Report to:

National Park Service
U.S. Department of the Interior
Olympic National Park
Port Angeles, Washington

Late Quaternary Sediment Source and Deposition History of Lake Ozette

7/1/2009

Andy Ritchie and Dr. Joanne Bourgeois

Earth & Space Sciences Department

University of Washington

TABLE OF CONTENTS

LIST OF FIGURES

LIST OF TABLES

Executive Summary

Purpose

This study was funded by the National Park Service to understand conditions in Lake Ozette prior to land-use changes in the 20th century, and to determine the magnitude of change that has occurred over the last 100 years. Lake Ozette is home to a genetically distinct stock of sockeye salmon (*Oncorhynchus nerka)*, which declined sharply in the 1950s, coincident with stream clearing activities and timber harvest in the basin. Despite nearly three decades of study and efforts to rebuild the population, Ozette sockeye remain depressed, and were listed as Threatened under the Endangered Species Act in March 1999. This study examines how modern land-use/land cover, lakeshore characteristics, and sediment accumulation rates in Lake Ozette differ from those prior to the collapse of Lake Ozette sockeye salmon.

Specific research goals include:

- Describe shoreline changes and changes in watershed land use at a sub-basin resolution in the context of fine sediment sources and sediment composition, and in the context of physical processes acting to create, maintain, and destroy habitat used by, or suitable for spawning sockeye salmon.

- Quantify sediment input rates to Lake Ozette over the past 500 years, at a decadal to centennial resolution, and at a sub-basin scale where possible.

- Document limnological characteristics of Lake Ozette with respect to isotopes of nitrogen and carbon over the past 500 years.

An additional original goal to quantify and describe changes in sediment composition and relative source contributions over the past 500 years was not accomplished due to a combination of sampling, time and fiscal constraints.

Goals and objectives

Describe shoreline changes and changes in watershed land use

The primary goal of the shoreline analysis was to quantitatively describe changes in unvegetated beach area between 1950 and 2003, as well as significant areas of accretion and erosion. Specific attention was devoted to the two extant sockeye spawning beaches on Lake Ozette, as well as to the Umbrella Creek delta, formerly utilized by sockeye. The purpose of this analysis is to determine how the shoreline has changed through the photographic record (from 1953 to 2003), to compare current and historic beach conditions, and to determine whether changes in coarse sediment flux at tributary mouths temporally corresponds to changes in land use and in accumulation rates measured in lake cores.

Watershed land use changes were characterized by sub-basin, documenting the shift from primary forest to industrial forestry through time, and comparing individual sub-basins to determine if sub-basin scale changes could be detected and contrasted in the sedimentary record of the lake. This analysis describes the timing of timber harvest and road building to allow comparison with sediment accumulation rates and shoreline changes at different time periods.

Both shoreline change and watershed land use were evaluated by compiling existing historic information, including aerial photographs and maps spanning the period from 1888 to 2006, and mapping changes in land cover, road density, shoreline extent, and shoreline vegetation through time.

Quantify sediment input rates to Lake Ozette over the past 500 years

The goal of this component was to determine recent and long-term sediment accumulation rates in Lake Ozette, and to evaluate whether historic changes in these rates can be detected. This enables us to understand to what degree recent accumulation rates differ from both peak rates and the long-term baseline (background) accumulation rate. A secondary goal is to determine whether changes in accumulation rates can be discriminated by sub-basin.

Reconnaissance seismic data were collected and used to target flat-lying sedimentary basins for coring. A coring apparatus was constructed, and eleven cores were collected over two years from depths of 20 to 100 m. Cores were analyzed for the radioisotope ^{210}Pb, which provides a detailed record of accumulation rates over the modern period (the last ~100 years). Long-term accumulation rates were derived through ^{14}C analysis from the midpoint and bottom of each core, allowing for a calculation of accumulation rates for the entire record in each core.

Document isotopic characteristics of Lake Ozette sediments

The primary goal of this research component was to use sediment cores to characterize the stable isotope record in Lake Ozette, to determine whether a detectable marine nitrogen signature exists, and to evaluate whether significant changes in stable isotopes of carbon or nitrogen are evident. A secondary goal was to determine whether isotope ratios or total N or C fluctuate significantly, and if so, whether changes in land use or salmon abundance temporally correlate with isotope or elemental composition of lake sediments.

Samples from seven cores were analyzed for carbon and nitrogen isotopes over a record spanning approximately the last 500 years.

Results

Shoreline and land-use changes

Significant changes in open beach area and shoreline morphology occurred between 1953 and 2003. More than half of the area mapped as open (unvegetated) beach in 1953 was covered by vegetation in 2003. Lake-wide, there was a decline of 56% in the measured area of unvegetated beach. On the two spawning beaches currently utilized by sockeye salmon, Allen's and Olsen's

beaches, the area of open beach declined by 67% and 66% respectively. The decline in open beach area was not limited to areas near tributaries, but was distributed throughout the shoreline of Lake Ozette.

The Umbrella Creek delta, a location formerly used by spawning sockeye salmon, was one of only two locations where the open beach area increased from 1953 to 2003. This can be attributed to aggradation and increased sediment flux. The proximal Umbrella Creek delta aggraded by about 2.4 ha from 1953 to 1994. Delta growth rates in Umbrella Creek track increases in timber harvest and road building. The maximum growth rate of Umbrella Creek delta occurred during peak timber harvest and road-building in the Umbrella Creek watershed.

At the beginning of the photographic record (1953), about 90% of the Ozette basin was still primary forest (old growth). From that point, timber harvest and road density grew rapidly. Peak harvest rates were largely synchronous across all sub-basins, occurring between about 1964 and 1984. During this period, between 50% and 80% of each sub-basin was harvested, and by 1994 about 94% of the primary forest on private lands had been converted to commercial forest. Virtually all of the remaining primary forest is found on federal and state lands, mostly on the west side of Lake Ozette, and to a lesser extent on state lands in the Crooked Creek sub-basin. Three of the four largest sub-basins in the Ozette watershed now have less than 5% primary forest. Umbrella Creek has only 1% of the original primary forest remaining, while Coal Creek has 3%, and Big River 4%. Annualized harvest rates climbed steadily from 1.4% per year in 1964 to a peak of 5.2% per year in 1979. By 1982, these rates dropped to pre-1964 levels, but have now stabilized at about 1.4%, with the onset of second-growth harvest.

Road density trends in the Ozette basin mirror timber harvest. Basin-wide, road density has grown steadily, increasing from about 0.4 km/km^2 in 1953 to 3.3 km/km^2 by 2006 for the entire watershed, and from 0.5 km/km^2 to 4.0 km/km^2 on private lands. Watersheds with the highest road densities are the same watersheds as those with the least remaining primary forest. Umbrella Creek has a road density of 4.6 km/km^2, followed by Big River, with a road density of 4.0 km/km^2, and Coal Creek, with a road density of 3.8 km/km^2.

Sediment accumulation rates

Recent sediment accumulation rates have increased significantly over background in Lake Ozette, coincident with timber harvest and development of the forest road network. The shift in accumulation rates occurred between 1960 and 1981, and varies by core location, with four of the five measured inflections occurring between 1960 and 1970. Of the eleven cores collected from Lake Ozette, seven showed continuous deposition without evidence of episodic deposition or erosion, and were sampled to develop ^{210}Pb profiles. The slopes of the profiles were used to calculate accumulation rates. Five of the seven cores showed an inflection in the slope, representing an increase in accumulation rates. The remaining two cores exhibited too much noise to be interpreted. No cores showed a decrease in accumulation rates.

Recent accumulation rates increased by 2- to 8-fold over background rates, with the highest increases measured near the mouths of Big River and Umbrella Creek. The highest increase in accumulation rates was found in a core from Swan Bay, closest to the mouth of the largest

tributary (Big River; 7.9 times higher than background), while the lowest increase was 2.0 times over background, in the deepest part of the lake. Since the recent increase in accumulation rates, those rates have remained high, rather than decreasing after the peak period of logging and road-building in the 1970s. Recent rates are the highest rates measured in all cores where inflection points were identified. Background sediment accumulation rates vary from 0.05 g/cm^2 to 0.20 g/cm^2, while recent accumulation rates range between 0.15 g/cm^2 and 1.00 g/cm^2.

All eleven cores were sampled at the midpoint and bottom of the core for ^{14}C so that carbon dates could be used to establish long-term accumulation rates to evaluate recent changes in accumulation with respect to long-term rates. The age of the oldest sediment sampled ranged from ~300 years in Swan Bay to ~2700 years in the western basin of the lake. Of the eleven cores sampled, seven had sufficiently well-constrained ^{14}C dates to enable comparison of accumulation rates in the upper and lower core halves. All of these cores showed an increase in accumulation rates in the upper half of the core (containing the recent shift in accumulation rates).

The ^{14}C analysis compared the top and bottom halves of each core, while the ^{210}Pb analysis examined only the modern fraction, going back about 100 years (the limit of ^{210}Pb dating). Because the modern fraction represents only a small portion of the top half of each core, no difference in accumulation rates between the upper and lower halves should be detectible if the recent increase is within the range of long-term variability. Thus ^{14}C data both provide additional evidence for the recent shift in accumulation rates within the modern fraction sampled for ^{210}Pb, and the combined data indicate that accumulation rates are now higher than in any comparable period for the last several thousand years.

Isotope values in lake sediments

Carbon and nitrogen stable isotope values from Lake Ozette fall within the range of other coastal temperate salmon-bearing lakes in the Pacific Northwest, and nitrogen isotope values are lower than values in lakes where salmon abundance has been successfully correlated with δ^{15}N values . Stable isotope values in sediments from Lake Ozette ranged from-27.7‰ to -26.7‰ (δ^{13}C), and from 0.6‰ to 3.1 ‰ (δ^{15}N). The C:N mass ratio varied from 11.5 to 20, the %C from 1% to 6.1%, and the %N from 0.1% to 0.4%. Six of seven profiles showed a down-core increase in C:N ratio, and 5 of 7 profiles showed a down-core decrease in δ^{15}N values. Down-core variations in δ^{13}C profiles showed both increases and decreases, varying by core.

No consistent temporal shifts in isotope ratios were observed between cores, although differences between cores were apparent. It appears that rather than indicating changes over time in lake chemistry or processes, isotope profiles track the depositional history of a given core. In general cores taken in deep water farther from terrestrial sources of organic material showed isotope profiles more consistent with algal-nutrient inputs, and had a higher organic content.

Interpretation

Shoreline and land-use changes in the Ozette watershed.

Both road densities and ongoing (annualized) harvest rates in the Ozette watershed fall into the highest watershed risk rating for cumulative risk of adverse effects to Threatened and Endangered species. Average basin road densities on private lands are 4.0 km/km^2 (6.4 mi/mi^2), which is about twice as high as the threshold for not properly functioning. This threshold is defined as significant (e.g. 20-25%) road-related increase in drainage network density. Moreover, with current annualized harvest rates of about 1.5%, roughly 45% of the lands in private holdings will be hydrologically immature (<30 years old) at any given time. Both increased drainage network density, and increased hydrologic immaturity can result in changes to runoff, including higher peak flows and reduced or increased low flows relative to background, depending on forest age.

Between 1953 and 2003, more than half of the open beach area on the lake was covered by vegetation, possibly related to increased fine sediment input, to changes in lake hydroperiod, or both. The loss of open beach is detrimental to spawning sockeye, which spawn in sand and gravel on open beaches along the lakeshore. In the last 50 years, more than 2/3 of the open beach area has disappeared on the two known sockeye spawning beaches in Lake Ozette, Olsen's Beach and Allen's Beach. Hypothesized causes for the increased vegetation include both an increase in fine sediment inputs and a change in the hydroperiod (the timing of water-level fluctuations) in Lake Ozette. Increased fine sediment around the lakeshore would provide more suitable substrate for vegetation to grow, and a change in the hydroperiod could both reduce wave energy acting on a given shoreline elevation, and reduce the time that the lakeshore is inundated, leading to a longer growing season at lower elevations on lake beaches.

In contrast to the rest of the lakeshore, unvegetated beach area increased at the Umbrella Creek delta in the last fifty years. Between 1964 and 1979, the delta grew by about 2.4 ha, and sockeye spawning ceased. In the same 15-year period, 72% of the watershed was harvested, and road densities increased four-fold, from about 1 km/km^2 (1.6 mi/mi^2) to about 4km/km^2 (6.4 mi/mi^2). Rough calculations of the volume of sediment required to increase the delta by this extent indicate that current estimates of sediment production in the Umbrella Creek watershed may underestimate sediment delivery to the lake over the last 50 years by as much as fourfold. Delta growth requires high sediment flux, which in combination with peak storm discharges and fluctuating lake levels, has created an unstable environment where vegetation cannot become established. Increased sediment flux makes the delta unsuitable for spawning sockeye salmon because eggs are easily buried or scoured, and survival to emergence is unlikely.

While it may seem counter-intuitive that both increased and decreased vegetation cover indicate degraded sockeye spawning habitat, these two examples illustrate the delicate balance required for proper habitat function. Sockeye salmon require clean, stable, oxygenated gravel/sand as spawning substrate for deposited eggs to survive. Ideal spawning areas are stable gravel and sand with a low proportion of fine sediments, which can suffocate incubating eggs. The same fine sediments that suffocate eggs can bury gravels and provide substrate for vegetation growth, while too much coarse sediment, or a high overall sediment flux, can prevent the establishment of vegetation, and at the same time bury and suffocate eggs. Additionally, while increased lake level fluctuations due to hydrologic modifications can provide better growing conditions for shoreline vegetation on beaches away from tributary mouths, such fluctuations can destabilize

tributary sediments because high flows occur over a wider range of lake levels, depositing and eroding sediment more dynamically.

Sediment accumulation rates through time

Both methods of quantifying accumulation rates (^{210}Pb and ^{14}C) indicate that recent rates have increased over background rates. While ^{14}C data provide only a coarse comparison between modern and long-term rates, more precise ^{210}Pb dates indicate that modern accumulation rates shifted recently as timber harvest and road-densities increased in the watershed. Recent accumulation rates are 2 - 8x higher than background and are higher than long-term averages. Elevated accumulation rates are seen throughout the lake, including in the western main basin, farthest from tributary inputs.

There is no evidence of an early peak in accumulation rates attributable to initial harvest or early logging practices in the Ozette watershed. Modern rates are the highest rates measured in all cores where inflection points were identified. Inflection points in ^{210}Pb profiles indicate that accumulation rates increased markedly between 1960 and 1980, and remained elevated thereafter (shifted), with the majority of locations shifting between 1960 and 1970. The greatest increases in accumulation rates were measured near the Umbrella Creek delta and the mouth of Big River, where accumulation rates increased by 5.5 and 7.9 times, respectively. Background sediment accumulation rates vary by site from 0.05 g/cm^2 to 0.20 g/cm^2, while modern accumulation rates range between 0.15 g/cm^2 and 1.00 g/cm^2.

Reconnaissance seismic data, in combination with accumulation rates from cores, indicate that Lake Ozette likely contains a continuous sedimentary record spanning the last 20 – 30 thousand years. The maximum age of cores collected from Lake Ozette was 2900 years, and the youngest core captured roughly a 400-year sedimentary record, but seismic profiles show that flat-lying sediment extends to depths of roughly 20 m in the North End, and about 30 m in the western basin. With pre-disturbance accumulation rates of about 1 mm/yr, these thicknesses imply that sediments in Ozette contain a valuable climate and environmental archive encompassing the last 20,000 – 30,000 years, extending into the last glaciation. It appears that Lake Ozette was at least partially ice-free during this time.

Isotope values in lake sediments

There does not appear to be a detectable marine-derived nitrogen signature in sediments from Lake Ozette. Relative to studies which have used δ^{15}N to track salmon abundance, both the range and the values of δ^{15}N are low in Lake Ozette sediments, although they are comparable to values reported in other sockeye lakes. This is probably due to both lower salmon abundance and a more active terrestrial component of the nitrogen cycle in mid-latitude temperate lakes than in those lakes farther north in Alaska where this technique has been used successfully.

While isotope data from sediments in Lake Ozette may not shed light on sockeye abundance, they still may provide valuable insight into the ecology and evolution of the lake. Trends by location were more apparent than trends by depth between cores. In general cores taken in deep

water farther from terrestrial sources of organic material showed isotope profiles more consistent with algal nutrient inputs, and had a higher organic content.

Stable isotope and elemental profiles in cores did exhibit down-core shifts. However these shifts fall within ranges reported by research studying diagenesis (post-depositional change) in lake sediments. This study was not able to distinguish between diagenetic and intrinsic fluctuations in isotopic or elemental values in lake sediments.

Major Conclusions

Land-use changes in the last fifty years have significantly affected Lake Ozette. Sediment accumulation rates more than doubled in Lake Ozette during the same period that the majority of the basin was converted from primary forest land cover to industrial forestry with a <50 year rotation. Near tributary mouths, accumulation rates have increased five- to eight-fold, and these elevated accumulation rates have persisted to the present. There are multiple indicators that the shoreline is continuing to respond to land-use modifications.

Shoreline response includes ongoing vegetation colonization of the shoreline and continuing delta growth at Umbrella Creek. Over half of the open beach area around the lake has been colonized in the last fifty years, and the Umbrella Creek delta has grown by 2.4 ha, representing an estimated 400,000 m^3 of sediment flux to the lake during this time. Sockeye spawning habitat has been significantly impacted by these effects of land-use changes. On existing spawning grounds, more than 2/3 of the open beach area in 1953 was overgrown with vegetation by 2003. Sockeye spawning at Umbrella Creek delta stopped as delta growth increased in the 1970s.

Unless the loss of open beach area is reversed, and/or the Umbrella Creek delta stabilizes, some mitigation may be necessary to maintain suitable habitat for sockeye. Research and monitoring of existing and former spawning habitat to understand factors creating, maintaining, and destroying this habitat should be a priority, but without a component of mitigation, such as vegetation removal, there is no reason to expect conditions on sockeye spawning beaches to do anything but worsen.

Despite the decline of sockeye salmon in Ozette, and increased sediment accumulation rates in the lake, carbon and nitrogen isotope values and ratios remain within the range of pre-disturbance values. The stability of the isotope record implies that fundamental drivers of ecosystem productivity may be relatively intact, and that the food web of the lake is capable of supporting sockeye salmon if limitations on spawning success can be overcome. Moreover, while stable isotope analyses have failed to reveal past patterns of salmon abundance, the sedimentary record in Lake Ozette clearly contains a valuable archive that can provide insights into climate and ecosystem dynamics that likely extend back beyond the last glacial maximum.

Acknowledgments

I would like to thank The National Park Service Water Resource Division and Olympic National Park for funding this study, and for their patience in awaiting its completion. Thank you also to the Washington Cooperative Ecosystem Studies Unit for administering the project, under Task Agreement #J9W88050001. A project of this scope would be impossible without the generous assistance of many people. John Meyers (retired) of Olympic National Park, was instrumental in helping with the project scope and grant application for this work. Cat Hoffman provided important feedback during the review process. Dr. Joanne Bourgeois and Dr. Chuck Nittrouer, Dr. Eric Steig, and Dr. Steven Fradkin provided extensive comments through the post-award project implementation, and throughout the project, and Dr. Nittrouer generously donated his time and the use of his equipment to make coring in Lake Ozette possible. I am also indebted to Dr. Charlotte Schreiber and Dr. David Montgomery for their encouragement and feedback during my research and report writing. My friend and fellow river scientist Mike Haggerty also helped to review this report and provided valuable constructive comments.

I would also like to thank Rayonier Timber Operating Company for allowing me to scan 1100 resource photos used in my shoreline and land use analysis. In particular, Julie Dieu, Frank Phillips and Mike Leavitt generously gave of their time to make this possible. Teresa Zena Alcock, of Olympic Natural Resource Center (ONRC) helped with space and equipment, so that I could scan the air photos locally. Harvey Greenberg and Charles Kiblinger loaned me a large format scanner and computer so that I could complete the work.

I am deeply indebted to local residents in the Ozette area. Rob Snyder, proprietor of The Lost Resort at Lake Ozette, provided invaluable assistance in everything ranging from food and accommodation to help with transporting and assembling my coring platform and assistance in the actual coring. Randi Knox also helped with lodging and motivation for this research. Larry Sears and his son Tim donated time and the use of his tractor for assembling the platform. Dave Easton (ONP – Ozette) provided tools and assisted with troubleshooting during collection of sub-bottom profiles. Don Hamerquist and Janeen Porter rallied the troops and helped immensely with processing the cores onshore. Carolyn Peterschmidt and John and Karolyn Burdick also helped with the shore-side core-processing work.

A great many people and organizations provided generous (and unpaid) donations of material and time throughout the project. I am especially grateful to the Makah Tribe, in whose employment I conceived of the need for this research. The Makah Tribe also generously donated an old smolt trap which served as the base from which the coring platform was constructed, and the use of a workboat to help with sediment coring in Lake Ozette. My friend Dean Reandeau was invaluable, and donated dozens of hours of brainstorming and welding. Without him, I never would have been able to finish building the coring platform in time for the first season of coring. Fellow graduate student Maureen Davies worked tirelessly with me on all aspects of my research. She helped with the initial setup and transport of the coring platform, with sub-bottom profile collection, and with coring in Lake Ozette. She also taught me the fundamentals of Kasten coring and ^{210}Pb analysis. Her grandfather, Rear Admiral Roger B. Horne Jr. (USN Ret.)

graciously allowed us to use his boat to collect seismic profiles in the lake. Another fellow graduate student, Tina Drexler, helped me with lab procedures and ^{210}Pb data interpretation.

My friend Gary Dougherty generously donated the use of his boat and his time to help me core in Ozette, and my sister Annalissa Ritchie, and my brother Tyler Ritchie, my friend Mike Haggerty, and friend and fellow grad student Matthew von der Ahe all helped in core collection and processing. To all of them, and to the others who helped in my research, and whose contributions I failed to mention, thank you for your invaluable assistance, and for believing in this work.

1 INTRODUCTION & RESEARCH OBJECTIVES

1.1 Background & Objectives

The National Park Service is funding this study to improve scientific understanding of the relationship between modern and pre-modern conditions in Lake Ozette. The project was funded by the National Park Service and implemented through the University of Washington Cooperative Ecosystem Studies Unit Task Agreement # J9W88050001. Study objectives are to determine sediment accumulation rates for approximately the last 600 years, to reconstruct watershed disturbance history by sub-basin, and to evaluate the magnitude of land-use related change in sediment accumulation rates in Lake Ozette.

Motivation for this research stems from the 1950s decline of Ozette sockeye salmon, and their subsequent 1999 listing as Threatened under the Endangered Species Act. Despite complete cessation of salmon harvest three decades ago, and more than 30 years of research and hatchery production aimed at understanding and overcoming limiting factors to sockeye salmon production, there has been no significant recovery of the population. While much previous research has examined historical population trends, food availability, and habitat conditions, there continues to be a poor understanding of how modern conditions differ from those found before the decline of Lake Ozette sockeye.

This project analyzes and quantifies disturbance history and shoreline changes in the Ozette basin in the 20th century (over the period of the photographic and map record). These modern changes are related to pre-disturbance, or equilibrium conditions in sediment accumulation in Lake Ozette over the last 500 years. Basin disturbance history is reconstructed and described by sub-basin from aerial photography and maps dating to ~1900. Shoreline changes over the period of the photographic record are analyzed and quantified, and the structure and composition of nearshore and deep basin sediment cores from Lake Ozette is described, including both sediment profiles for stable isotopes of N and C, and sediment accumulation rates based on ^{14}C and ^{210}Pb isotopes.

1.2 Physical Setting

1.2.1 Geography

The Ozette Basin is located near the northwest tip of the Olympic Peninsula, in Washington State, midway between the coastal towns of Neah Bay and La Push (Figure 1). The basin is drained by the Ozette River, which originates at the North End of Lake Ozette, and meanders for 8.5 km (5.3 mi) to the Pacific Ocean, losing only 10.4 m (34 ft) of elevation. The Ozette Basin occupies part of a narrow strip of Pacific coastal temperate rainforest which extends from northern California to southeast Alaska. This productive and diverse rainforest is characterized by some of the highest biomass accumulation and most productive forests in the world (Franklin and Dyrness 1973).

Figure 1. Ozette watershed location map with sub-basins.

The Ozette basin falls within the Olympic Section of the Pacific Northwest Coast Ecoregion of Vander Schaff et al (2006), and the Coastal Lowlands, Coastal Uplands, and Low Olympics subdivisions of the Coast Range Ecoregion of Pater et al (1997). About 95% of the basin lies within the Sitka Spruce Vegetation Zone of Henderson et al (1989), with the remainder, a small section of highly dissected mountainous terrain in the headwaters of Big River, in the Western Hemlock Vegetation Zone.

From Lake Ozette to the Pacific coast, and along the broad, gentle valley of Big River for some distance upstream to an elevation of about 100 m (300 ft), the landscape can be characterized as Coastal Lowlands, with abundant freshwater lakes and wetlands, and black-water streams. (Pater et al, 1997). Prairies dot the coastal plain between Lake Ozette and the Pacific Coast, and bogs are common where poorly drained glacial sediment impedes groundwater drainage through the hummocky terrain. Inland, and through an elevation of about 150 m (500 ft) Pater et al (1997) define the Coastal Uplands Ecoregion, corresponding roughly with the historic distribution of Sitka spruce. A small portion of the northern Ozette basin above 150 m (500 ft) falls within the Low Olympics subdivision of Pater et al (1997), characterized by a lush western hemlock, western red cedar, and Douglas-fir rainforest rich in epiphytes.

The more localized study of Henderson et al (1989) defines the Sitka spruce vegetation zone as a function of elevation, aspect, and precipitation. Henderson et al (1989) map the Sitka spruce vegetation zone as extending through about 95% of the watershed, and identify a single dominant forested plant association of Sitka spruce/Swordfern-Oxalis. Dominant tree species in this forest type are Sitka spruce, western hemlock, and western redcedar. Red alder and bigleaf maple are common early seral species (Henderson et al 1989). Dominant understory species (shrubs and herbs) include oxalis, swordfern, vine maple and salmonberry. Close to the coast, salal and evergreen huckleberry become more common. The Washington Native Plant Society has documented at least 223 species as present in the Ozette catchment (WNPS unpublished data).

The total Ozette basin area is about 229 km^2 (88 mi^2). Mean basin elevation, (excluding bathymetry of Lake Ozette) is 91 m (299 ft), with a maximum elevation of 592 m (1943 ft) at Sekiu Mountain, in the NE corner of the catchment, to sea level, at the confluence of the Ozette River with the Pacific Ocean (USGS 1994). Topography varies from gently undulating, low-elevation coastal hills along the western margin of the basin to steep, highly dissected mountainous terrain at the headwaters of Big River in the northeast portion of the catchment.

Lake Ozette occupies about 13.5 % of the Ozette Basin. Ozette is the third largest natural lake in Washington, and the largest with an uncontrolled outlet (Walcott, 1973). The lake is approximately 13 km (8 mi) from north to south and 3.2 km (2 mi) wide, and has three islands (Garden, Tivoli, and Baby). Lake Ozette has a surface area of 30.6 km^2 (11.8 mi^2; 3,056 ha; 7,550 acres), with 57.4 km (36.5 mi) of shoreline. The maximum depth is 98 m (320 ft) (Dlugokenski et al. 1981), with an average depth of about 40 m (130 ft). Lake Ozette's mean water surface elevation is 10.4 m (34 ft) above mean sea level (National Geodetic Vertical Datum of 1929[NGVD 1929]), with a maximum range of about 3.4 m. Minimum summer water surface elevation typically ranges between 9.4 and 9.8 m (31 – 32 ft), and correlates reasonably well with summer precipitation. Maximum winter water surface elevation has a wider range,

from 11 to 12.6 m (36 – 41.5 ft) and correlates with winter precipitation. The Ozette River is the lake's only modern outlet, although basin topography suggests that the lake may have emptied through Allen's Slough (in the southwest part of the lake) and possibly at other points along the western shore in the past.

1.2.2 Climate

Climate on the northwest Olympic Peninsula and in the Ozette watershed is strongly influenced by proximity to the Pacific Ocean. The region is characterized by abundant seasonal precipitation and mild temperatures throughout the year (NCDC 2007). Prevailing winds are from the southwest and west in the winter, and from the northwest and west in the summer (NCDC 2007). In the summer and early fall, fog and low clouds commonly form offshore and move inland at night, often disappearing by midday. This is a source of fog-drip, which can contribute significantly to dry season precipitation (Oberlander 1956; Azevedo and Morgan 1974; Harr 1982; Dawson 1998), but is poorly quantified on the Olympic coast (Stone 1936; Court and Gerston 1966; WRCC 2003).

The wet season begins in September or October, as the Aleutian Low builds over the Gulf of Alaska. During the rainy season, storms are frequent, and gale-force winds are not unusual. Rainy season temperatures show little fluctuation, with maximums typically in the 40s and minimums in the mid-30s. A few arctic outflow events each winter typically produce periods of cold, dry weather and transient snowfall at low elevations. However, snow rarely accumulates during the winter and typically doesn't reach depths greater than 25 cm (10 in) or persist longer than a few weeks at most elevations within the Ozette watershed. In winter months, rainfall is often nearly continuous. Between October and January, rain can be expected about 26 days per month. On average, about 82% of the precipitation falls from October through April (NCDC 2007).

The dry season begins in May, as the Aleutian Low weakens and the North Pacific High expands northward (Phillips 1960; NCDC 2007). During the warmest months, high temperatures are typically in the upper 60s and lower 70s, occasionally reaching the upper 70s and lower 80s. Rarely, hot dry outflow from east of the Cascades brings temperatures into the 90s. From July to September, rain can be expected about ten days per month. Dry season precipitation averages about 18% of total annual precipitation (NCDC 2007).

Mean annual precipitation in the Ozette watershed is similar to measured precipitation at Quillayute State Airport, about 20 km (12 mi) south, and at Tatoosh/Neah Bay, about 25 km (15 mi) north. A thorough review of precipitation and other regional climate records from nearby weather stations (Forks 1E, Quillayute Airport, and Neah Bay 2E), as well as short-term records from Lake Ozette, indicates that rainfall regimes at low elevations are similar for the Ozette Ranger Station location and Quillayute Airport (Haggerty et al 2008).

The most precise available estimates of precipitation are model data from PRISM (Parameter-elevation Regressions on Independent Slopes Model), an expert climate mapping system that incorporates point data and complex climate factors such as temperature, elevation, and

prevailing wind direction (Daly et al 1994; http://www.prismclimate.org). The PRISM dataset for mean annual rainfall from 1971 to 2000 was queried for the Ozette watershed. Mean rainfall for the watershed was calculated to be 266 cm (105 in), with a maximum of 336 cm (132 in) in the south-facing, upper-elevation headwaters of Big River, and a minimum of 230 cm (91 in) over Lake Ozette. The standard deviation of modeled precipitation values was 18.8 cm (7.4 in). Of the approximately 5% of the watershed with modeled precipitation more than two standard deviations from the mean, 81% of the area was in the headwaters of Big River, with the remainder in Umbrella Creek and Coal Creek.

These data differ somewhat from those reported by the United States Bureau of Reclamation (BOR) (Lieb and Perry 2005). The BOR reports average annual precipitation ranging from 330 cm (130 in) in the headwaters to 185 cm (73 in) at the southwest edge of the catchment, citing a digitized isohyetal map of Washington as the source - Plate 1 of USGS Water Resources Investigation Report 97-4277 (Sumioka et al 1998). However, this figure is digitized and interpolated from a 1965 map of mean annual precipitation in Washington from 1930 to1957, produced by the U.S. Weather Bureau (Sumioka et al 1998).

1.2.3 Limnology & Lake Ecology

The dramatic difference between dry season and wet season precipitation in the Ozette Basin are reflected in physical and ecological characteristics of the lake itself. Distinct beaches ring the lake, and conifer species are excluded from areas inundated in the winter. Many of these beaches are covered with submersion-tolerant grasses, forbs, and shrubs, and distinct vegetation communities inhabit various elevations of the shoreline. Shoreline vegetation surveys conducted by Meyer and Brenkman (2001) identified 24 taxa: grasses (2), sedges (1), rushes (3), forbs (11), shrubs (3) and aquatics (4). These surveys were not exhaustive, and likely omit many species present in the shoreline and littoral environment. However they serve to illustrate the diverse nature of shoreline habitat. Springs are also present, as are gravel and sand beaches, particularly on the windward shores and at the mouth of Umbrella Creek.

Lake Ozette is a (humic), monomictic, oligotrophic to mesotrophic lake (Beauchamp and LaRiviere 1993; Meyer and Brenkman 2001). Like many lakes and rivers in areas of high primary productivity, Ozette is a brown-water lake, characterized by tea-like color from dissolved organic carbon. This increases absorption of sunlight in the visible and UV, and can temporally stabilize thermal stratification, as well as increase the total amount of energy absorbed and stored as heat (Caplanne and Laurion 2001). Available water temperature profiles indicate that the lake begins to stratify in April and begins to mix in October (Meyer and Brenkman 2001, Beauchamp and LaRiviere 1993).

During the dry season, days are long, solar radiation and ambient air warm the surface waters, and the lake is thermally stratified. The epilimnion reaches a depth of 10 to 15 m, and a maximum temperature of about 21 ºC (Meyer and Brenkman 2001). While the lake is stratified, the hypolimnion is about 30 to 40 m deep, with a temperature of 7 to 8 ºC. During the rainy season, inputs of water at or near ambient air temperature are high, days are short, the lake is well mixed, and temperature is confined to a narrow range throughout the water column,

reaching a minimum of about 6 to 7 ºC in February (Bortleson and Dion 1979; Meyer and Brenkman 2001).

Detailed studies of plankton community and lake productivity have been conducted by Bortleson and Dion (1979), Dlugokenski et al (1981), and Meyer and Brenkman (2001). These studies are summarized in Haggerty et al (2008). At least nine crustacean and 15 rotifer taxa have been identified, with densities highest in spring and summer months, and lowest in late fall and winter. (Meyer and Brenkman 2001, Bortleson and Dion 1979). While researchers have differed significantly in their estimates of total available zooplankton biomass, they have all agreed that the lake is productive. This is evident by the size and diversity of fish species the lake supports.

At least 25 fish species have been identified as present as lake Ozette (Haggerty et al 2008). This includes seven species of salmonids (*Oncorhynchus),* five species of sculpin (*Cottus*), and two species of lamprey (*Lampetra*). Additional fish species have been observed in the estuarine portion of the lower Ozette River. River otters frequent the lake and tributaries throughout the year, and seals feed on adult salmon spawning or staging in the lake during winter months when the Ozette river is at a high enough stage to facilitate seal passage into the lake.

Two species of freshwater sponge, *Spongilla lacustris* and *S. fragilis* have been identified in Lake Ozette (Gee 1934), as have two species of freshwater mussel, the western pearlshell, *Margaritifera falcata,* and the Oregon floater, *Anodonta* cf. *oregonensis* (Gustafson and Iwamoto 2005). These mussels are obligate parasites on gills and fins on freshwater fishes.

1.2.4 Geology

The geologic history of the northwestern Olympic Peninsula, in combination with its climate and vegetation, strongly influences potential sediment yield in the Ozette basin. The evolution of the peninsula tells a story of mountains eroded to the sea and buried deep beneath the ocean floor, of half-baked continental sediments half-subducted, then driven back into the continent by the Juan de Fuca plate and thrust up in a fractured mélange against a buckled backstop of basalt, to be weathered and driven seaward again by the inexorable forces of erosion.

The story that this cycle of uplift and erosion tells in the rocks of the Ozette basin has been largely obscured by an extensive mantle of Pleistocene glacial sediments deposited over the last 1.8 Ma. The chronicle of repeated glaciation and deglaciation is in turn complicated by multiple advances of the ice itself, as well as by the sheer quantity of precipitation, and the consequent erosion and dense vegetation in the Holocene. A brief outline of the geologic setting of the Olympic Peninsula is useful to understand the history of the rocks of Ozette.

The Olympic Peninsula is a textbook example of a subduction complex – a thick accretionary wedge of sediment scraped off of the subducting Juan de Fuca plate and added to the continental margin (Tabor and Cady 1978). The Olympic Mountains are the only place along the active subduction zone where the accretionary wedge is uplifted and exposed (Brandon and Vance 1992). The wedge is formally designated as the Olympic Structural Complex (OSC) by Stewart and Brandon (2004). The OSC lies structurally below, or inside of, the Crescent Formation, a

~16 km thick sequence of submarine to subaerial basalt flows that erupted about 50 Ma (Babcock et al 1992).

While structurally the Crescent Formation overlies the OSC, stratigraphically it lies below the accretionary wedge, forming a resistant 'backstop' to the more deformable sedimentary rocks. The uplift and exposure of the OSC has deformed the Crescent Formation and related Coast Range terrane into a horse-shoe shape open toward the coast. Bedding planes along the inland apex of the horse-shoe have been inclined near vertical, dipping east, in the eastern Olympics near the Dosewallips River (Babcock et al 1992). The Crescent Formation wraps from the Pacific coast at Cape Flattery, around the core of the Olympics where it creates steep topography west of Hood Canal, then back again to approach the coast in the vicinity of Grays Harbor. The contact between the OSC and the Crescent Formation is delineated by the Calawah Fault and the Hurricane Ridge Fault, which define a major discontinuity in the structural geology of the Olympic Peninsula.

The peninsula began to emerge above sea level about 15 Ma, as a large arch developed in the subducting Juan de Fuca plate (Brandon and Vance 1992). The Ozette basin lies within the northwestern portion of the OSC, described as an uplifted subduction-related mélange of primarily marine volcanic and sedimentary rocks. These rocks are derived from source sediments derived from terranes in the region of the Idaho batholith (Aalto et al 1998) to the Omineca crystalline belt in the Canadian Rockies (Stewart and Brandon 2004), and deposited in water depths greater than 2000 m (Stewart and Brandon 2004), from the Eocene through the Oligocene, about 50 to 30 Ma (Brandon and Vance 1992). Little record of the post-emergence geologic history exists, and the modern story begins with stagnation and retreat of the Juan de Fuca lobe of the Cordilleran ice sheet in the vicinity of the Ozette basin about 13,000 yr BP (Heusser 1973), based on radiocarbon dates of wood buried in ablation till near Lake Ozette.

The Ozette basin is underlain primarily by Quaternary sediments, and by relatively incompetent marine sedimentary rocks, which have been heavily faulted (Schasse 2003), and have never been subjected to deep burial (Stewart and Brandon 2004). As a consequence, these rocks weather rapidly into readily erodible soils. Measurements of in-stream bedrock erosion in comparable accretionary marine sedimentary rocks within the OSC on the southern Olympic Peninsula have found modern bedrock weathering and erosion rates surpassing 100 mm/yr over a 7 year period (Stock et al 2005).

Spatial analysis of digital data from Washington Department of Natural Resources (2005) was performed to quantify the relative area of distinct geologic sources in the Ozette basin (Figure 2). Unconsolidated Quaternary glacial and nonglacial sediment sediments dominate the surficial geology of the basin, comprising 72% of the basin land area. These sediments lie primarily in the low-relief, low elevation portions of the basin, typically occupying valley bottoms and gentle slopes, including everything west of Lake Ozette, and gentle slopes and valley bottoms below elevations of about 100 m in the northern portion of the watershed, and below elevations of about 80 m south of Crooked Creek, on the east side of the lake.

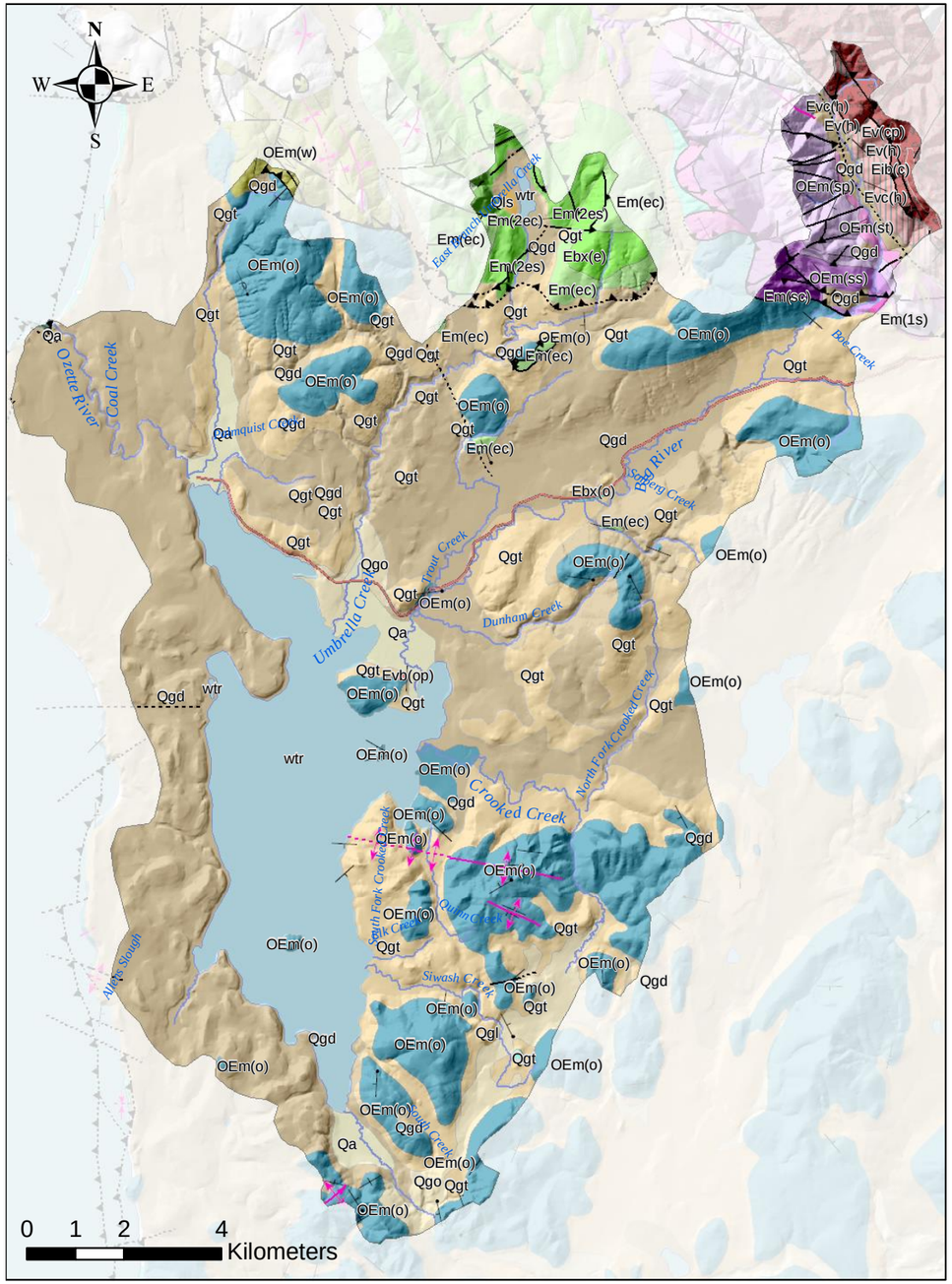

LEGEND

Geologic Map Units

Quaternary Nonglacial Deposits

- open water
- Qa - alluvium
- Qls - mass-wasting deposits, mostly landslides

Quaternary Glacial Deposits of the Fraser Glaciation

- Qgd - continental glacial drift, Fraser-age
- Qgt - continental glacial till, Fraser-age
- Qgo - continental glacial outwash, Fraser-age
- Qgl - glaciolacustrine deposits, Fraser-age

Ozette Terrane

- Ebx(o) - Ozette Lake-Calawah Ridge block, tectonic breccia
- Evb(op) - Ozette Lake-Calawah Ridge block, basalt flows
- OEm(oc) - Ozette Lake-Calawah Ridge block, conglomerate
- OEm(o) - Ozette Lake-Calawah Ridge block, sandstone & siltstone
- Om(c) - Cape Alava coastal block, sandstone

Sooes Terrane

- OEm(e) - Elk Lake block, siltstone unit
- Em(ec) - Elk Lake block, sandstone and conglomerate unit
- Ebx(e) - Elk Lake block, melange unit
- Em(2es) - Elk Lake block, sheared siltstone & sandstone
- Em(2ec) - Elk Lake block, conglomerate and sandstone
- OEm(sp) - Snag Peak block, sandstone and siltstone unit "p"
- OEm(ss) - Snag Peak block, siltstone and sandstone unit
- OEm(st) - Snag Peak block, siltstone unit
- Em(1s) - Snag Peak block, concretionary siltstone & claystone
- Em(sc) - Snag Peak, sandstone and conglomerate
- OEm(w) - Washburn Hill block, turbidite sandstone unit

Terrane S of Crescent Fault & N of Calawah Fault

- Ev(h) - volcanic rocks of Hobuck lake
- Evc(h) - volcaniclastic deposits or rocks

Crescent Terrane

- Ev(cp) - pillow basalt flows and breccias
- Em(1c) - siltstone and sandstone
- Eib(c) - silicified intrusive volcanic rocks

Geologic Symbols

- Fault, unknown offset
- Fault,unknown offset, concealed
- Thrust fault, sawteeth on upper plate
- Thrust fault, concealed, sawteeth on upper plate
- Right-lateral strike-slip fault
- Right-lateral strike-slip fault, concealed
- Left-lateral strike-slip fault
- Left-lateral strike-slip fault, concealed
- Normal fault, bar and ball on downthrown side
- Normal fault, concealed, bar and ball on downthrown side
- Anticline
- Anticline; concealed
- Anticline;large arrowheads show direction of plunge
- Syncline
- Syncline; concealed
- Bedding - showing srike and dip
- Overturned bedding - showing strike and dip
- vertical bedding - showing strike
- Bedding - showing strike and dip; top known
- Overturned bedding - showing strike and dip; top known

Figure 2. Geologic Map of the Ozette basin (from Washington DNR 1:100,000 digital data)

Glacial sediments are the most common mapped unit, comprising 70% of the geologically mapped surfaces in the basin. These Pleistocene sediments are dominated by drift (59%) and till (37%), with minor outwash components, primarily near the Umbrella Creek delta and along the southeastern edge of the basin, and a single small glacio-lacustrine unit mapped in the upper portion of Siwash Creek, about 3 km E of Lake Ozette. Nonglacial sediments comprise just 2% of the mapped area, and are almost entirely mapped as Holocene alluvium, primarily in the modern floodplains and valley bottoms of Big River, Umbrella Creek, Coal Creek, and South Creek. The entire basin west of Lake Ozette is mapped as glacial drift.

Bedrock in the Ozette basin is mostly mapped on higher elevation hilltops and highly dissected terrain, and is not mapped west of Lake Ozette (Schasse 2003). Bedrock typically crops out at elevations above about 100 m in areas north of Crooked Creek, and at elevations above approximately 80 m in the hills south of Crooked Creek. Bedrock units make up just a quarter of the basin area. These are primarily mapped as marine sedimentary rocks of the Ozette terrane (19%), or Sooes Terrane (6%). The remainder is either transitional terrane between the Crescent Fault and the Calawah Fault, or Crescent Formation marine basalts and related volcanics.

“Bedrock” in the Ozette basin is not only hard to find, but hardly rock. About 95% of the bedrock units mapped in the Ozette basin are heavily faulted, highly disrupted mélange and turbidite units of the Ozette (69%) and Sooes (23%) terranes, and unnamed terrane lying between the Crescent and Calawah faults (3%). The remaining 5% are basal rocks of the Crescent Formation, comprising primarily lower Eocene basaltic pillow lava and breccias and silicified intrusive volcanic rocks.

Ozette terrane is the most abundant bedrock in the basin, comprising over 2/3 of the mapped rock units. Ranging in age from early Eocene to early Oligocene, nearly all Ozette terrane exposures in the Ozette basin are mapped as unit OEm(o); medium- to thick-bedded Oligocene to Eocene sandstone, with minor interbeds of thin-bedded sandstone and siltstone turbidites (Figure 2). Locally this unit contains carbonaceous and calcareous intraclasts with rare lenticular coal seams. Also locally present are deposits of siltstone-chip conglomerate, pebble conglomerate, and debris flow mudstone (Schasse 2003).

Sooes terrane comprises nearly a quarter of the bedrock in the Ozette basin, and is confined primarily to the steep upper reaches of Big River and Umbrella Creek, where a combination of steep slopes, intense deformation, and steeply dipping beds (Schasse 2003) in units of the Elk Lake and Snag Peak blocks makes these landforms particularly susceptible to landsliding. Highly disrupted units of the Elk Lake and Snag Peak blocks make up about 23% of the Sooes terrane, primarily in the East Fork of Umbrella Creek north of the inferred location of the Ozette fault, and in upper Big River southwest of the inferred location of the Calawah Fault. Sooes terrane is primarily Oligocene to lower Eocene sandstone, siltstone, conglomerate and mélange. Conglomerate and coarse sandstone are common in some members of this unit, as are finer grained sandstone and siltstone. Graded channel deposits, metavolcanic rocks, laminated siltstone, and carbonaceous and coaly layers are present in some members. Chert pebbles in conglomerates within the Elk Lake block contain late Triassic radiolarians (Schasse 2003).

About 5% of the basin area, entirely within the portion of the headwaters of Big River lying northeast of the Calawah Fault, is underlain primarily by rocks of the lower Crescent Formation. These rocks are primarily basalt pillow lava and breccias, with 1-5 m beds of pelagic limestone and calcareous silts. Beds dip from 42º - 80º, and landslides are common in this bedrock unit.

1.2.5 Watershed Land Use and Disturbance History

Natural disturbance in Pacific coastal temperate rainforests is primarily driven by wind and other geomorphic events such as landslides and flooding (Alaback 1996). While forest fire return intervals are estimated at about 900 years in the Sitka spruce vegetation zone (Henderson et al 1989), and great earthquakes occur approximately every 400-600 years along the Cascadia margin (Atwater and Hemphill-Haley 1997; Goldfinger et al 2003), hurricane-force winds occur on the Washington coast with an average return interval of about 20 years (Henderson et al 1989). The ’21 Blow of 29 January 1921 blew down an estimated 7-8 billion board feet of timber from the Columbia River to Vancouver Island, and the Columbus Day Storm of 12 October 1962 toppled about 11 billion board feet in Washington and Oregon. Based on estimates of about 50,000 board feet/acre (Bolsinger 1969) in mature forest on the Olympic Peninsula, the ’21 Blow blew down the equivalent of about 650 sq km (250 sq mi) of mature forest, and the Columbus Day Storm blew down timber equal to 900 sq km (350 sq mi) of mature forest.

Humans clearly have been present in the Ozette basin for at least the last several thousand years. Evidence of human presence on the northwestern Olympic Peninsula is found back to about 3800 ^{14}C years bp in Neah Bay (McMillan 1999), and to at least 2700 years ago at the mouth of the Hoko River (Hutchinson and McMillan 1997). Wray and Anderson (2003) report that ^{14}C-dates indicate human habitation near the mouth of the Ozette River about 3500 ^{14}C years bp, and McMillan (1999) reports evidence of continuous occupation by about 2000 ^{14}C years bp in the Ozette region.

The Makah Village of Ozette, near the mouth of the Ozette River, shows evidence of occupation from about 3500 ^{14}C years bp to the first part of the 20th century. In 1893 the Ozette Reservation was established by Congress to protect the rights of remaining Makah Indians living at the Ozette village. At that time there were 64 Ozette Indians who had not yet relocated to Neah Bay. While there is no evidence for year-round settlements within the basin prior to European settlement, tribal oral history, as well as the character of archaeological sites around Lake Ozette and the Ozette River, indicate that sites within the Ozette basin were occupied at least seasonally (Swindell 1941).

The most obvious extensive pre-European signature on Ozette watershed landscape was the maintenance of a few small prairie areas between Lake Ozette and the Pacific coast. The Makah people regularly burned these prairies to keep forest vegetation from encroaching (Wray and Anderson 2003). This was a common practice among tribes in the region. The practice both facilitated harvest of cranberries, camas and fern and created forage for game. It was widely reported by early settlers to the region, and remains well known in oral regional history (Riley 1968).

European settlers began moving into the Ozette basin shortly after the 1855 Treaty of Neah Bay was signed with the Makah. From the 1850s to the 1890s, the Makah population in the Ozette watershed steadily declined as the population of homesteaders increased. The Ozette village was largely deserted by the early 1900s, as the Makah Agency's Indian Agents forced children from the Ozette village to relocate to Neah Bay for boarding school (Riley 1968). By 1915, the Office of Indian Affairs listed 15 adults (8 men, 7 women) as the only population of the Ozette Village (Sells 1915).

Residential and non-industrial agricultural development in the watershed has been confined to the low elevation, low relief bottomlands along Big River, following the county road to Lake Ozette, and to the shore of the lake. Homesteading in the Ozette basin as a whole reached a peak in the late 1800s. Government Land Office (GLO) surveys conducted from 1892 to 1897 identified 39 homesteads around the lake, and another 26 throughout the watershed, 8 of which were in the bottomlands along Big River. The 1935 USGS map shows only 10 buildings around the lake, and another 32 homes and other buildings along Big River, with about 116 ha (288 acres) of cleared land (USGS 1935). USGS maps in 1956 show 11 buildings near the lake and 19 buildings with 485 acres of cleared land along Big River (USGS 1956). In 1984, USGS maps record 21 buildings around the lake, and 34 homes with 176 acres of cleared land along Big River (USGS 1984). As of 2006, there are 15 buildings on private in-holdings around the lake, and another five comprising the Olympic National Park facilities at the lake outlet. Along Big River, there are 62 houses and other buildings, and about 245 acres of cleared land (Haggerty et al 2008).

The legislative history of the basin plays a role in both the lack of settlement and the development of industrial forestry in Ozette. President Grover Cleveland created the Olympic Forest Reserve by Executive Order in February 22, 1897 (Gannett 1897), closing the area to further settlement. Many discouraged settlers moved away, and by the time land was reopened to settlement in 1907, timber companies rapidly consolidated their holdings in the area, and little further settlement occurred. The area west of the lake was acquired by the 1939 Public Works Program, and transferred to the Olympic National Park by President Harry S. Truman by Presidential Proclamation on January 6, 1953. A thin buffer along the eastern shoreline of Lake Ozette was added to the park under Public Law 94-578, on October 21, 1976, and the surface of Lake Ozette and the Ozette River were added to the park in Public Law 99-635 on November 7, 1986.

With the exception of the development of industrial forestry, little change in agricultural land development in the Ozette basin has occurred since the early 20th century. East of the coastal strip, industrial logging began in the 1930s. Logging accelerated through the latter half of the 20^{th} century, reaching a peak in the 1970s and 1980s. By the 1990s, virtually all of the private timberlands in the Ozette basin had been harvested, and the second cut had begun.

2 METHODS

2.1 Shoreline and watershed land use history

Data acquisition

Data sources were compiled from existing historic information, and attempts were made to locate and digitally archive all available imagery for the Ozette Basin (Table 1). Rayonier Timber Operating Company (Rayonier) was particularly helpful in this regard. Their Forks office provided access to ten-inch 1:12,000 scale aerial photos ("resource photos") from 1953, 1964, 1971, 1977, and 1985. Over 1,100 aerial photos were scanned in 16-bit grayscale at 400 dpi (about 0.75 m pixel size) for this project using a large-format Microtek Scanmaker 6400XL scanner. Portions of the 1953 and 1971 aerial photos containing shoreline areas of the lake were also scanned at 2,400 dpi, 16-bit grayscale, using an EPSON Perfection 3200 scanner (about 0.1 m pixel size). Entire photos could not be scanned due to scanner (and file) size. USGS maps from 1935 and 1956 were scanned by the University of Washington Map Collections staff at 300 dpi. Government Land Office maps were acquired from a digital collection at the University of Washington Map Library.

Georeferencing

Aerial photographs were initially ortho-rectified using ERDAS IMAGINE OrthoBase software at 2' pixel size. Camera information was not available. However the approximate flight height and the camera focal length were recorded at the top of each photograph for the first and last photos in each flight line. Washington State DNR black & white 3' pixel digital orthophotos were used for horizontal reference, and a 10m USGS DEM as vertical reference. The resulting digital photos were of sufficient quality to perform a preliminary shoreline analysis. Because of a lack of complete high-resolution scans, incomplete camera data, poor DEM quality, and software performance issues, ERDAS software was only used to rectify a partial coverage for 1953.

All other aerial photographs were rectified using the georeferencing tool in ArcMap. Ten (10) to twenty (20) control points were located in each photo, and transformations were performed using a first-order polynomial transform, except in a few cases where aerial photos spanned significant elevation changes. In these cases, 2nd order transformations were used when the RMSE of the control points could be significantly reduced, and no appreciable losses of accuracy occurred. Visual assessments of the offset of forest roads in old aerial photos from roads on existing orthophotos were the primary aide in assessing accuracy in these cases.

Existing resource aerial photographs were georeferenced to 2000 and 1994 orthophotos for the Ozette watershed land use analysis and the Umbrella sub-basin analysis. Resource aerial photographs were georeferenced to 2003 orthophotos (the highest resolution shoreline data available) for the shoreline analysis. GLO maps were georeferenced to digitized, georeferenced 1984 USGS 1:24,000 maps (USGS 1994) using section corners. USGS maps from 1935 and 1956 were georeferenced to the 1984 UGSG maps using section corners and horizontal control points which were shown on both maps.

All spatial analysis of land use was performed using ArcMap Geographic Information System (GIS) software, published by Environmental Systems Research Institute, Inc. (ESRI). Versions 9.0-9.2 of the software were used for this project.

Table 1. Map, satellite, and aerial photograph imagery used for shoreline analysis and catchment land use history.

Year	Description	Lake Shoreline	Ozette Basin	Umbrella Catchment
1888-9	GLO Survey Map		**X**	**X**
1935	USGS 1:24K Map		**X**	**X**
1953	Rayonier 1:12K photo	**X**	**X**	**X**
1956	USGS 1:24K Map		**X**	**X**
1964	ONP 1:12K photo	**X**	**X**	**X**
1971	Rayonier 1:12K photo	**X**	**X**	**X**
1976	LANDSAT MSS		**X**	
1977	Rayonier 1:12K photo	**X**		**X**
1979	LANDSAT MSS		**X**	
1983	LANDSAT MSS		**X**	
1984	USGS 1:24K Map		**X**	
1985	Rayonier 1:12K photo	**X**		**X**
1988	LANDSAT TM		**X**	
1994	DNR B/W orthophoto	**X**	**X**	**X**
2000	DNR B/W orthophoto	**X**	**X**	**X**
2003	Makah color orthophoto	**X**		**X**
2006	NAIP color orthophoto	**X**	**X**	**X**

2.1.1 Shoreline analysis

A preliminary qualitative comparison of shoreline morphology and vegetation density on the shore of Lake Ozette was completed by comparing ortho-rectified aerial photos from 1953 with 2003 orthophotos. The purpose of this analysis was to determine whether detectable change in the unvegetated shoreline area had occurred. This in turn would determine whether a more detailed analysis of shoreline vegetation and morphological changes was warranted.

Because the results of the preliminary study indicated that significant changes in shoreline vegetation had occurred, a quantitative shoreline assessment was carried out which compared high-resolution scans of 1953 aerial photos to the 2003 orthophotos to better understand the magnitude and spatial distribution of changes in shoreline morphology and vegetation cover. The quantitative analysis was designed around the hypothesis that there has been a decrease in unvegetated beach area (an increase in vegetation around the shoreline of Lake Ozette).

In addition to the high-resolution analysis, a time-series analysis of changes in shoreline morphology at the Umbrella Creek delta was performed using aerial photos from 1953, 1964, 1971, 1977, and 1985, as well as orthophotos from 1994, 2000, 2003, and 2006. For the delta

analysis, all aerial photos were carefully georeferenced to the 2003 orthophotos using the same control points for each year.

2.1.1.1 Preliminary shoreline analysis

A detailed shore outline was produced from the 2003 photos. This layer was hand-drawn as an overlay on the 2003 aerial photos at a scale of 1:500 or larger (better). For areas where the shoreline could not be resolved in the 2003 dataset, no line segment was created. The resulting outline was used to generate line segments for the preliminary analysis. Aerial photos from 1953 were compared with 1994, 2000, 2003 orthophotos. Variations in illumination, glare, shadow, and camera angle made it useful to refer to two modern photosets rather than a single set when comparing with the 1953 photos. No significant differences were noted between the modern photo sets; however they were not specifically compared with each other.

The shore outline was segmented where significant qualitative changes occurred in the relative character of the 1953 and 2000/2003 photoset. Areas where large, obvious relative change occurred in a short distance were used to break segments. In all cases, deposition, erosion, or no change was noted as a segment attribute. In many areas of the modern vegetated shoreline, it appeared that slight overall shoreline deposition (progradation into the lake) occurred. This was not used to break analysis segments, and is not captured by the analysis. The following general methods were practiced during preliminary shoreline analysis:

For each portion of the shoreline, the 1953 photoset was compared with the 2000 photoset. If photo quality in the 2000 ortho was insufficient (due to sun glare or shade), either the 1994 ortho or the 2003 color ortho was used. In most cases, the 2000 or 2003 orthophotos were sufficient to determine whether obvious change had occurred. Only in a few cases where glare or shadow obscured both the 2000 and the 2003 orthophotos were the 1994 orthophotos used.

Analysis consisted of two distinct variables: shoreline sediment dynamics and shoreline vegetation. These variables are represented in two separate columns in the dataset. For the shoreline sediment dynamics variable, the allowed values were: no change, erosion, deposition, unknown, and null value (not analyzed). For the shoreline vegetation variable, the allowed values were: no change, increase, decrease, unknown, and null value (not analyzed).

Where significant sediment deposition or erosion was detected, nearby features were evaluated to determine if there were errors in ortho-rectification. If errors in ortho-rectification appeared to be on the same order as shoreline changes, no value (null value) was entered for that segment. If ortho-rectification errors appeared minimal, the area where change occurred was noted. If an area was obstructed from viewing, “unknown” was entered as a value.

Vegetation detection was based on vegetation patterns and shoreline brightness. Because of glare and poor resolution in some 2000 and 1953 orthophotos, high-resolution, unrectified scans of the 1953 photos, and high resolution 2003 color orthophotos were referred to where there was uncertainty in image interpretation. This was particularly true for beaches with high glare (image saturation), areas of shadow, and narrow, steep beaches where vegetation change was difficult to detect. If there was uncertainty, “no change” was recorded. If the image could not be resolved,

"unknown" was entered for the segment. If the image could not be interpreted due to rectification error, the field was left blank (null value). When significant erosion or deposition was encountered, "no change" was entered for the vegetation field if the character of the shoreline vegetation remained the same, even though the vegetation occupied additional area. If the character of vegetation in an erosion or deposition segment changed, the appropriate value was entered in the vegetation field.

2.1.1.2 Quantitative Shoreline Analysis

Detailed quantitative shoreline analysis was performed using high-resolution scanned images (0.1 m pixel size, 2400 dpi) from 1953, and comparing these images with high-resolution orthophotos (1 ft pixel size). For this analysis, 1953 aerial photos were georeferenced to the 2003 aerial photos using boulders along the shoreline of the lake, road intersections, and trees which had clearly remained stationary from 1953 to 2003 as control points in the 1953 photos. Polynomial transformations were limited to first-order polynomial, since the shoreline (water surface) is basically flat. This assured that beach area measured in the 1953 photos would accurately compare to that of the 2003 photos.

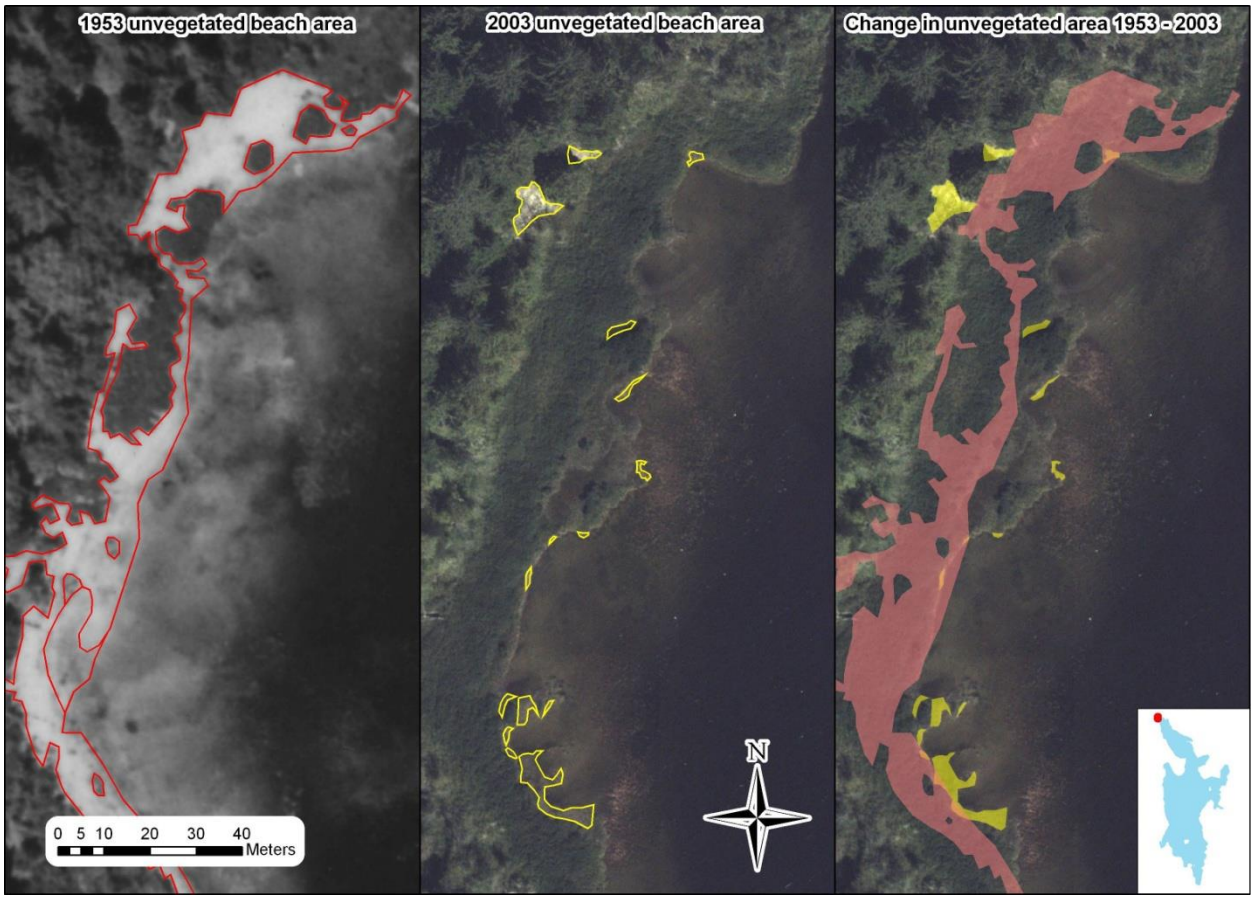

Figure 3. Lake Ozette shoreline directly SW of the Ozette River outlet, in 1953 and 2003.

After georeferencing the 1953 aerial photos, ArcMap was used to delineate polygons around all areas of unvegetated beach in both the 1953 and the 2003 photosets at a scale of 1:300 or larger (better). This resulted in a high-resolution coverage of historic (1953) beach area, as well as beach area in 2003, and enabled comparison of the area of unvegetated beach per unit length of shoreline between the 1953 and 2003 photo sets (Figure 3).

The area of vegetated beach was not delineated, since the transition from beach to upland vegetation is not clear due to overhead foliage. A necessary assumption of this method is that the area of overhanging foliage obscured roughly the same portion of beach in 2003 as in 1953. In areas where either the 2003 or the 1953 coverage of the shoreline was obscured due to shadow, no polygons were delineated for either year. In this way, bias due to difference in sun angle was eliminated.

The main difficulties in this exercise were related to photo quality, lighting, and the difference between color and black & white photos. For example, the color photos showed three primary types of beach cover – light brown or white for sand, brown/gray for mud, dark (or wet) rock, or brown vegetation, and green, where there was green vegetation. The black and white photos showed various shades of gray. I resolved this in several ways. First, since the study is designed around the hypothesis that there has been a decrease in unvegetated beach, I biased myself to delineate the brown areas on the 2003 photos as unvegetated beach unless it was clearly vegetation. I also avoided delineating medium-gray areas of the 1953 photos as unvegetated if there were no other indicators (such as shadows or texture) that indicated they were unvegetated. In addition, where the color photos were brown, I avoided delineating bare ground on either black & white or color photo, unless there were other indicators on both photo sets that allowed me to be confident in my judgment.

Figure 3 shows a typical area of significant change.

After unvegetated shoreline area was delineated for both photosets, the data were analyzed by change in area per length of shoreline. The Washington State Department of Ecology shoreline GIS coverage for Lake Ozette was used for this portion of the analysis. The shoreline coverage was segmented into 500 m sections (a total of 96 segments), and a 150 m buffer was applied on the shore-side of each segment. The buffer layer was edited to remove overlap and other artifacts, and the length of shoreline within each buffer was calculated (this was necessary since some convoluted shore features resulted in more than 500 m of shore per buffer segment, and because the shore length is not evenly divisible by 500 m). Both the 1953 and 2003 beach polygon coverages were then intersected with the buffer segment coverage, and the area of unvegetated beach in 1953 and 2003, and difference between photo years, was calculated for each segment. All results were then calculated in units of square meters per 100 meters of shoreline, normalizing results by shoreline length.

2.1.1.3 Umbrella Creek Delta Analysis

An analysis of changes in Umbrella Creek delta was performed using aerial photography from 1:12,000 photos of the shoreline from 1953, 1964, 1971, 1977, 1985, 1994, 2000, and 2006. For horizontal control, rocks, stumps, roads, and logs were identified from high-resolution scans of

the 1953 photos which had remained stationary in the 2003 orthophotos. Shoreline boulders were used to georeference the photos initially, then roads, stumps, and downed trees were compared between the 1953 and the 2003 coverages, and added as georeferencing control points where it was clear they had not moved. The same control points identified in the 1953 photos were used for the 1964, 1971, 1977, and 1985 photos. For 1994, 2000, 2003, and 2006, the photos were previously orthorectified, and no adjustments were made. Table 3 lists aerial photographs used in this analysis, along with their acquisition dates.

Table 2. Acquisition dates and sources of aerial photography for Umbrella Creek delta analysis.

Year	Date	Photograph
1953	Jul 16 1953	CL 5-11 and CL 5-10
1964	May 15 1964	OLY 64 6-25
1971	Jul 17 1971	OLY 379-7-28
1977	Aug 09 1977	OL-77 7B-20
1985	Jul 02 1985	OL-85 29-007-198
1994	Jul 10 1994	WADNR ORTHO T30NR15W
2000	Aug 28 2000	WADNR ORTHOT30NR15W
2003	Sep 07 2003	MAKAH ORTHO h,i,j 7-11
2006	Jun 24 2006	NAIP Clallam County

Following georeferencing, shorelines were drawn delineating the interface between the shore and the lake for each photo-year. Polygons were then created by intersecting a shape drawn perpendicular to the shore with the shorelines. Two polygons were created, one (delta) which extended about a km from the Umbrella Creek mouth to the north, and about 350 m to the southeast, and a second (proximal delta) which was a subset of the first, extending about 350 m in both directions (Figure 4). Polygon edges (perpendicular to shoreline) were chosen where the shoreline had exhibited little accretion or erosion from photo-year to photo-year.

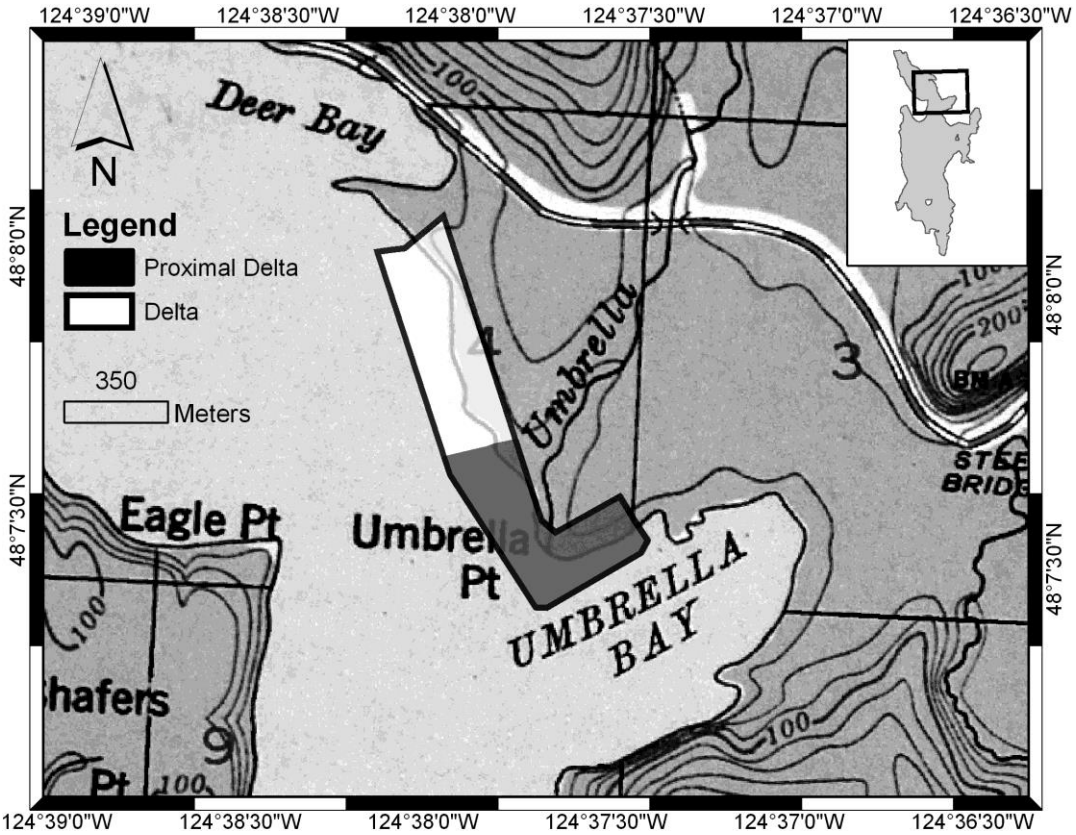

Figure 4: Umbrella Creek delta analysis polygons.

Since each shore polygon had the same landward boundary, any differences in polygon area were changes in the lakeward area of the delta. This allowed temporal comparison of relative delta area between photo-years. To compare delta area between years, the area of each shoreline polygon was calculated within ArcMap, and the area of the initial polygon (from the 1953 photos) was subtracted.

2.1.2 Watershed Land-use Analysis

Land cover and road density were mapped for the Ozette catchment from GLO maps, USGS maps, aerial photography, and satellite imagery (Table 1). One analysis was performed for the Ozette Watershed and sub-basins using available coverages for the entire watershed, and a second, slightly higher-resolution analysis was performed on the Umbrella Creek sub-basin (Figure 1), in part to compare sub-basin changes to changes on Umbrella Creek delta.

Because cleared area was not reliably indicated on GLO maps or USGS maps, these data sources were not used in the quantitative analysis, although clearing polygons and homestead points were digitized for reference.

2.1.2.1 Ozette Watershed land use analysis

For each image-year from 1953 to 2006, the area harvested was delineated for clear-cut and road right-of-way (ROW) harvests. While early harvests (1953 and to a lesser extent 1964) sometimes

had areas of selective harvest, where some trees were left standing, these areas were not differentiated from clear-cut harvest. Areas where substantial trees were left standing were not marked as clearcut polygons. Each polygon was given a year attribute for image-year showing harvest, image source, and notes, where the type of harvest was described.

Total road length was also delineated for each image-year from 1953 to 2006. As with the harvest layer, each road length was assigned a year-built, an image source, and a category for notes. In addition, the 1984 USGS map was used to verify and digitize some roads that could be seen but not accurately resolved on the 1979 and 1983 Landsat MSS imagery. Change in area harvested and road length over time was then calculated using ArcMap and summarized with Microsoft Excel.

Both cumulative timber harvest and remaining primary forest through time were evaluated. Cumulative harvest was simply calculated as the sum of the area harvested in each photo year. Remaining primary forest through time was quantified by clipping the total watershed area with successive years of harvest data. Polygons less than 500 sq. m. in area were removed to minimize artifacts of harvest unit boundary alignment errors.

2.1.2.2 Umbrella Creek detailed sub-basin land use analysis

Delta area for Umbrella Creek could only be accurately calculated using aerial imagery, since available satellite imagery resolution is too coarse. Two photo-years (1977 and 1985) were used in the delta analysis that were not used in the Ozette Basin analysis. These photos had largely complete coverage of the Umbrella Creek catchment, but only partial coverage of the Ozette Basin.

Because dates were offset between the satellite imagery (1979, 1983, 1988) and the aerial photographs (1977 and 1985), it was determined that a more meaningful comparison between land use and delta change in Umbrella Creek could be performed if the same photo-years used in the delta analysis were used to analyze the Umbrella Creek catchment A detailed analysis was performed in the Umbrella Creek catchment in order to facilitate comparison of delta land use with changes in the morphology of Umbrella Creek delta.

Road length and clear-cut area were delineated for each photo-year in the Umbrella Creek catchment. In the few locations where aerial photos were missing, USGS index photos were georeferenced and used to identify and delineate harvest units and roads. A portion of road in the area not covered by the 1985 aerial photos was delineated from the 1984 USGS map. Total road lengths constructed, and area clearcut between each photo year were calculated.

2.2 Sediment Accumulation History

Reconnaissance data were analyzed to select sites likely to produce a continuous record in sediment cores. A sediment coring platform was constructed to enable collection of sediment cores from depths up to 100 m in Lake Ozette. Based on the reconnaissance data, a first round of cores were collected from flat-lying sediment in the main depositional basins in the lake. Following this analysis, a second round of cores was collected in shallower water near tributary

mouths of the major tributaries to target areas of more rapid sediment accumulation and improve temporal resolution over the duration of the targeted time period.

2.2.1 Reconnaissance surveys

In order to construct a sediment accumulation history, the nature of the lake bed and sediment were evaluated prior to selecting locations to extract sediment cores. Reconnaissance surveys, consisting of grab sampling and seismic profiling, were conducted in July and September, 2005.

2.2.1.1 Sediment grab-sampling

Grab sampling was conducted at 27 locations around Lake Ozette in July 2005, using a .025 m^2 stainless steel Van Veen sampler, deployed from a small boat with a hand line. The goal of grab sampling was to determine grain size distribution by depth (essentially to determine the depth of wave-base at the lake), and to determine the consistency of lake sediments before finalizing coring plans. Grab samples are stored at the School of Oceanography at the University of Washington. Sample locations are shown on Figure 5.

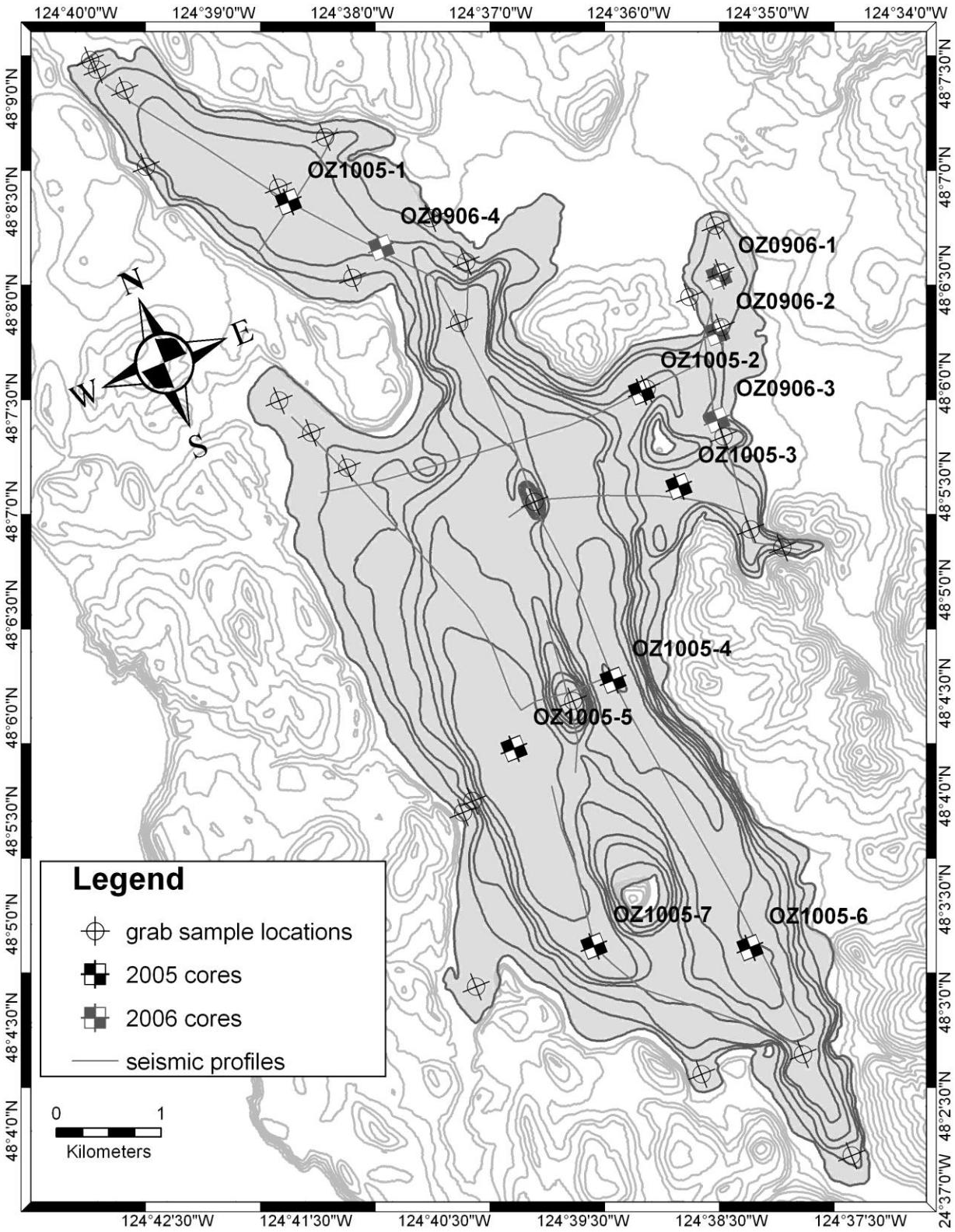

Figure 5: Seismic profile, grab sample, and Kasten core locations from 2005 and 2006 Ozette field seasons. Elevation and depth contours are 40 ft intervals due to source data limitations.

2.2.1.2 Seismic profiling

The objective of the seismic survey was to identify flat-lying sediment, and to learn more about sediment structure and bottom character in Lake Ozette. Seismic profiles were collected on 7-8 September 2005 (Figure 5). The survey was conducted from a 14' Arima, using a Uniboom power supply (EG & G 230-1) operating at 300 J, powering a Uniboom transducer mounted on a kneeboard for flotation and stability, while increasing portability over the standard Uniboom sled, an EPC 3200 analog data recorder, a 100 element hydrophone streamer, and a Kronheit signal processor w/ center frequency set to 900 Hz and bandwidth of 1 kHz.

The seismic profiles represent transects across at least one axis of the major basins in the lake. Approximately 33.2 km of profile data were collected (Figure 5). An unresolved source of electronic interference significantly degraded data resolution. The original analog data were very noisy, with vertical stripes at high densities throughout the entire dataset (Figure 6). This made it difficult and distracting when attempting to interpret the data. Substantial post-processing was necessary to make the data usable.

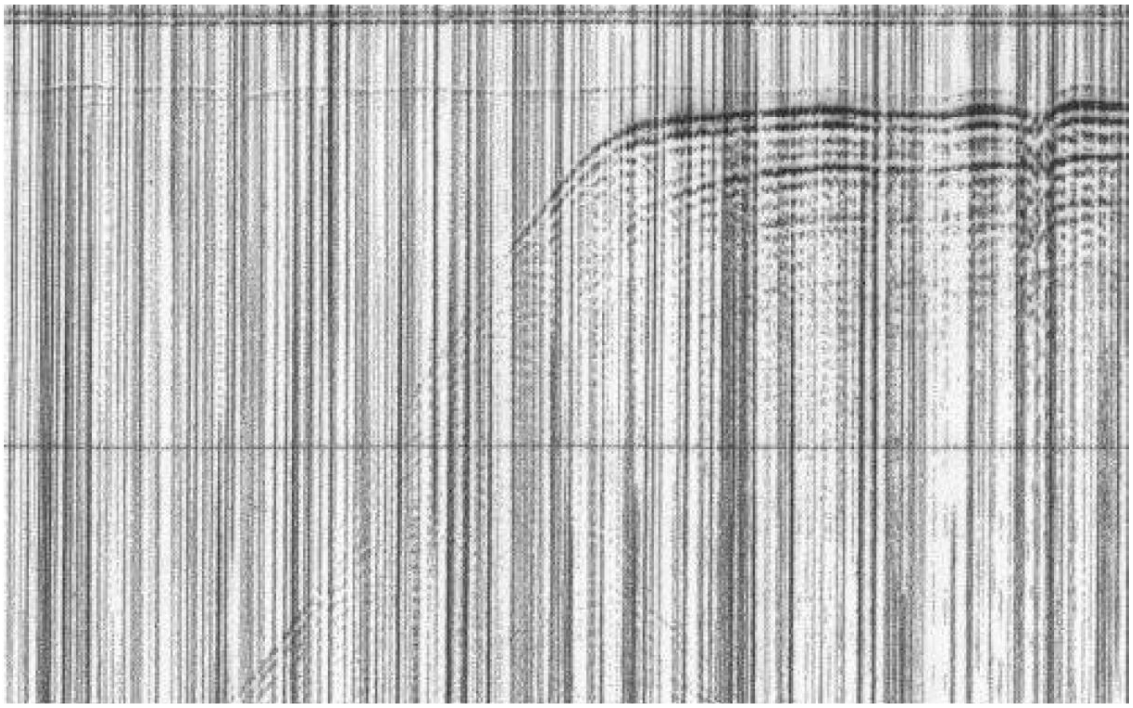

Figure 6: A portion of original seismic data, scanned at 100 dpi. Vertical stripes are noise. Seismic data were post-processed by cutting the chart roll into sections so each survey transect was a separate chart. Each chart was scanned at 100 dpi, 8-bit grayscale, at the University of Washington Engineering Services office Facilities Records unit. Image files were processed using the open-source GNU Image Manipulation Program (GIMP) . A Fast Fourier Transform (FFT) was performed on each image, using a FFT plug-in for GIMP authored by Rémi Peyronnet. This resulted in an image in "frequency space" (Figure 7) which showed strong contrast in a horizontal line in the center of the image, corresponding to vertical noise in the original data. I selected the 30-50 center rows of the image, the rows with noticeably higher

contrast, and 5-10 rows above and below the high contrast region. I then limited the maximum and minimum pixel values in these rows to about 20% of their original range (Figure 7).

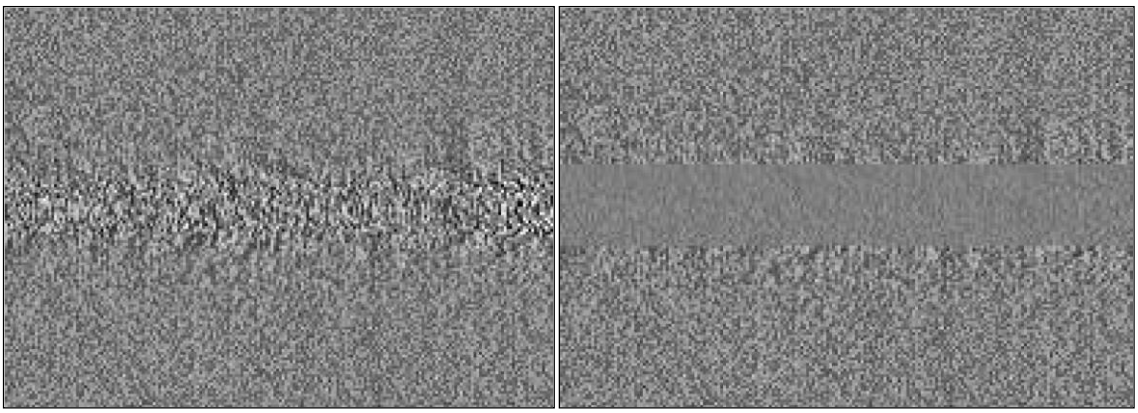

Figure 7: A portion of the center of the FFT of the scanned chart depicted in Figure 9, before (left) and after (right) restricting pixel values in the high contrast region.

After adjusting pixel values, an inverse FFT was performed on the edited image. The resulting image had no noticeable reduction in data quality, since the majority of the information contained in seismic data is vertically discontinuous but horizontally (or near-horizontally) continuous. Vertical noise was substantially reduced by this operation (Figure 8).

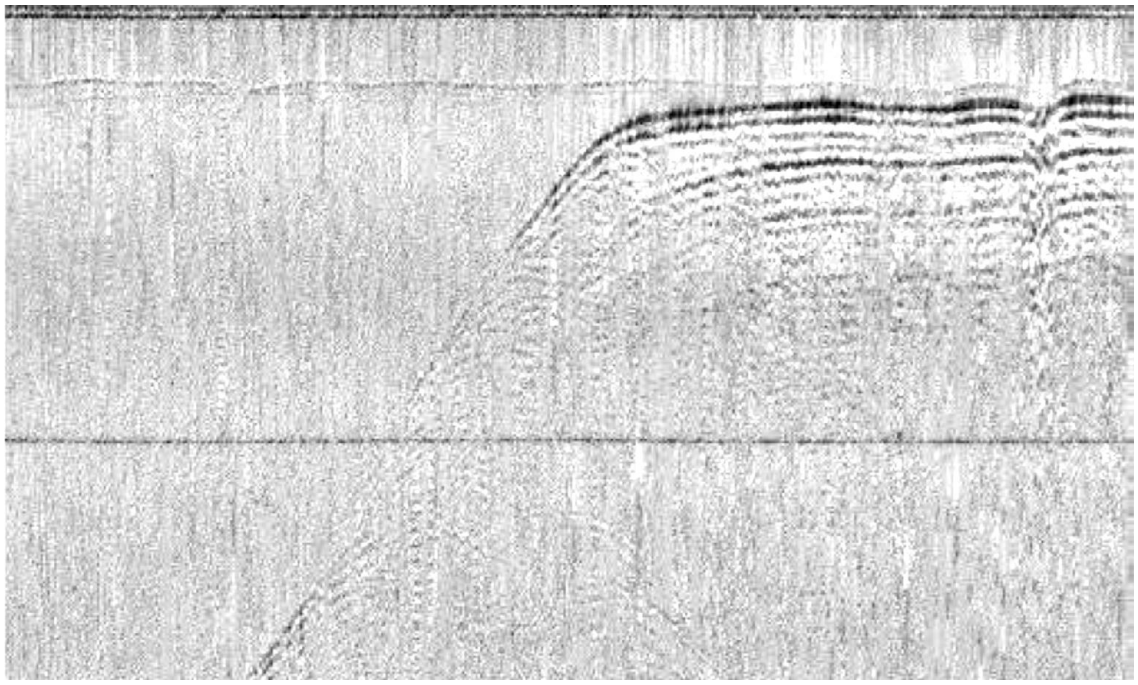

Figure 8: Resulting de-striped image corresponding to the same area as Figure 6.

After de-striping, acoustic profile data were further processed by compressing the horizontal axis using Adobe Photoshop CS2, and resampling the horizontal scale at ¼ the number of original pixels, using a bicubic interpolation algorithm. The reduction in horizontal scale made

identification easier for both primary features such as bedrock, till, and lacustrine surfaces, and secondary features like rotational slumps.

Horizontally and vertically scaled profiles were also created. Print resolution was kept equal to scan resolution of 100dpi for this purpose. Horizontal scale of the profile was calculated between each GPS waypoint by first measuring the actual distance in meters between each GPS waypoint, then measuring the distance between each waypoint in cm on the scanned profiles. This corrects for changes in vessel speed over each transect, improving accuracy of the scaled sub-bottom profiles.

Vertical scaling was calculated based on a sound velocity of 1,420 m/s, and seven uncalibrated depth locations read from an onboard depth-sounder and recorded periodically on the acoustic charts. Two depth locations were used to calibrate sound velocity, because both had relatively flat bottoms. Based on sound velocity calculations, the vertical scale is 7.27 m/cm. Based on the seven depth measurements, the scale is 7.26 m/cm. The 7.27 number was used because of uncertainty surrounding the actual location of other points, because of the steepness of slope where the measure was taken. The ratio of m/cm for each GPS segment of the profile was then divided by four times the vertical scale. This produced a scaling factor by which each segment of the scanned image was adjusted to create a 4x vertically exaggerated image.

Acoustic data are available in Appendix A.

2.2.2 Lake sediment core acquisition

In the summer of 2005, a coring platform was constructed to acquire sediment cores from the 100m deep lake. The coring platform was deployed in 2005 and 2006, and 11 cores were retrieved from depths ranging from 20m to 100m.

2.2.2.1 Coring platform construction

After evaluating available coring equipment and technology, it was determined that Kasten coring was the most feasible way to collect sediment cores from Lake Ozette. Kasten corers collect cores with sufficient sediment quantity and cross-sectional area to minimize deformation, perform X-ray analysis, and subsample for ^{210}Pb, δ^{13}C, and δ^{15}N. These corers are regularly deployed at similar and greater depths for oceanographic research, and several Kasten corers were made available for this research from Dr. Charles Nittrouer at the University of Washington.

These Kasten corers collect cores up to 3m long, in a 13.5 cm square tube with one removable side. The core barrel mounts into a weight stand and is secured with 2 pins. The weight stand is capable of being loaded with up to 500 kg of square lead weights. For this project, 100 kg of added weight were used in 2005, and 150 kg in 2006. together with the weight stand and the core barrel, total Kasten corer weight was approximately 200-250 kg empty. With sediment, corer weight was about 250-300 kg.

Typically, Kasten cores are collected from an A-frame on the back of an oceanographic research vessel. No vessels could be located for this project which had suitable winches or cranes, and could be transported to, and deployed in, Lake Ozette. Therefore, it was determined that the most logical course of action would be to construct a coring barge, consisting of a platform, a tower, and a power winch.

A suitable platform was constructed consisting of four aluminum compartments that bolted together into two 6.3 m pontoons, separated by 2.1 m, and connected with two aluminum braces (Figure 9). The pontoons displaced a total of 4.43 m^3 of water. Total platform weight was under 400kg. For buoyancy calculations, total excess buoyancy was estimated at 4,000 kg.

Figure 9. Coring platform constructed to collect sediment cores from Lake Ozette.

A tower was designed and constructed to allow sufficient clearance for the core barrel when attached to the weight stand, and provide sufficient strength to avoid risk of buckling. The tower was designed to withstand at least 4,000 kg of stress. The tower was constructed of standard 1-1/2" steel water pipe, with an outside diameter of 1.9", and a wall thickness of 0.145". cross-braces were added at 1/3 and 2/3 of the tower height (Figure 9). The braces consisted of 3/4" galvanized water pipe, and were fastened with Kee-Klamp® swivel sockets. Tower legs mounted to brackets located in the center of gravity of each of the four compartments. Brackets were

made from ¼" angle-iron, welded to ¼" steel plates, designed to distribute the weight from each leg across the skin of the pontoon. Each plate had a surface area of 0.25m^2. Cross braces constructed from 1-1/2" pipe held each base in position, and a 8" x 2 ½" x 3/8" U-channel spanned the pontoons and provided a mounting base for the winch and hydraulic power-pack. The tower was stress-tested to 2,000 kg using a tensiometer after braces were installed.

A hydraulic winch and powerpack were rented from the University of Washington School of Oceanography pooled equipment. The winch was tested to pull a maximum of 1,000 kg. Total weight of the winch, hydraulic powerpack, and tower was less than 1,000 kg.

2.2.2.2 Sediment core collection

A total of eleven sediment cores were collected from Lake Ozette in 2005 and 2006. Seven sediment cores were collected from Lake Ozette on 22-23 October 2005, and four cores were collected on 10-11 September 2006. The 2006 cores targeted areas closer to tributary mouths, with a goal of targeting areas of more rapid sediment accumulation to improve temporal resolution while maintaining a 2-cm sampling interval in the kasten cores. GPS locations were chosen based on a combination of lake bathymetry data and seismic data. GPS positions for cores are shown in Figure 5.

The Kasten corer was deployed with 100 kg of weight in 2005, and 150 kg in 2006. The corer was lowered continuously at a velocity (depending on drum diameter with line) of about 0.7 m/s, until slack appeared on the Spectra© line. At this point the winch was slowly played out until the corer stopped sinking into the lakebed. The low elasticity of Spectra© allowed for accurate assessment of when the corer had stopped sinking into the lake bottom. The advantage of this "slow deployment" is that the sediment-water interface is better preserved.

Core retrieval consisted of raising the Kasten core to the coring platform, tilting it to about a 45º angle, and packing the top with foam to prevent displacement of surface sediments. The core was then transferred to a skiff and taken to shore while the platform was towed to the next coring location.

2.2.3 Sediment core processing and storage

Following retrieval of the sediment cores, X-ray trays measuring 30 cm long by 13.5 cm wide by 2.5 cm deep were collected from each core before sub-sampling the core in 2-cm intervals. Two cores from the 2005 trip were not prepared for x-radiograph analysis because there were an insufficient number of x-ray trays available in the field.

Digital X-radiographs were taken of each tray to aid in interpretation of ^{210}Pb and ^{14}C profiles. Sub-samples of 7 cores that showed no indications of post-depositional disturbance were analyzed for ^{210}Pb and ^{14}C in order to constrain sediment accumulation rates. In addition, 8 cores were sub-sampled for stable isotopes of carbon and nitrogen.

2.2.3.1 Lake sediment X-ray analysis

X-ray subsamples were obtained by pushing three-sided Plexiglas x-ray trays into the exposed surface of the cleaned kasten core, inserting vertical steel plates between trays,then inserting the fourth side of each tray working systematically from the top down (Bentley 2003). X-ray trays were brought to the University of Washington and processed using a Kramex portable x-ray unit and digital film. Because the x-ray unit was a point source, rather than a scanning unit, exposure was not constant throughout the slab. This limited x-radiograph interpretation to qualitative parameters such as whether deposition was continuous or showed signs of disturbance. A sample composite (multiple x-ray slabs from a single core) is shown in (Figure 10).

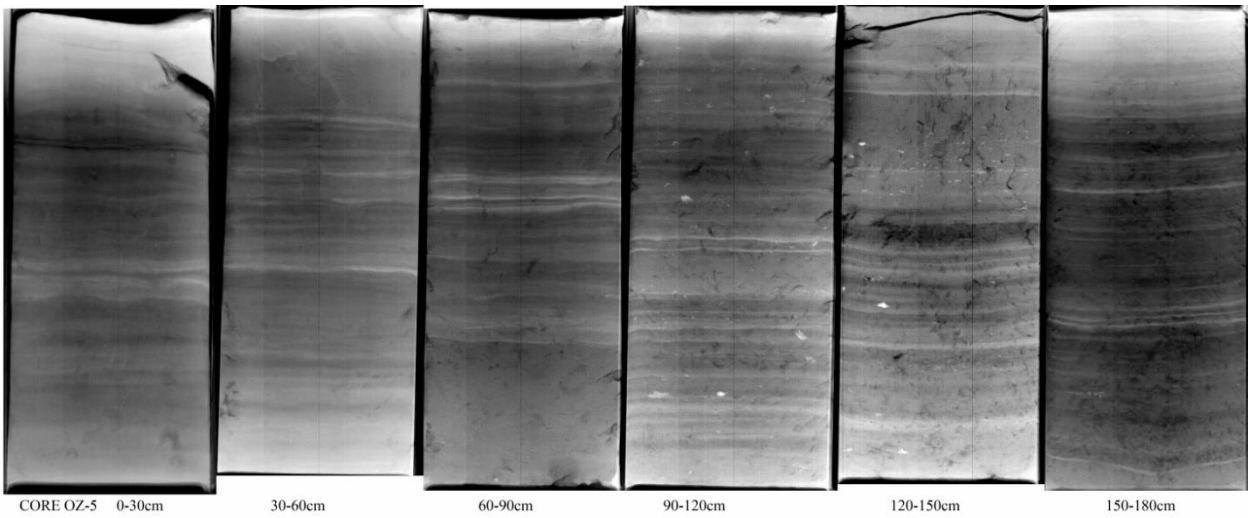

Figure 10. Composite X-ray negative of core OZ1005-5. Each column is one 30 cm X-ray tray. Light laminae represent more dense, X-ray opaque sediment. Bright specks below 90 cm are crystals of the mineral vivianite.
X-radiograph negatives are included in Appendix B.

2.2.3.2 Lake sediment radioisotope analysis

2.2.3.2.1 *210-Pb analysis for short-term accumulation rates*

The radioisotope ^{210}Pb is an alpha particle emitter with a half-life ($t^{1/2}$) of 22.3 years. The use of ^{210}Pb as a sediment accumulation rate tracer has been well established in the earth and ocean sciences (Nittrouer et al 1979, Appleby et al 1986, Aalto et al 2005). ^{210}Pb is produced through the ^{238}U decay series. It forms naturally in rocks and sediment as a result of ^{238}U decay, as well as in the atmosphere, as a result of the decay of ^{222}Ra. When formed *in situ* from the decay of parent elements, ^{210}Pb activity is *supported*, and will be in secular equilibrium with ^{226}Ra. When formed in the atmosphere from the decay of ^{222}Ra, ^{210}Pb falls out of the atmosphere onto the earth surface. This added concentration of ^{210}Pb is termed *excess* activity. After burial of surface sediment, no additional ^{210}Pb is added, and the excess ^{210}Pb activity will decrease over time until it reaches supported levels.

^{210}Pb is strongly adsorbed to clay particles, and can be introduced to lake basin sediments through tributary streams, or directly by adsorption onto clay particles when they enter the lake through tributary sediment inputs. ^{210}Pb activity varies as a function of particle size and geographic location, but atmospheric inputs are generally considered to be constant for a specific location.

^{210}Pb analysis of Ozette lake sediments was performed at the University of Washington using lab facilities and methodology developed by Dr. Charles Nittrouer (Nittrouer et al. 1979) to evaluate sediment accumulation rates on the Washington continental shelf. α-spectroscopy of ^{210}Po, a granddaughter decay product of ^{210}Pb, was used to determine ^{210}Pb activity. Partial digestion of sediment samples was performed using HCl and HNO_3 to extract ^{210}Po, which was analyzed in combination with a known level of ^{209}Po added to the sample, as described in Nittrouer et al. (1979). Excess ^{210}Pb activity was determined by subtracting the mean supported activity from the total activity. Supported activity was determined from the lowest sampled ^{210}Pb values in cores where the ^{210}Pb activity reached a constant value. Where the lowest analyzed intervals did not reach a constant value, supported activity from cores with the most similar mass-depth plots were substituted. Mass accumulation rates are reported in (g/cm^2yr) to eliminate the need to account for the effect of compaction on evaluation of sediment accumulation.

2.2.3.2.2 14-C analysis for long-term accumulation rates

Sub-sampling, pre-treatment, and ^{14}C age measurement.

Core sample intervals were chosen from the middle and bottom of each sediment core collected from Lake Ozette. This enabled comparison between the lower and upper half of each core, and maximized the utility of a limited number of ^{14}C age dates, which are limited by cost. Samples were washed through a 150 micron sieve with de-ionized H_2O. Ephemeral terrestrial macrofossils such as winged seeds, conifer needles, or hardwood leaves were extracted. These fossils are generated over a period of 1 to several years, and decay rapidly in an oxidizing environment, so are the least likely to represent time periods far-removed from their appearance in the sedimentary record. Macrofossils were placed in clean culture tubes rinsed with de-ionized H_2O, and 0.01N HCl was added. Samples were refrigerated in 0.01N HCl until pre-processed for AMS dating with an acid-base-acid treatment (< 72 hrs).

Each sample was pre-treated using an acid-base-acid rinse. Using a new pipette for each sample and each step, the samples underwent a series of washes. First, 0.01N HCl was pipetted off, and tubes were filled with 1N HCl. samples were then heated at 90 C for 15 minutes, and the 1N HCl was pipetted off. Only one HCL rinse was required. Tubes were then filled with 1N KOH and heated at 90 C for 45 minutes. This step was repeated 1-3 times for each sample until the KOH was not significantly discolored. Samples then underwent a final treatment in 1N HCl for 15 minutes at 90 C, and were rinsed twice with de-ionized H_2O before being placed in glass Wheaton scintillation vials with polyethelene screw caps. The vials were filled with 0.01N HCl to prevent biological activity prior to processing. Following pretreatment, samples were sent to the National Ocean Sciences Accelerator Mass Spectrometry Facility (NOSAMS) at Woods Hole Oceanographic Institution for AMS dating. NOSAMS reports uncalibrated ^{14}C ages and

activities following the convention of Stuiver and Polach (1977) and Stuiver (1980). ^{14}C ages were corrected for fractionation using measured $\delta^{13}C$ values, normalized to -25‰.

I converted uncalibrated ^{14}C years reported by NOSAMS to calibrated calendar years before present (Cal BP) using OxCal 4.0 with the IntCal 04 calibration curve (Bronk Ramsey 2001). The relative standard deviation (RSD) for each date was calculated, based on the probability distribution of the calibrated date curve. The RSD is a dimensionless number, useful for determining precision of a measurement. It is defined as the absolute value of the ratio of the standard deviation (σ) to the mean (μ).

I corrected core depths for compaction based on porosity vs. depth as measured in samples taken for ^{210}Pb analysis. Sediment compaction can exhibit a linear trend (Revil et al 1999; Törnqvist et al 2008). Compaction can also be highly nonlinear (Boudreau and Bennett 1999). Since porosity data were limited to samples analyzed for ^{210}Pb, these data were used to determine if a linear or nonlinear regression provided a better fit. Based on samples analyzed for ^{210}Pb in the upper 60 cm of cores, a linear regression of porosity vs. depth was chosen to decompact sediments and calculate accumulation rates based on ^{14}C dates from the midpoint and base of each core (Figure 32). Because 2005 cores and 2006 cores were taken at different depths and distances from sediment sources, two separate regressions were performed, one for each coring year. Equations used to decompact sediment depth intervals are shown in Figure 32.

Long-term accumulation rates were calculated for upper-, lower-, and whole-core intervals. I used decompacted depths: (1) from the surface to midpoint (upper); (2) from the surface to the base (whole); and (3) from the midpoint to the base (lower). The first two calculations derive minimum and maximum accumulation rates (cm/y) from the midpoint and basal ^{14}C dates based on depth of the sample divided by the age range given by the 95.4% (2 σ) probability distribution, as reported by OxCal. The third calculation derives the accumulation rate between the midpoint and basal ^{14}C samples for a given core. The accumulation rate range is calculated by dividing the decompacted interval between ^{14}C dates by the maximum and minimum age range given by the 2 σ probability distribution for each date.

2.2.3.3 Lake sediment stable isotope analysis

Seven cores were analyzed for stable isotopes of carbon and nitrogen. Samples were dried at 50º C for 24 hours, then ground to a fine powder and packaged for shipping to the Cornell University Stable Isotope Laboratory. Samples were weighed and run by Cornell University Stable Isotope Laboratory staff using a Finnigan MAT Delta Plus Isotope Ratio Mass Spectrometer (IRMS).

The depth to sample in each core was determined based on ^{14}C ages with a goal of sampling through approximately the last 500 years. The two cores showing the youngest ^{14}C ages were sampled for their entire length with a goal of reconstructing a high resolution recent stable isotope record for $\delta^{13}C$ and $\delta^{15}N$ from existing cores.

3 RESULTS

3.1 Quantification and description of shoreline and watershed changes

Shoreline and watershed analyses indicate that significant changes in vegetation distribution and shoreline morphology have occurred in the latter half of the 20th century. Preliminary shoreline analysis results indicate that significant changes in both vegetated beach area and shoreline morphology occurred between 1953 and 2003. Changes in vegetated area were notably widespread, occurring throughout the watershed. The Umbrella Creek delta was identified as an area of particular interest, due to significant changes in delta area and morphology, and because it was one of only a few shoreline areas around the lake that did not show in increase in vegetation cover. Based on these results, a quantitative analysis of the change in shoreline unvegetated area was conducted.

The quantitative shoreline analysis found that over half of the area of unvegetated beach identified in 1956 had been lost by 2003. The loss of unvegetated beach was not confined to areas near the main tributaries to the lake. In fact, the only areas showing an increase in unvegetated beach were deltas that showed evidence of rapid aggradation, likely overwhelming vegetation growth. Quantitative analysis of subaerial delta evolution at the mouth of Umbrella Creek found that delta growth peaked in the early 1980s, and continues through the present.

Land use analysis reveals that prior to the 1950s, roughly 90% of the Ozette basin, and more than 85% of current private ownership was still mature forest. Industrial timber harvest accelerated rapidly and peaked in the early 1980s. By 1990 only about a quarter of the watershed remained mature forest, most of this being federal trust lands. Mature forest area on private lands and state and federal trust lands has remained largely unchanged since the mid-1990s. Roughly 5% of private lands and 20% of state lands are in mature forest, while Over 90% of federal trust lands are unharvested. A higher resolution study of the Umbrella Creek sub-basin found similar results, but included additional data points by analyzing additional aerial photograph coverage.

3.1.1 Preliminary shoreline analysis

About 50 km of lake shoreline was classified, roughly 88% of the 57 km perimeter. About 45.6 km was suitable for vegetation trend analysis, and 44.8 km was analyzed for deposition and erosion. (Figure 11). The length of shoreline in each category is presented in Table 3.

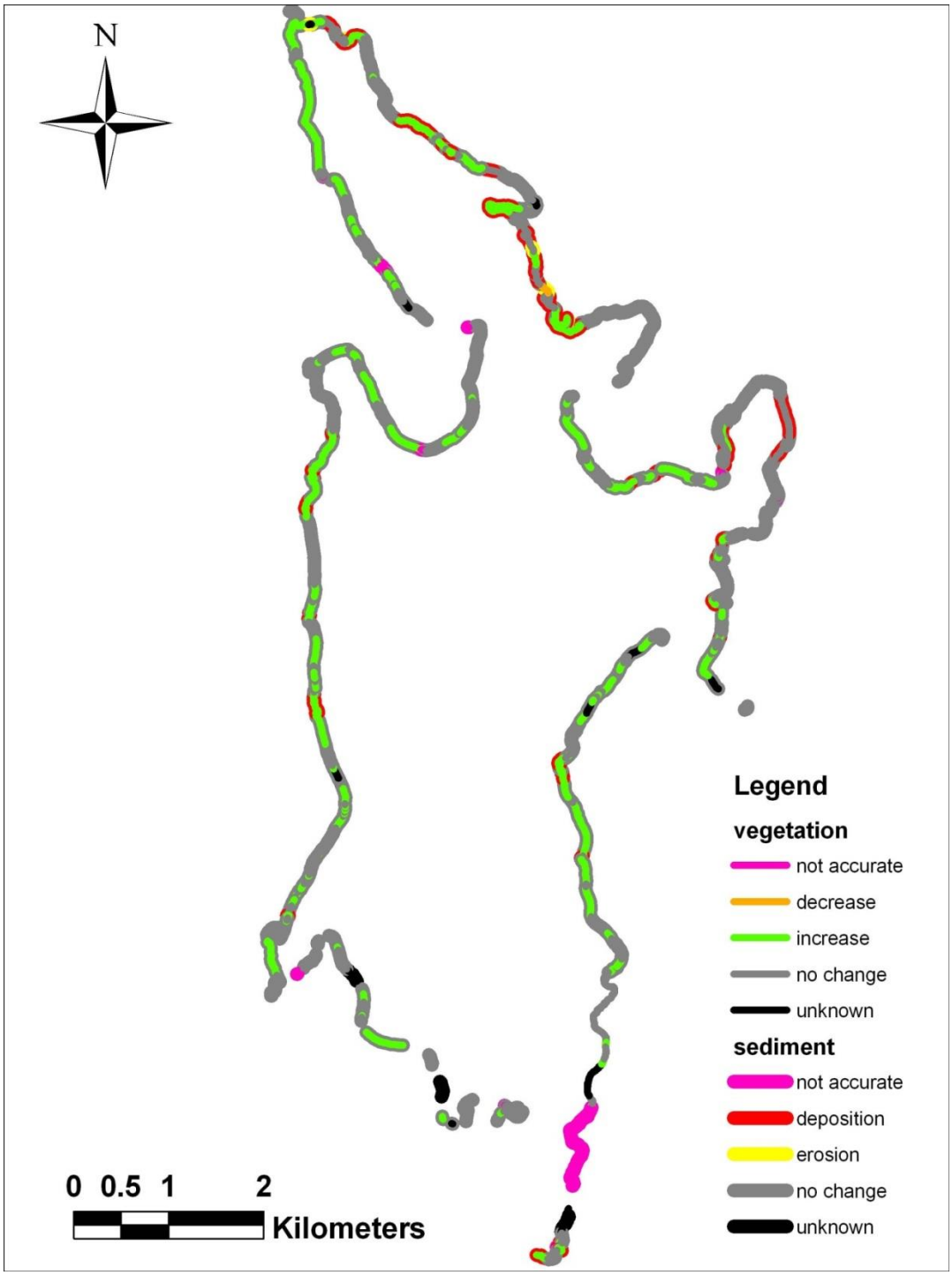

Figure 11. Changes in Lake Ozette vegetation and shoreline from 1953 to 2003.

Table 3. Measured length in each category for vegetation and sediment shoreline variables.

Vegetation	length (m)	**Sediment**	Length (m)
Increase	18,403	Deposition	7,742
Decrease	160	Erosion	373
No change	27,025	No change	36,710

More than 40% of the surveyed shoreline showed evidence of increased plant cover. Even without further map analysis, significant changes are apparent in shoreline vegetation distribution at Lake Ozette. While introduced plant species could cause widespread changes in shoreline plant distribution, it is unlikely in this case. Only minor infestations of *Phalaris arundinacea* (Reed canarygrass) have been observed in the lake itself (Meyer and Brenkman 2001), and the primary species that appears to be increasing its distribution is *Myrica gale* (sweet gale), a submergence-tolerant native species. In most cases, increased vegetative cover appears to have spread from plant communities that were already growing. (Figure 12).

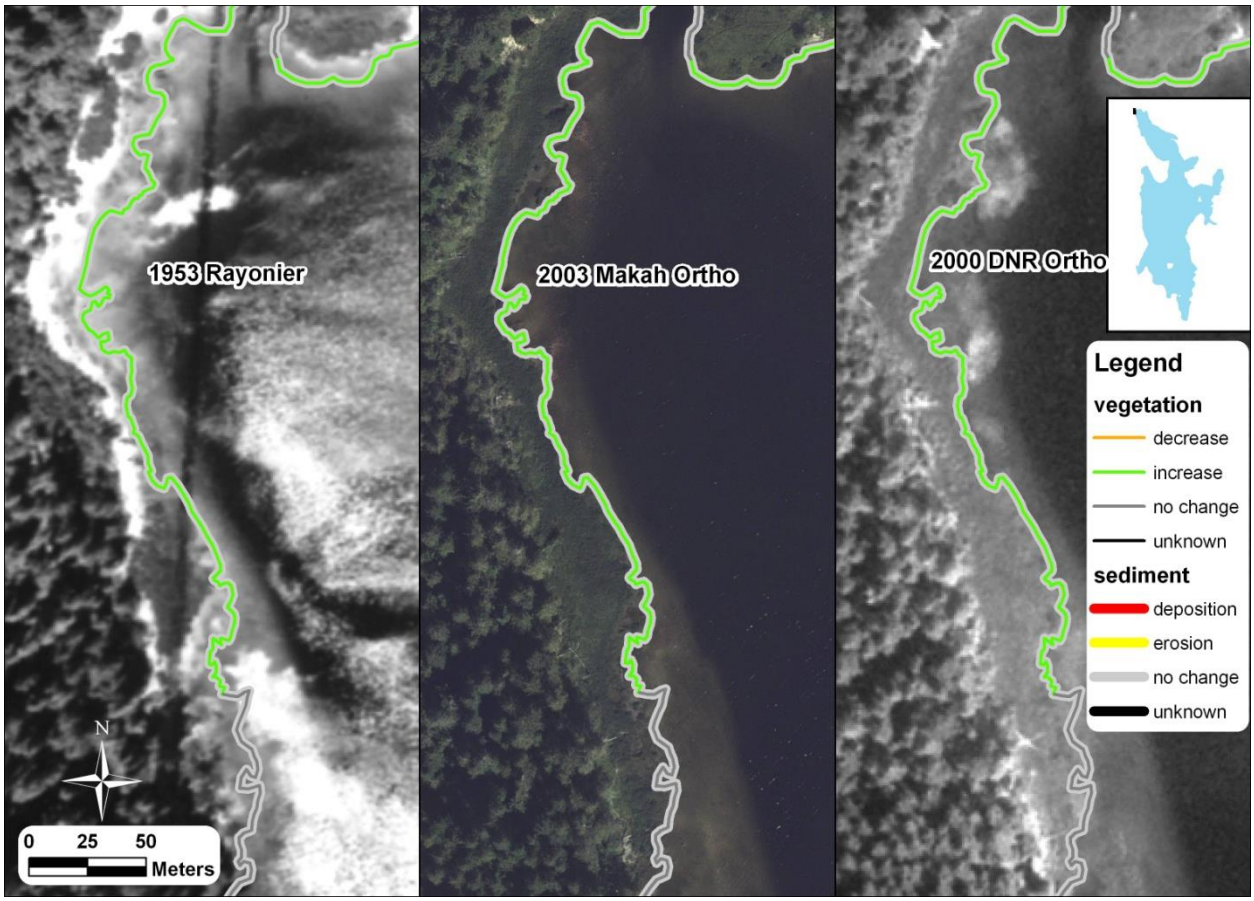

Figure 12. Vegetation changes from 1953-2003 at Lake Ozette at the Ozette River outlet.

Much of the southern shoreline, particularly the southeast shore, was unresolveable due to shadows from trees on the 2003 photo set, which served as a primary tool for this project. At the southeast end of the lake, between the south end of Olsens Bay and South Creek, there is also significant error in the orthorectification of the low-resolution 1953 photographs. This error precluded any analysis of sediment dynamics for this area. Orthorectification errors did not prevent vegetation analysis though, and from those results (no change in vegetation cover), it is reasonable to assume that shoreline change has not been significant in this area. Further analysis of shoreline change in this section of the lake should focus on tributary confluences with the lake, as these are the most dynamic locations, where shoreline change would be expected to occur.

Tributary and Outlet changes:

Some minor changes were evident at the mouths of Elk, Siwash, and South Creek. South Creek, which in 1953 appears to have recently avulsed, has entirely abandoned its old channel by 2003. However, the most obvious geomorphic change in Lake Ozette shoreline from 1953 to 2003 is the evolution of the Umbrella Creek Delta (Figure 13).

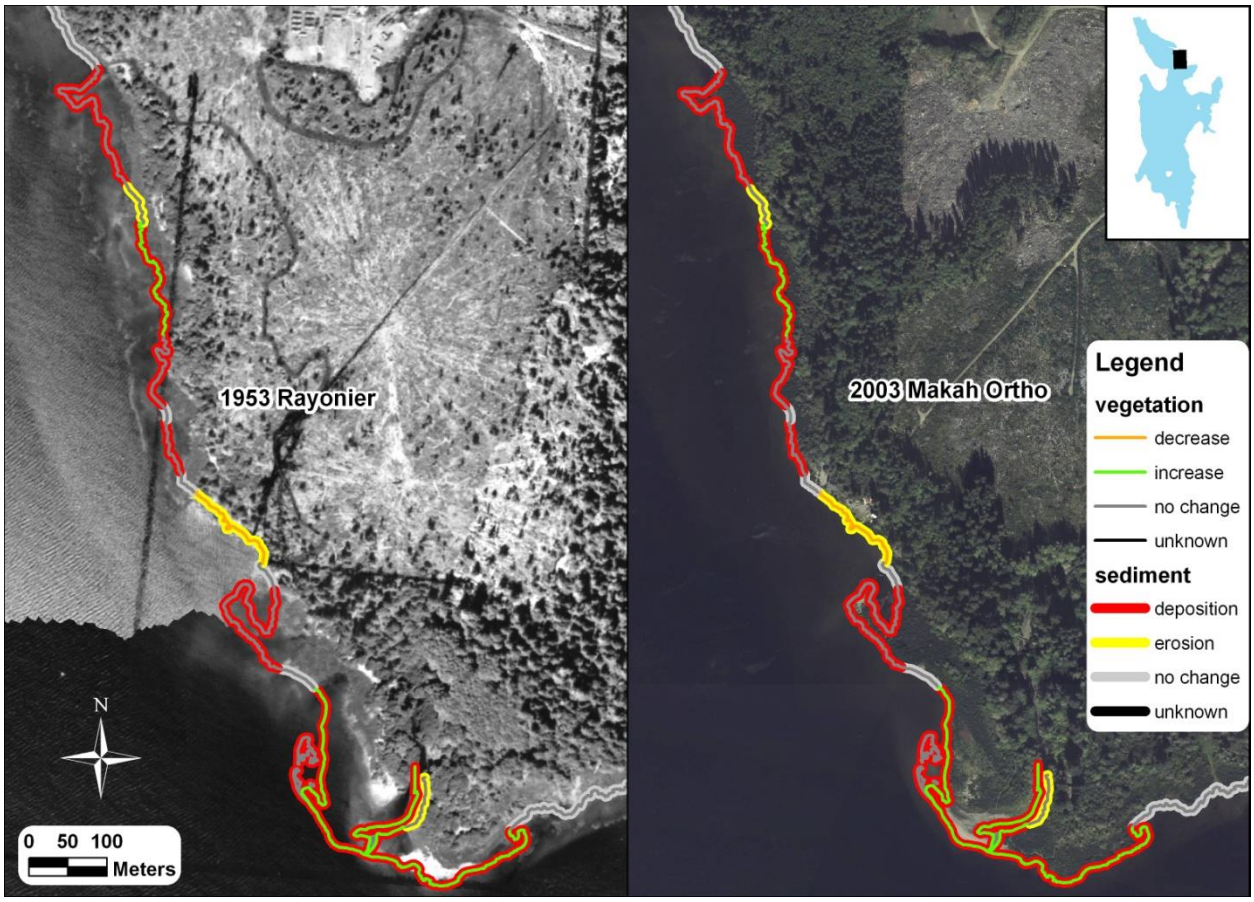

Figure 13. Shoreline changes at the mouth of Umbrella Creek on Lake Ozette.

The shape of spits migrating north along the shoreline clearly indicates sediment transport direction to the north. Note that significant erosion has occurred north of the smaller spit, with additional deposition extending well north, at the top of the right image (Figure 13). Also note that the clear-cuts in both images are recent; timber harvest rotation here appears to be almost exactly fifty years.

With the exception of the Umbrella Creek delta, most depositional features were located in small, shallow embayments. Often the deposition was concurrent with plant colonization, particularly north of Umbrella Creek on the east side of the lake (Figure 13).

3.1.2 Quantitative Shoreline Analysis

Quantitative analysis of unvegetated beach area was performed to determine the magnitude of change illustrated by the preliminary analysis. I measured 96,144 m^2 of unvegetated beach in 1953, and only 41,951 m^2 in 2003, a decrease of 56%. The mean area of unvegetated beach was 200 m^2 per 100m of shoreline in 1953, and only 87 m^2 per 100m in 2003. Both range and variance declined from 1953 to 2003, which implies shoreline vegetation complexity has been reduced at the scale of this analysis, which binned the shoreline into 500 m segments. A histogram of the difference in unvegetated beach area from 1953 to 2003 shows that only three segments showed an increase of >50 m^2 of unvegetated beach per 100m, while many (49) showed a decrease of >50 m^2 unvegetated beach per 100m (Figure 14).

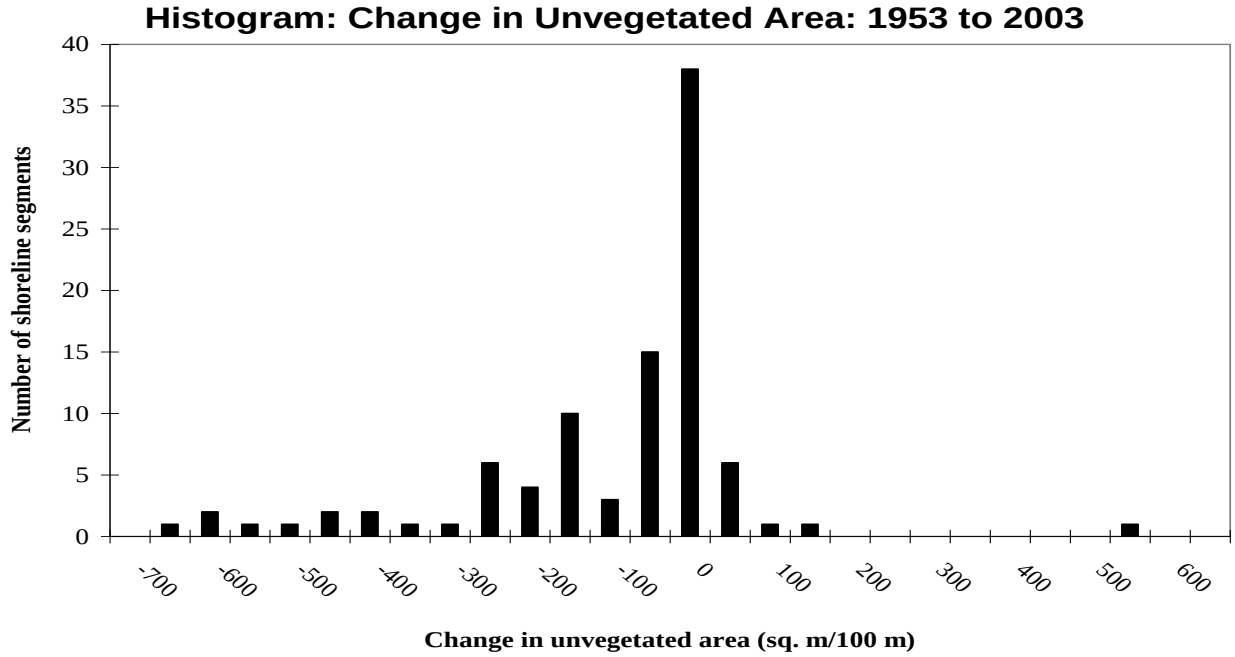

Figure 14. Change in shoreline unvegetated area, binned in intervals of 50m^2 per 100m length of shoreline. Note negative skewness of the distribution.

All three segments showing an increase in unvegetated beach area are located on tributary delta landforms, two on the delta of Umbrella Creek, and the third on the delta of tributary 20.0078, a small, steep stream east of Baby Island. Thus the only areas showing an increase in unvegetated beach appear to be tributary deltas (Figure 15), and the decline in open beach area is well distributed throughout the area where there is (or was) unvegetated beach, rather than concentrated near the tributary mouths and deltas.

The area of unvegetated beach at the two remaining sockeye spawning beaches in Lake Ozette declined slightly more than the lake as a whole during the same period. Unvegetated area at Allen's Beach declined by 67%, from 11,673 m^2 in 1953, to 3,876 m^2 in 2003, over a shoreline length of 2,643 m (Figure 16). At Olsen's Beach, unvegetated shoreline declined by 66%, from 2,538 m^2 to 868 m^2 over a shoreline length of 855 m (Figure 17)

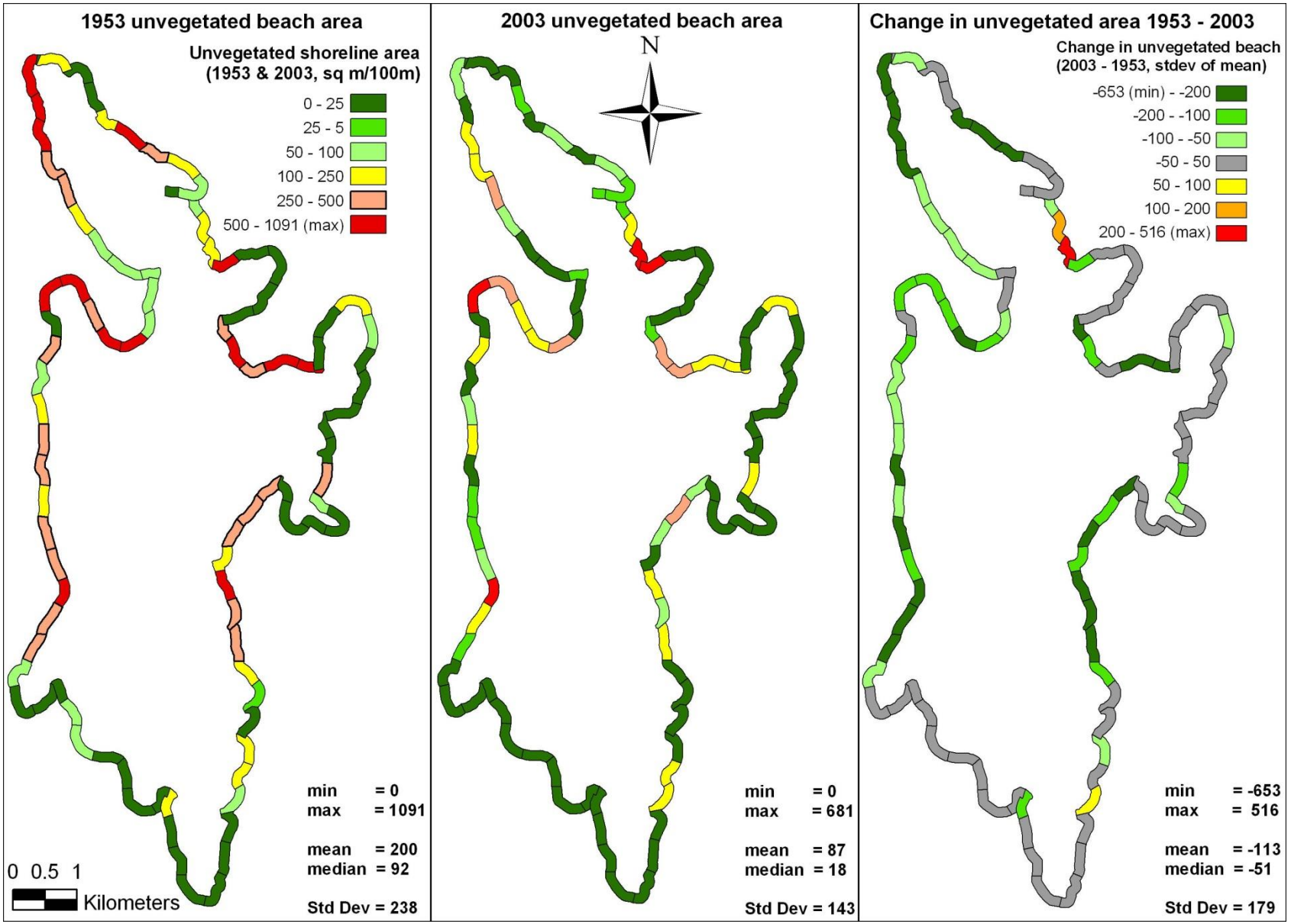

Figure 15. Unvegetated beach area in 1953 and 2003, and change in unvegetated area from 1953 to 2003.The red and orange segments in the right portion of the figure are north of Umbrella Creek, and the yellow segment is north of Tributary 20.0078.

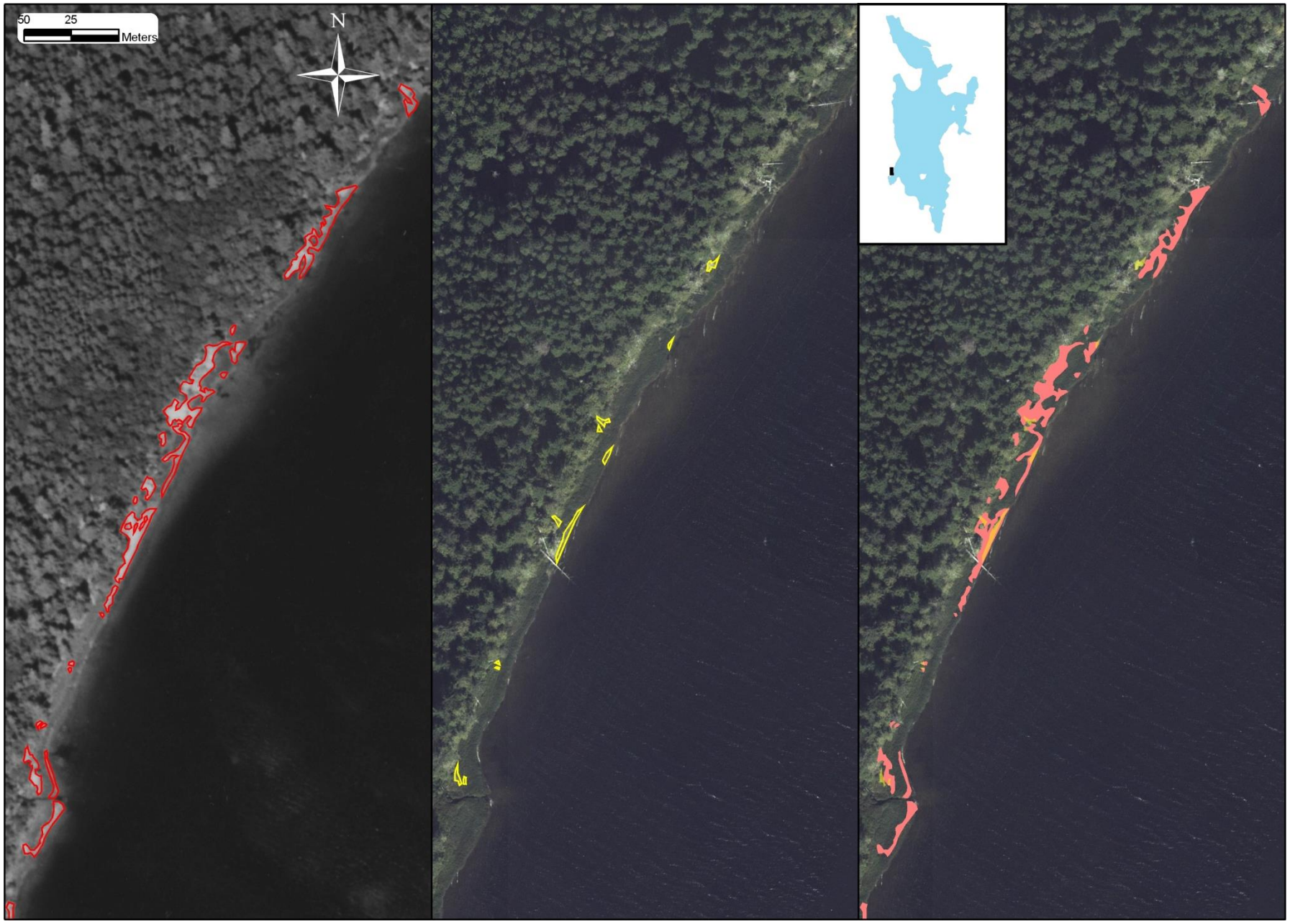

Figure 16. Comparison of south Allen's Beach from 1953 to 2003. Red polygons delineate unvegetated shoreline in 1953 (left image) and yellow polygons delineate unvegetated area in 2003 (middle image). Rightmost image highlights differences between photo-years.

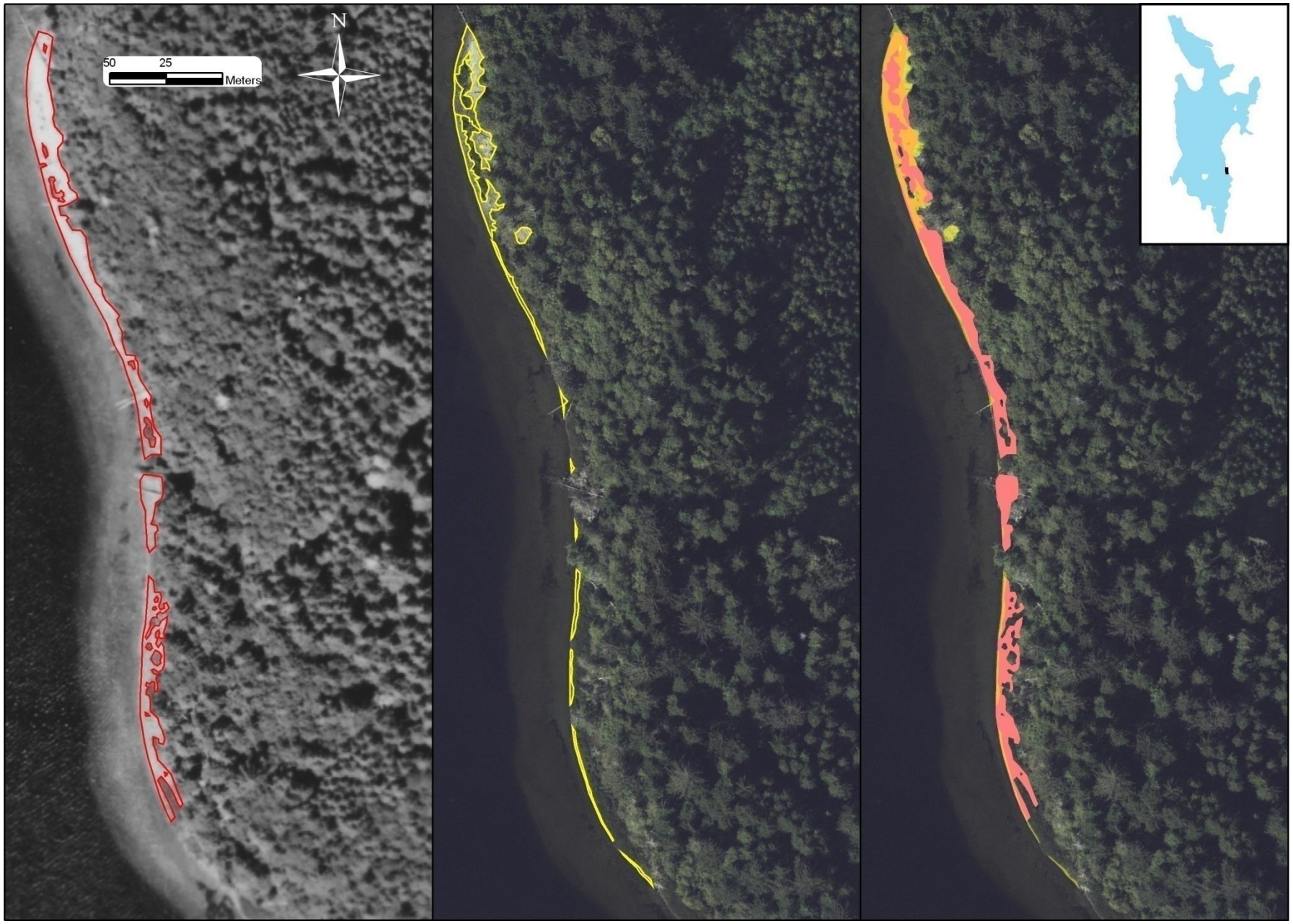

Figure 17. Vegetation changes at Olsen's Beach from 1953 to 2003. Red polygons delineate unvegetated shoreline in 1953 (left image) and yellow polygons delineate unvegetated area in 2003 (middle image). Right image highlights differences between photo-years.

3.1.3 Umbrella Creek Delta Analysis

The Umbrella Creek delta has grown noticeably from 1952 to present (Figure 18 and Figure 19). Aerial photo analysis shows that delta growth was more rapid from 1964 to1977, slowing noticeably from 1977 to 2006. While a few data points (1964 and 2006) show a decrease in delta area over previous photosets. However, the 1964 and 2006 aerial photos were taken earlier in the year than other photos (Table 2), and thus lake level would be higher, giving an underestimate of delta growth through time. Mean lake stage for the period 1976 through 2005 is about 10.2 m (33.5 ft) in May, compared with about 9.7 to 9.9 m (31.8 to 32.5 ft) in July and August (Haggerty et al 2008).

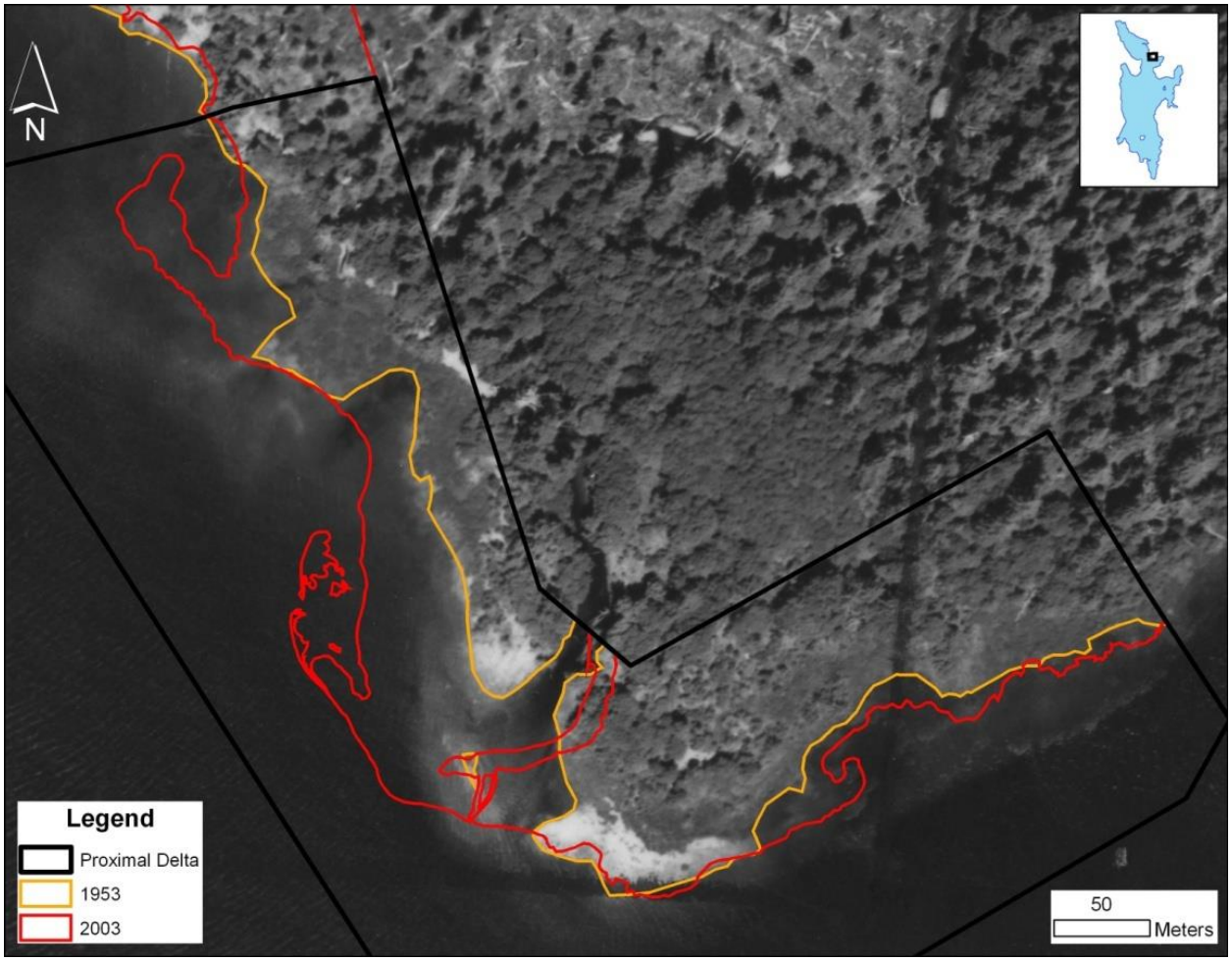

Figure 18. Umbrella Creek Delta in 1953. 1953 (orange) and 2003 (red) shorelines are shown.

The 1985 photos showed a decrease in the whole delta area, but an increase in the proximal delta (Figure 20). This may be due to complex patterns of sediment transport, such as spit formation and migration (Figure 18 and Figure 19). Excluding the 2006 photo year, which was taken

abnormally early, and the 2000 and 2003 photos which were taken unusually late, delta growth over the period of 1953 to 1994 appears to be about 1.7 to 2.4 hectares (4.1 to 5.9 acres) (Figure 20, Table 4).

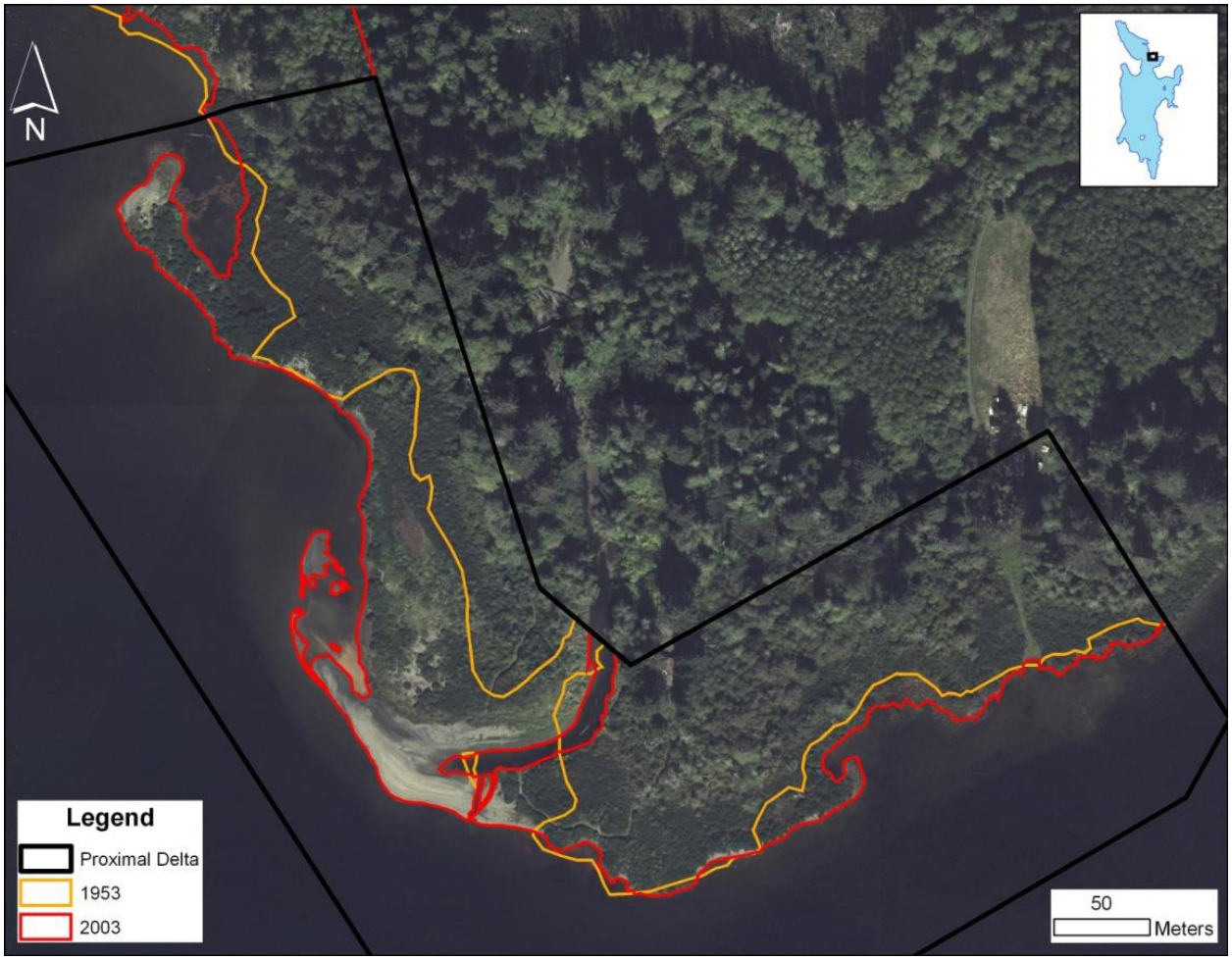

Figure 19. Umbrella Creek Delta in 2003. 1953 (orange) and 2003 (red) shorelines are shown.

While a few analysis years deviate from the long-term delta growth trend (Figure 20, Table 4), the two most notable years (1964 and 2006) can be explained by the early timing of the aerial photography in these years (Table 4. Change from 1952 sub-areal Umbrella Creek delta Table 2). Both the proximal delta and the whole delta analysis area show a consistent trend in delta growth over time. Unfortunately, accurate surveys, or aerial photography from prior to 1952 have not been located. This reduces the certainty of conclusions drawn from this time series, since no baseline delta trend can be established for the period prior to the onset of rapid timber harvest.

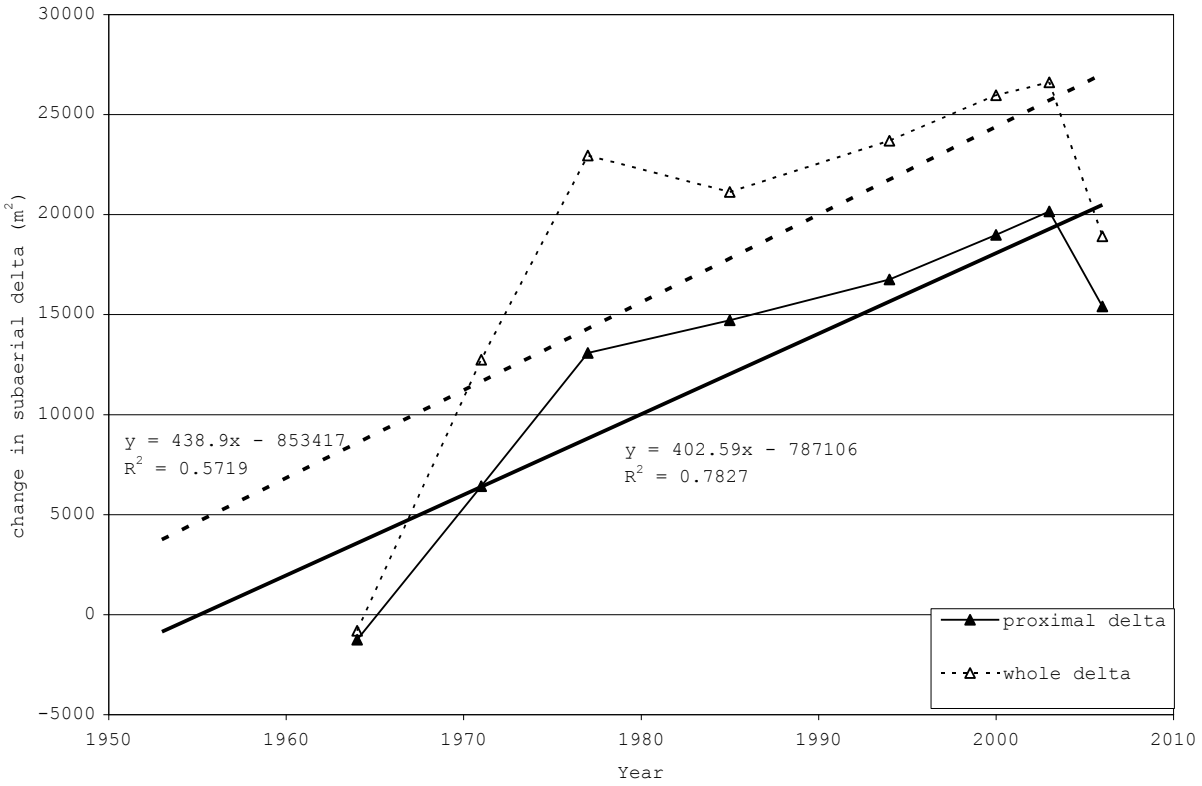

Figure 20. Change in proximal and whole Umbrella Creek subaerial delta area since 1952.

Table 4. Change from 1952 sub-areal Umbrella Creek delta within polygons shown in Figure 4.

Proximal Delta					
Photo year	Area (sq ft)	Change (sq ft)	Change (acre)	Change (sq m)	Change (ha)
1953	555,298	NA			
1964	541,736	-13,562	-0.31	-1260	-0.13
1971	624,390	69,092	1.59	6419	0.64
1977	696,143	140,845	3.23	13085	1.31
1985	713,676	158,378	3.64	14714	1.47
1994	735,686	180,387	4.14	16759	1.68
2000	759,681	204,383	4.69	18988	1.90
2003	772,263	216,964	4.98	20157	2.02
2006	721,135	165,837	3.81	15407	1.54
Whole Delta					
Photo year	Area (sq ft)	Change (sq ft)	Change (acre)	Change (sq m)	Change (ha)
1953	1,471,682	NA			
1964	1,462,959	-8,723	-0.20	-810	-0.08
1971	1,608,830	137,148	3.15	12741	1.27
1977	1,718,699	247,017	5.67	22949	2.29
1985	1,699,164	227,481	5.22	21134	2.11
1994	1,726,649	254,967	5.85	23687	2.37
2000	1,751,109	279,426	6.41	25960	2.60
2003	1,758,131	286,449	6.58	26612	2.66

2006	1,675,221	203,539	4.67	18909	1.89

3.1.4 Ozette Watershed Land Use History

Timing of the "first cut," or primary forest depletion, was largely synchronous. At most, about 15 years separate peak harvest rates in the various sub-basins (Figure 21). Similar depletion trends occur in each major watershed, with peak harvest rates occurring over a ten to 20 year period, between about 1964 and 1984, when between 50% and 80% of each sub-basin area was harvested. The increasing harvest trend through the 1970s is followed by decreasing depletion rates as accessible primary forest is largely eliminated in the 1980s. By 1994, virtually all remaining stands of primary forest are either found on state or federal lands, or consist of low-value or inaccessible timber. Depletion of primary forest in Ozette has stabilized at about 80%, with remaining stands primarily on the east side of the lake and in Crooked Creek.

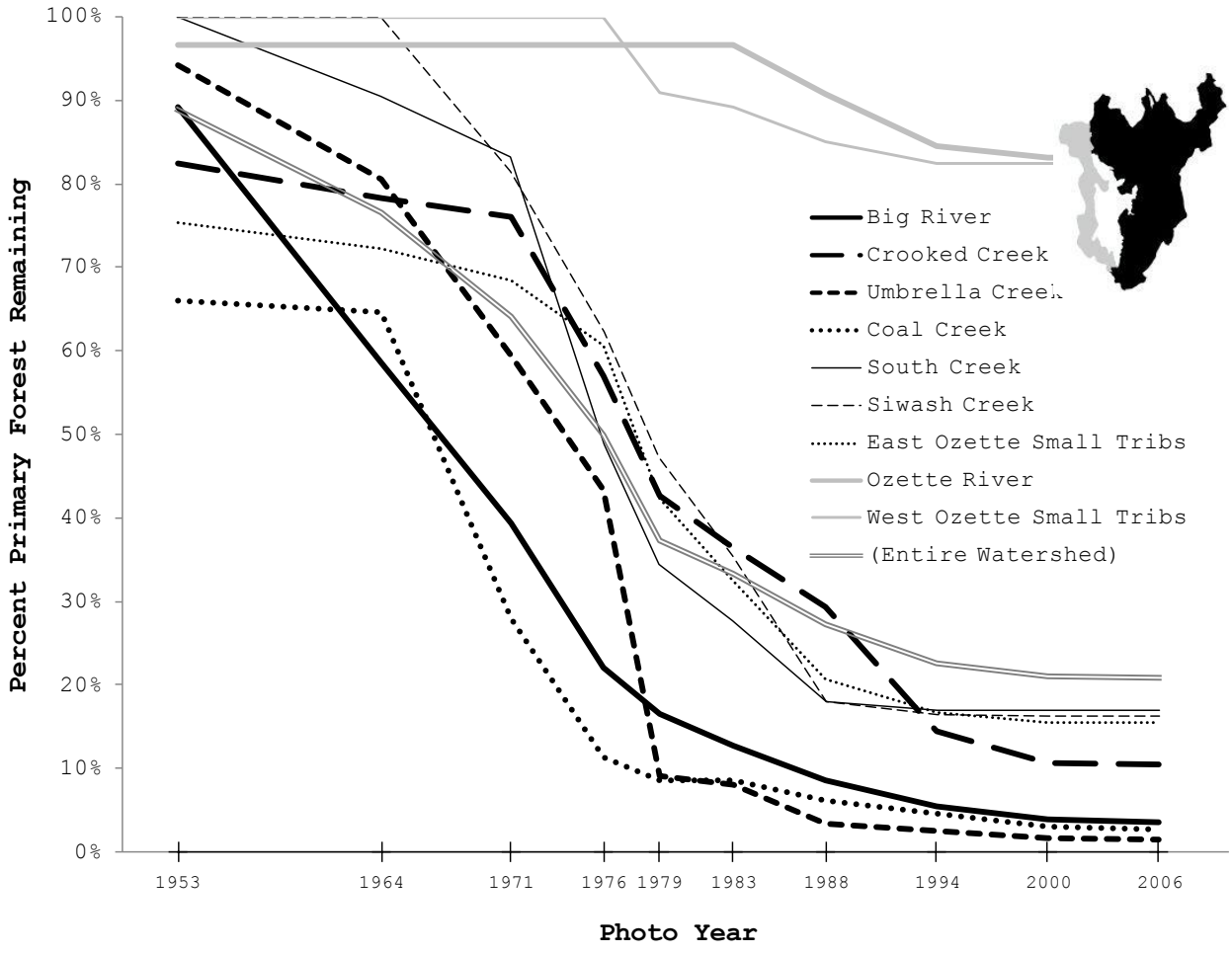

Figure 21. Primary forest fraction remaining from photo year1953 – 2006 by sub-watershed. The west side of the lake, which is primarily park and tribal land, is shown in gray.

In 1953, the first year in which accurate aerial imagery permits remote assessment of harvest history, approximately 90% of the watershed is still primary forest. By that time, harvest had

occurred primarily along the easily accessible bottomlands of Big River, Coal Creek, and Crooked Creek. Harvest occurred primarily on low relief topography, and was concentrated along the logging railroad coming into Ozette from Crooked Creek and Little Hoko, to the east and northeast, respectively. After 1964, primary forest depletion rates in the Ozette watershed increased, peaking at an average annualized rate of over 4% between 1976 and 1979 before falling back to levels at or below that measured from 1953-1964 (Table 5).

Table 5. Remaining primary forest over time as percent of watershed and percent of ownership.

	1953	**1964**	**1971**	**1976**	**1979**	**1983**	**1988**	**1994**	**2000**	**2006**
Primary forest remaining by sub-watershed										
Big River	89%	59%	39%	22%	17%	13%	9%	6%	4%	4%
Crooked Creek	82%	78%	76%	57%	43%	36%	29%	14%	11%	10%
Umbrella Creek	94%	81%	59%	43%	9%	8%	3%	2%	2%	1%
Coal Creek	66%	65%	28%	11%	9%	9%	6%	5%	3%	3%
South Creek	100%	90%	83%	49%	35%	28%	18%	17%	17%	17%
Siwash Creek	100%	100%	82%	62%	47%	35%	18%	16%	16%	16%
E. Ozette Sm. Tribs	75%	72%	68%	61%	42%	32%	21%	17%	15%	15%
Ozette River	97%	97%	97%	97%	97%	97%	91%	85%	83%	83%
W. Ozette Sm. Tribs	100%	100%	100%	100%	91%	89%	85%	83%	83%	83%
Primary forest remaining by ownership type										
Ozette Reservation	100%	100%	100%	100%	100%	100%	100%	100%	100%	100%
Private Ownership	85%	70%	55%	39%	23%	18%	12%	6%	4%	4%
Federal Land	98%	98%	98%	98%	97%	97%	96%	96%	96%	96%
Washington State	100%	91%	77%	53%	41%	40%	26%	24%	21%	21%
(Entire Watershed)	***89%***	***77%***	***64%***	***50%***	***37%***	***33%***	***27%***	***23%***	***21%***	***21%***

State and private lands show similar trends in depletion of primary forest, with an earlier decrease in depletion rates, and more remaining primary forest held by the state (Figure 22). Minor harvest in lands acquired by Olympic National Park can be seen in the mid-1970s. This is primarily composed of the buffer strip and areas near the Ozette River, which is land acquired by the park in 1976 – likely shortly after it was harvested. The Makah Tribe's Ozette Reservation is also shown as a baseline, since no harvest has occurred here.

Since original ownership is not known, few – if any – conclusions can be drawn from historic data on relative rates of harvest by private industry and Washington State. However it is clear that the only significant holders of remaining primary forest in the Ozette Basin are the United States (including lands held in Trust for the Makah Tribe) and the State of Washington.

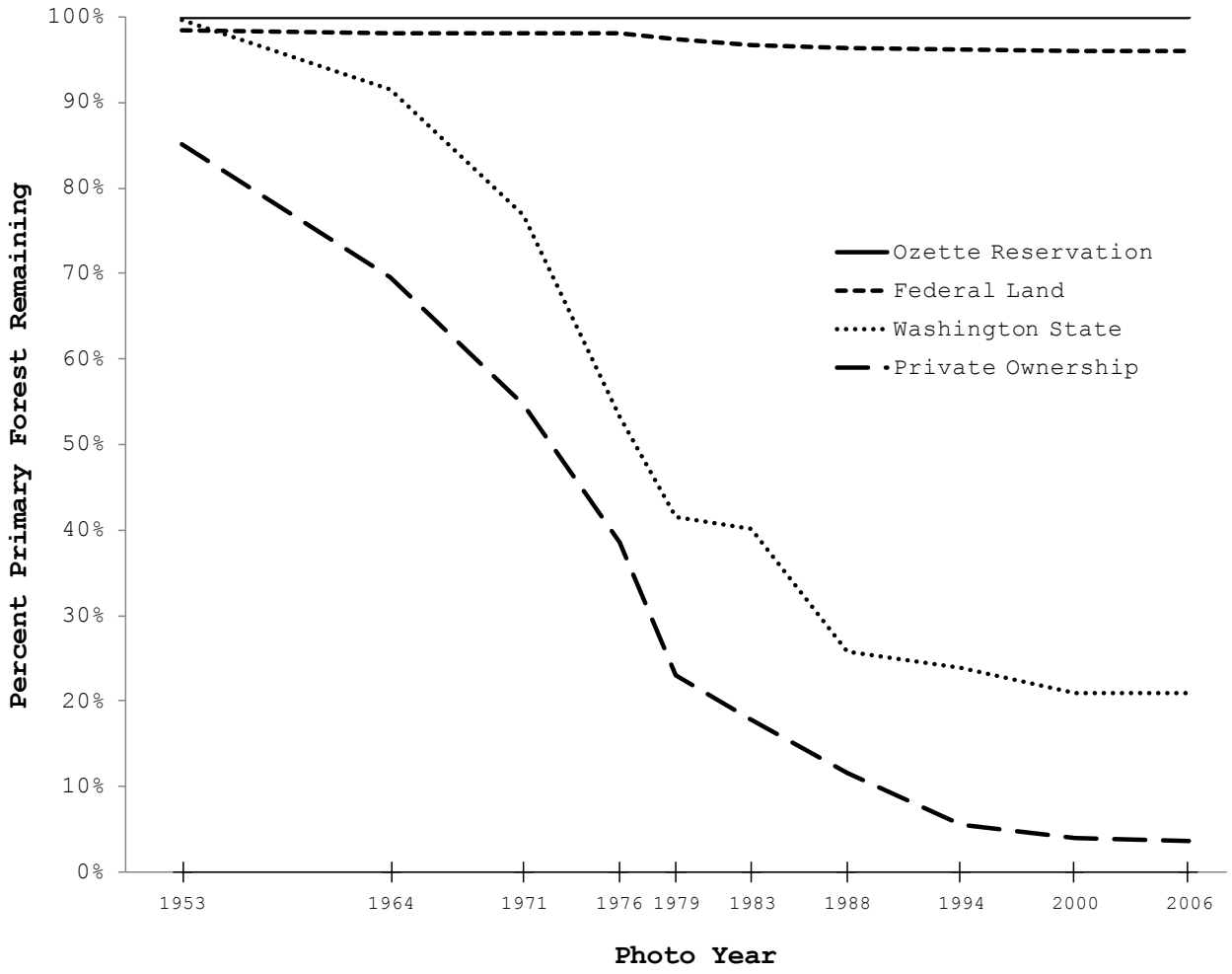

Figure 22. Primary forest fraction remaining from 1953 – 2006 by ownership category.

Harvest rates (shown as annualized harvest in Figure 23 and Table 6) peaked on both private and state lands in the late 1970s and fell rapidly by the early 1980s. By the mid 1990s, annualized harvest on state lands dropped to less than 1% of the watershed area, and stabilized on private timberlands at about 1.5%. This is likely a function of the quantity of timber that has reached maturity for the second cut. Cumulative harvest values (Figure 23) show that roughly 15% of the watershed in private ownership was harvested a second time between about 1994 and 2006.

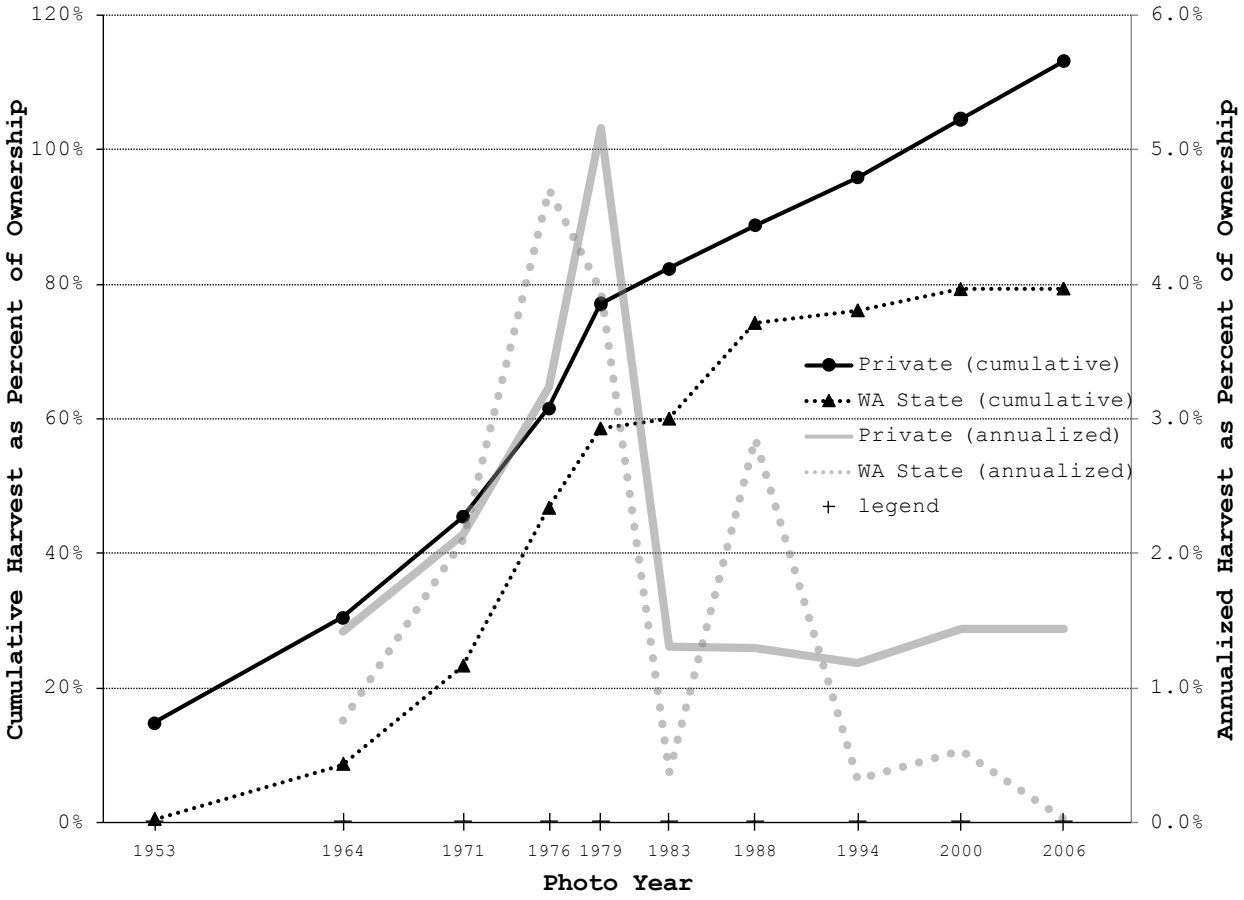

Figure 23. Cumulative and annualized harvest as percent of ownership area for state and private lands from 1964 – 2006.

Table 6. Annualized harvest rates from from 1964 – 2006 by sub-basin and owner type.

	1964	**1971**	**1976**	**1979**	**1983**	**1988**	**1994**	**2000**	**2006**
Big River	2.8%	2.8%	3.5%	1.8%	1.0%	0.9%	0.7%	1.5%	1.6%
Crooked Creek	0.4%	0.3%	3.8%	4.9%	1.6%	1.4%	2.6%	1.4%	0.8%
Umbrella Creek	1.2%	3.0%	3.2%	11.4%	0.3%	0.9%	0.2%	0.9%	1.7%
Coal Creek	0.1%	5.3%	3.3%	1.0%	0.0%	0.5%	0.4%	2.5%	1.9%
South Creek	0.9%	1.0%	6.9%	4.8%	1.7%	1.9%	0.2%	0.0%	1.0%
Siwash Creek	0.0%	2.6%	3.8%	5.1%	2.9%	3.5%	0.3%	0.0%	0.0%
E. Ozette Sm. Tribs	0.3%	0.5%	1.6%	6.2%	2.5%	2.5%	0.9%	1.8%	0.8%
Ozette River	0.0%	0.0%	0.0%	0.0%	0.0%	1.2%	1.1%	0.2%	0.2%
W. Ozette Sm. Tribs	0.0%	0.0%	0.0%	3.0%	0.4%	0.8%	0.4%	0.0%	0.0%
Private Ownership	1.4%	2.1%	3.2%	5.2%	1.3%	1.3%	1.2%	1.4%	1.4%
Washington State	0.7%	2.1%	4.7%	3.9%	0.4%	2.9%	0.3%	0.5%	0.0%
(Entire Watershed)	***1.1%***	***1.8%***	***2.8%***	***4.2%***	***1.0%***	***1.2%***	***0.9%***	***1.1%***	***1.1%***

Harvest trends are similar for all of the major sub-basins in the Ozette basin (Figure 24). The three basins which are almost entirely in private ownership (Big River, Umbrella Creek, and Coal Creek) all have surpassed 100% of the basin area harvested, while Crooked Creek and the

Ozette basin as a whole have lower cumulative harvest percentages due to remaining blocks of primary forest.

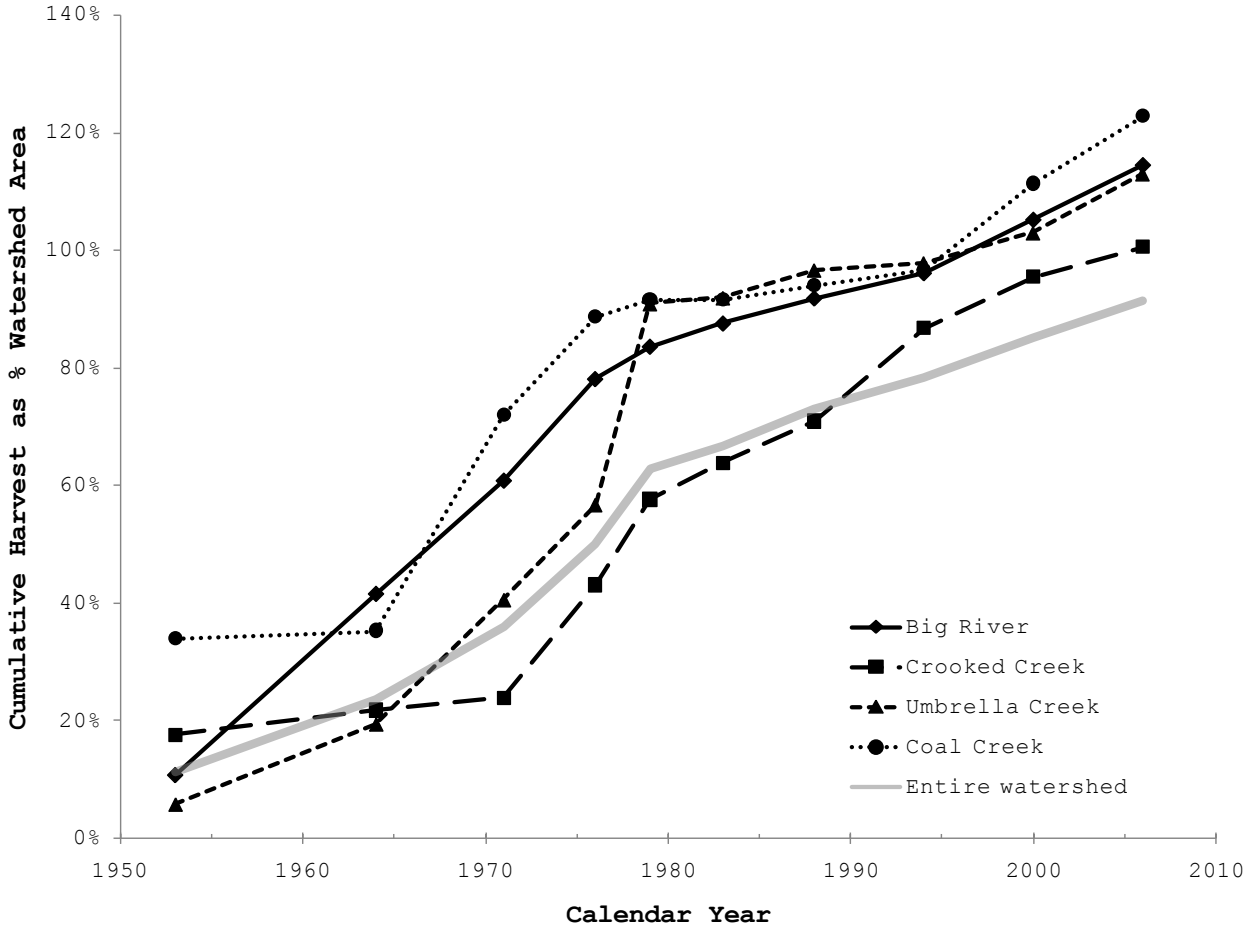

Figure 24. Cumulative harvest as percent of watershed area for major Ozette tributaries.

Increases in road density in the Ozette watershed closely parallel timber harvest (Table 7, Figure 25, Figure 26), and reach their highest values in Umbrella Creek, where densities are greater than 4.6 km/km^2 (7.4 mi/mi^2). While primary forest depletion stabilized by 2000, road density on private lands continued to climb from 2000 to 2006, likely due to changes in harvest methods and equipment. Road densities on State land stabilized from 2000 to 2006 (Figure 26). A plot of road density as a function of cumulative harvest in the five largest watersheds shows a close fit between the two, with scatter increasing above a cumulative harvest of 100% (Figure 27). The increased scatter above 100% may be due to differences among watersheds in topography, harvest methods, or timing and methods used for the first harvest.

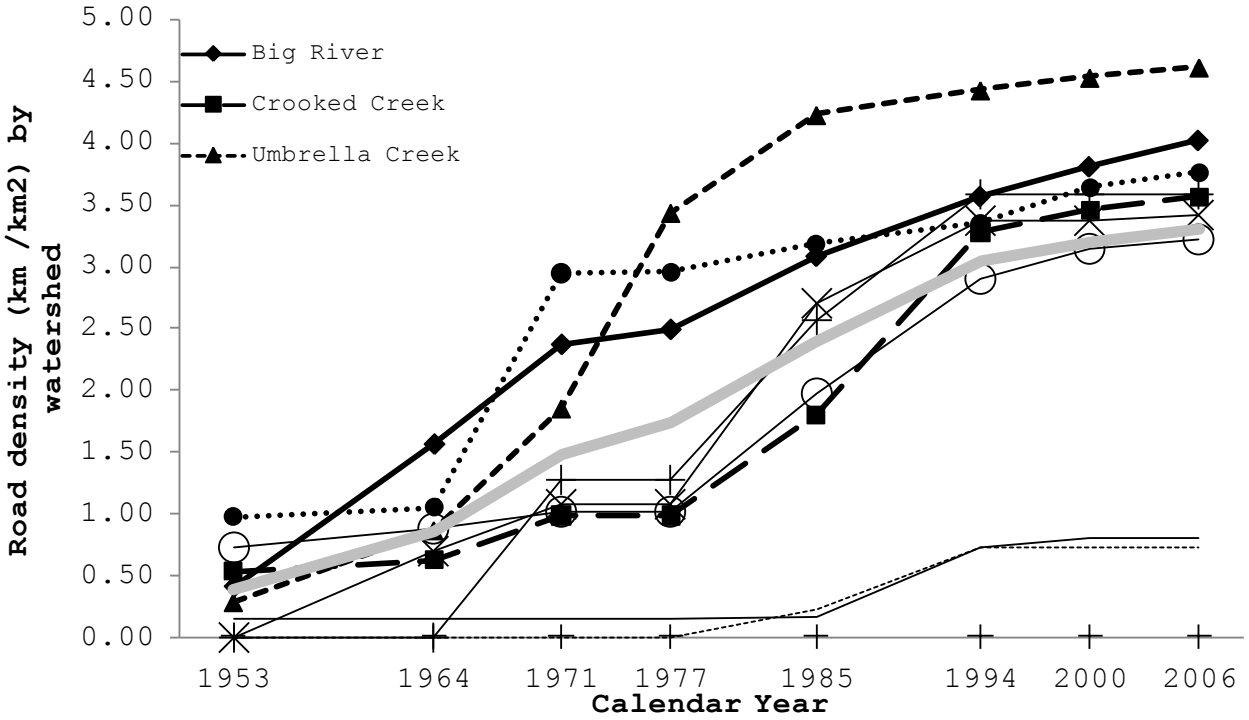

Figure 25. Road Density through time for entire watershed (gray) and subwatersheds (black).

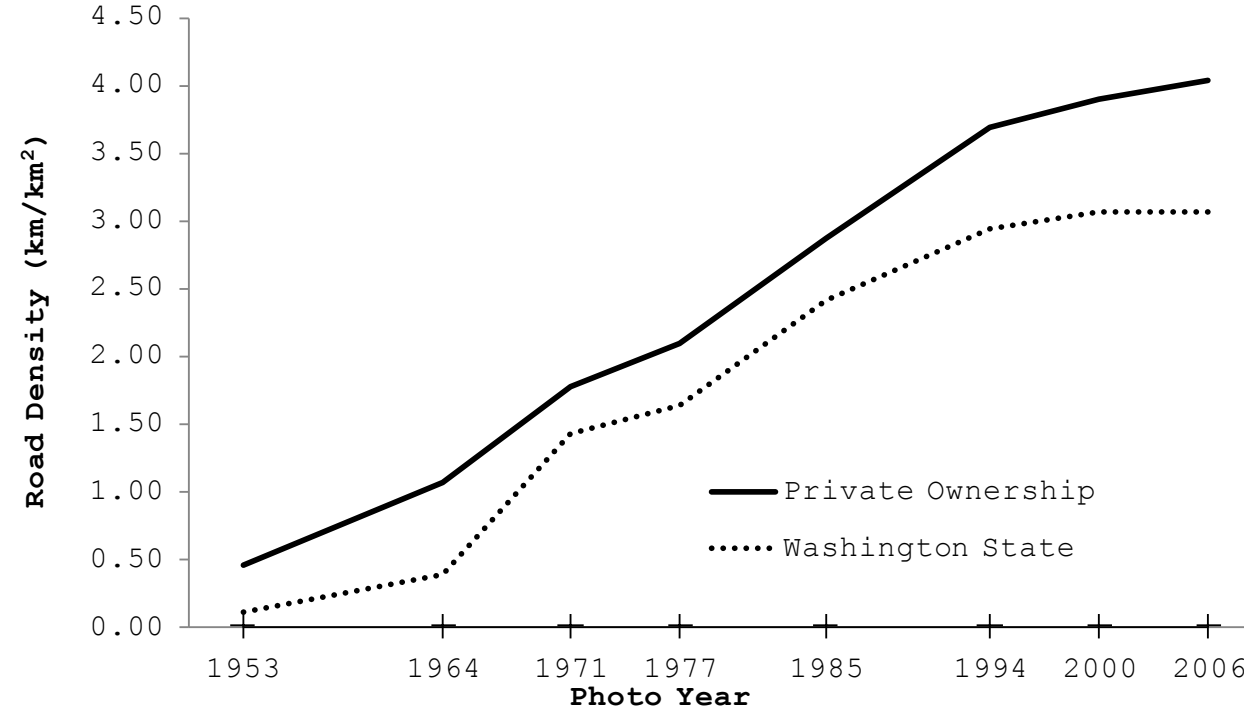

Figure 26. Road density by ownership for private and state lands.

Table 7. Summary of road density by sub-watershed and ownership type.

	1953	1964	1971	1977	1985	1994	2000	2006
Road Density (km/km^2) by sub-watershed								
Big River	0.4	1.6	2.4	2.5	3.1	3.6	3.8	4.0
Crooked Creek	0.5	0.6	1.0	1.0	1.8	3.3	3.5	3.6
Umbrella Creek	0.3	0.9	1.9	3.4	4.2	4.4	4.5	4.6
Coal Creek	1.0	1.0	2.9	2.9	3.2	3.3	3.6	3.8
South Creek	0.0	0.7	1.1	1.1	2.7	3.4	3.4	3.4
Siwash Creek	0.0	0.0	1.3	1.3	2.6	3.6	3.6	3.6
East Ozette Lake Small Tribs	0.7	0.9	1.0	1.0	2.0	2.9	3.1	3.2
Ozette River	0.1	0.1	0.1	0.1	0.2	0.7	0.8	0.8
West Ozette Lake Small Tribs	0.0	0.0	0.0	0.0	0.2	0.7	0.7	0.7
Road Density (km/km^2) by ownership type								
Private Ownership	0.5	1.1	1.8	2.1	2.9	3.7	3.9	4.0
Federal Land	0.2	0.2	0.2	0.2	0.2	0.2	0.2	0.2
Washington State	0.1	0.4	1.4	1.6	2.4	2.9	3.1	3.1
(Entire Watershed)	0.4	0.9	1.5	1.7	2.4	3.0	3.2	3.3

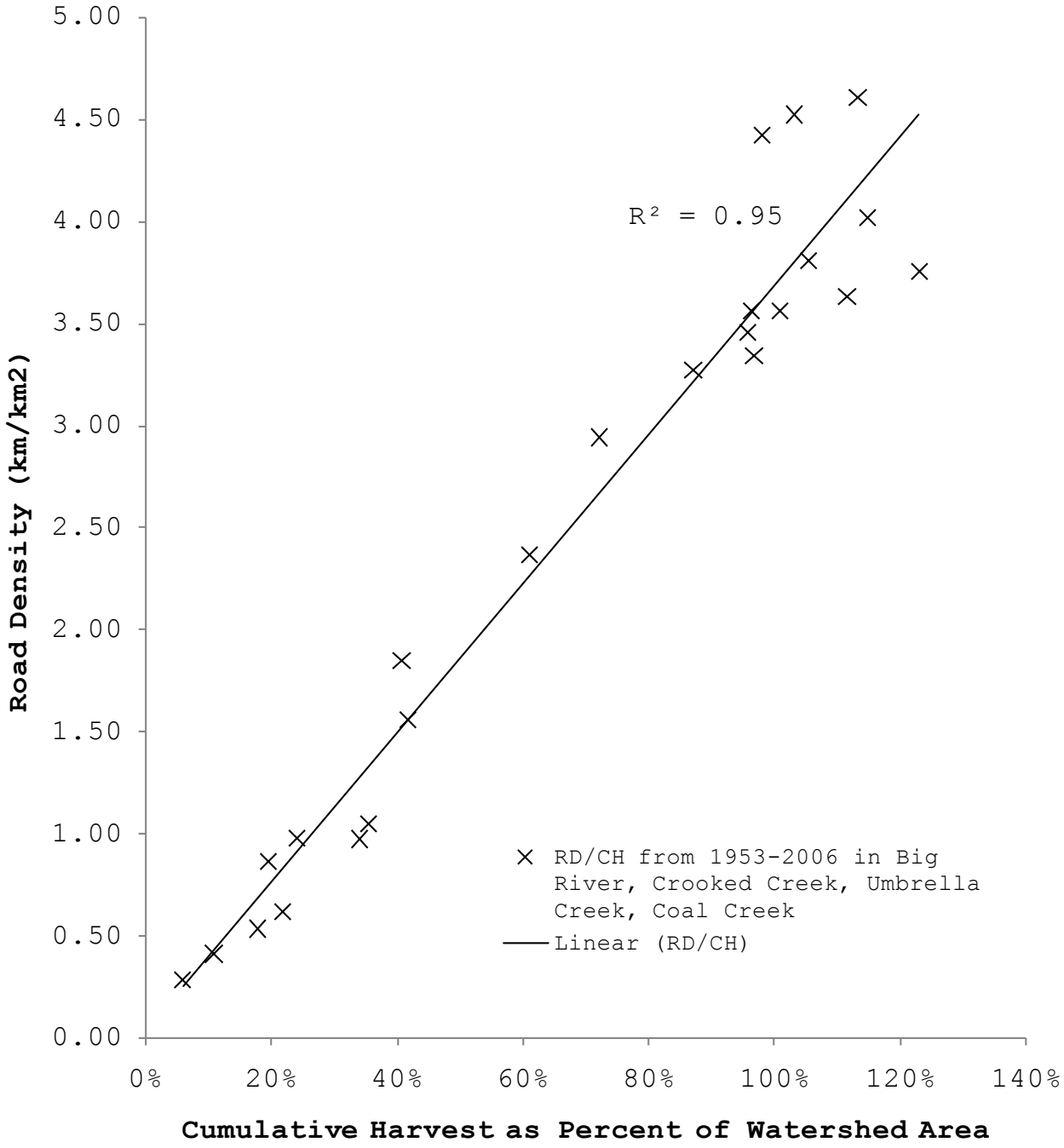

Figure 27. Road density as a function of cumulative harvest. Based on data from Big River, Crooked Creek, Umbrella Creek, and Coal Creek from 1953-2006.

3.1.5 Umbrella Creek detailed sub-basin analysis

In order to compare delta growth and land use history in the Umbrella Creek watershed, it was necessary to analyze land use for years in which high-resolution (aerial photography) data were available for the Umbrella delta. Because the delta imagery was temporally offset from satellite data used for the Ozette watershed land use analysis (Section 3.1.4) in the 1976-1988 period, two

additional photo years (1977 & 1985) were georeferenced and analyzed for only the Umbrella Creek catchment. This allowed comparison of land-use and delta growth in the Umbrella Creek sub-basin. Because Umbrella Creek showed the most rapid harvest of any Ozette basin (Figure 24), this higher-resolution sub-basin analysis also provided an independent error-check of low-resolution (satellite) image analysis results. Figure 28 shows the results of this comparison.

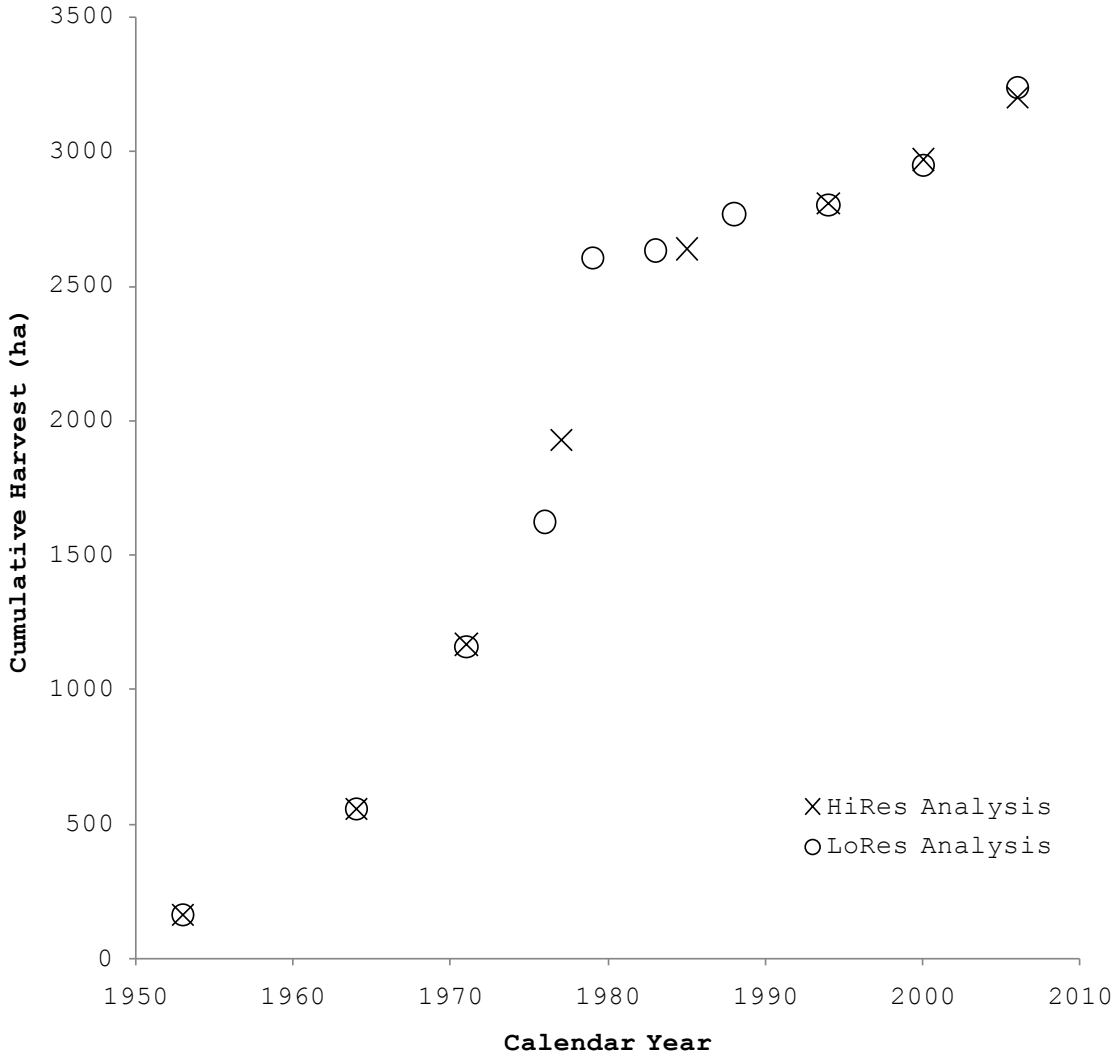

Figure 28. Comparison of high- and low-resolution analysis of cumulative harvest in Umbrella Creek watershed."X" is analysis using photo data, "O" uses satellite data.

While harvest rates in Umbrella Creek do not appear to peak as dramatically when only the photographic data are analyzed (Figure 28), this is likely a function of temporal, not spatial resolution. The data in Figure 28 show that each point in the high resolution analysis is intermediate in value between adjacent points in the low resolution analysis. In other words, if the low-resolution analysis significantly over-estimated harvest, we would not expect to see these data points form a continuous positive trajectory.

Road density and cumulative harvest track each other closely throughout the analysis period (Figure 29), although road density increases more rapidly than harvest during the peak period of harvest in the late 1970s. By 2006, road construction appears to be reaching a saturation density at just over 4.5 km/km^2 (Figure 29).

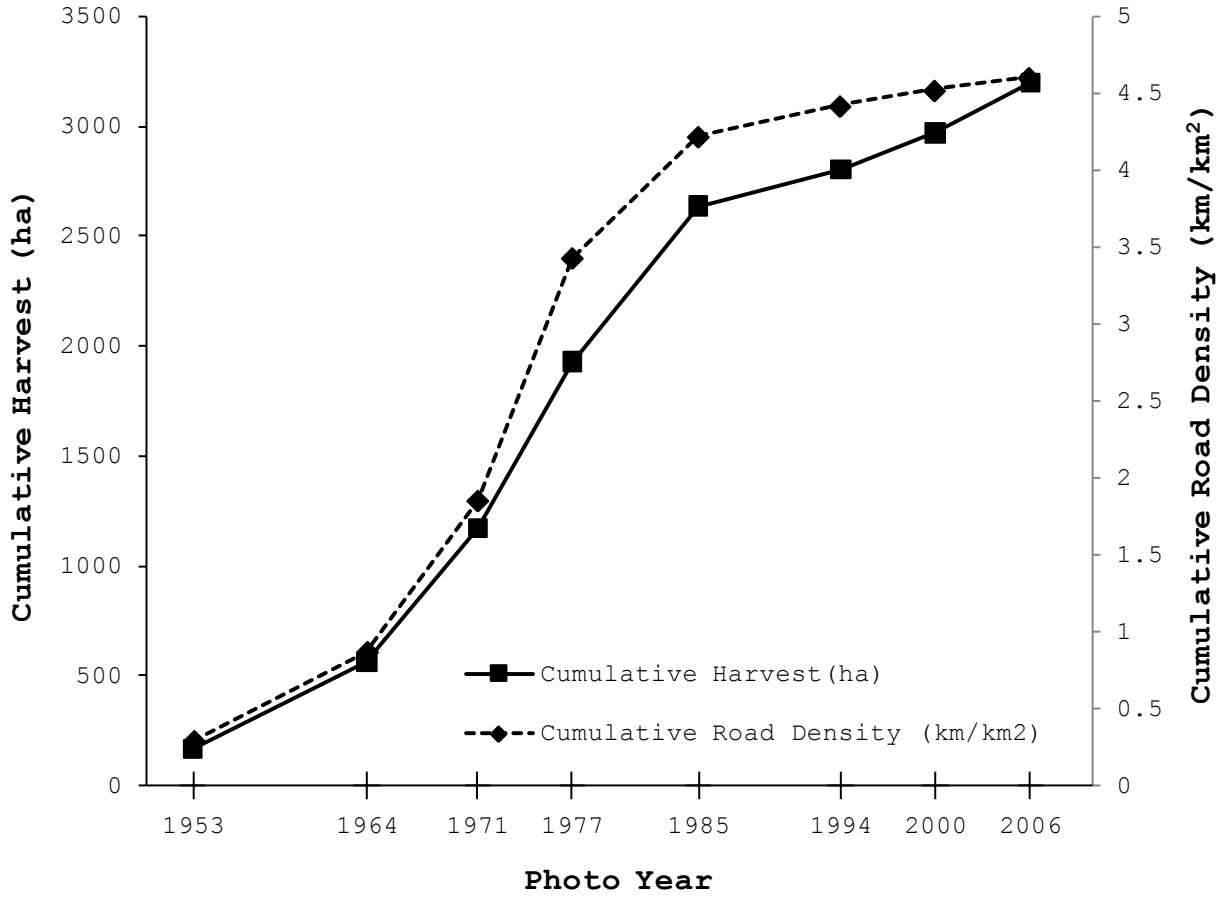

Figure 29. Cumulative harvest and cumulative road density by photo year in Umbrella Creek watershed.

Road densities this high can have significant impacts on watershed hydrology. Road connectivity to streams was measured by Wemple et al (1996) in two drainages in the Western Oregon cascades and 57% of the surveyed road length was connected to the stream network by surface flow paths. Cederholm et al (1982) found that road densities higher than about 1.8 km/km^2 (2.9 mi/mi^2) were consistently correlated with fine sediment in salmon spawning gravels that exceeded the highest levels found in undisturbed basins. A recent USFS review of road-related research found that evidence of increased erosion and sediment delivery to streams from roads is strong (Gucinski et al 2001).

Both road density and cumulative harvest in the Umbrella Creek sub-basin show a strong positive correlation with delta growth (Figure 30), with R^2 values of greater than 0.96. In other words, delta growth covaries with timber harvest and road construction.

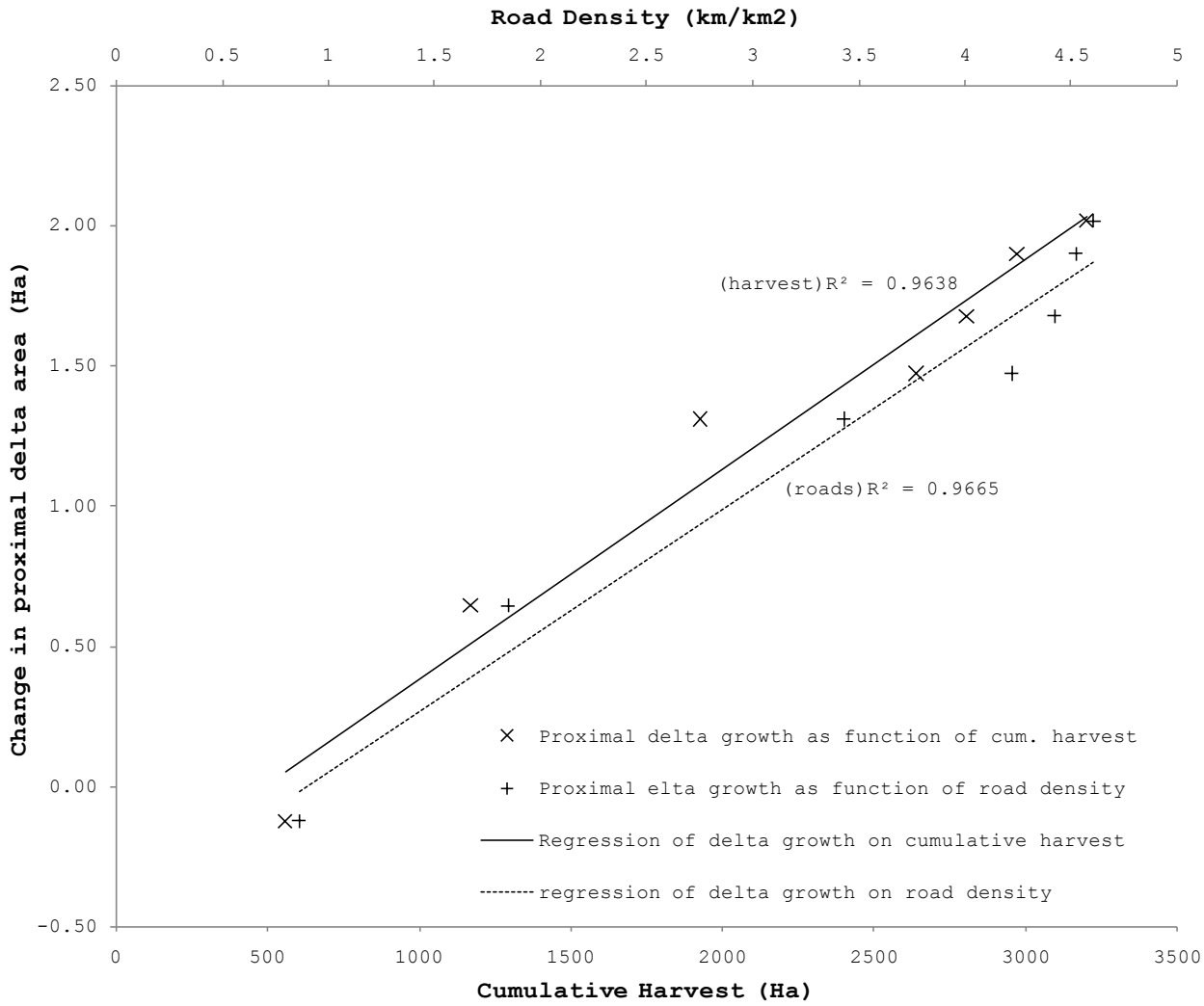

Figure 30. Proximal delta growth plotted against cumulative harvest (bottom axis) and road density (top axis).

3.2 Lake Ozette sediment accumulation history

3.2.1 Short-term accumulation rates (^{210}Pb isotope analysis)

^{210}Pb profiles were measured on seven cores, five from cores collected in 2005 and two from cores taken in 2006. Relative differences in sediment size between cores can be inferred from cumulative mass values (Figure 31), and from porosity data (Figure 32). Coarser sediment shows lower initial porosity and less response to compaction (Figure 32) and a higher bulk density, resulting in greater cumulative mass by depth (Figure 31). Coarser grain size is also indicated by lower excess activity in plots of OZ0906-1 and OZ0906-2 (Figure 34 and Figure 35).

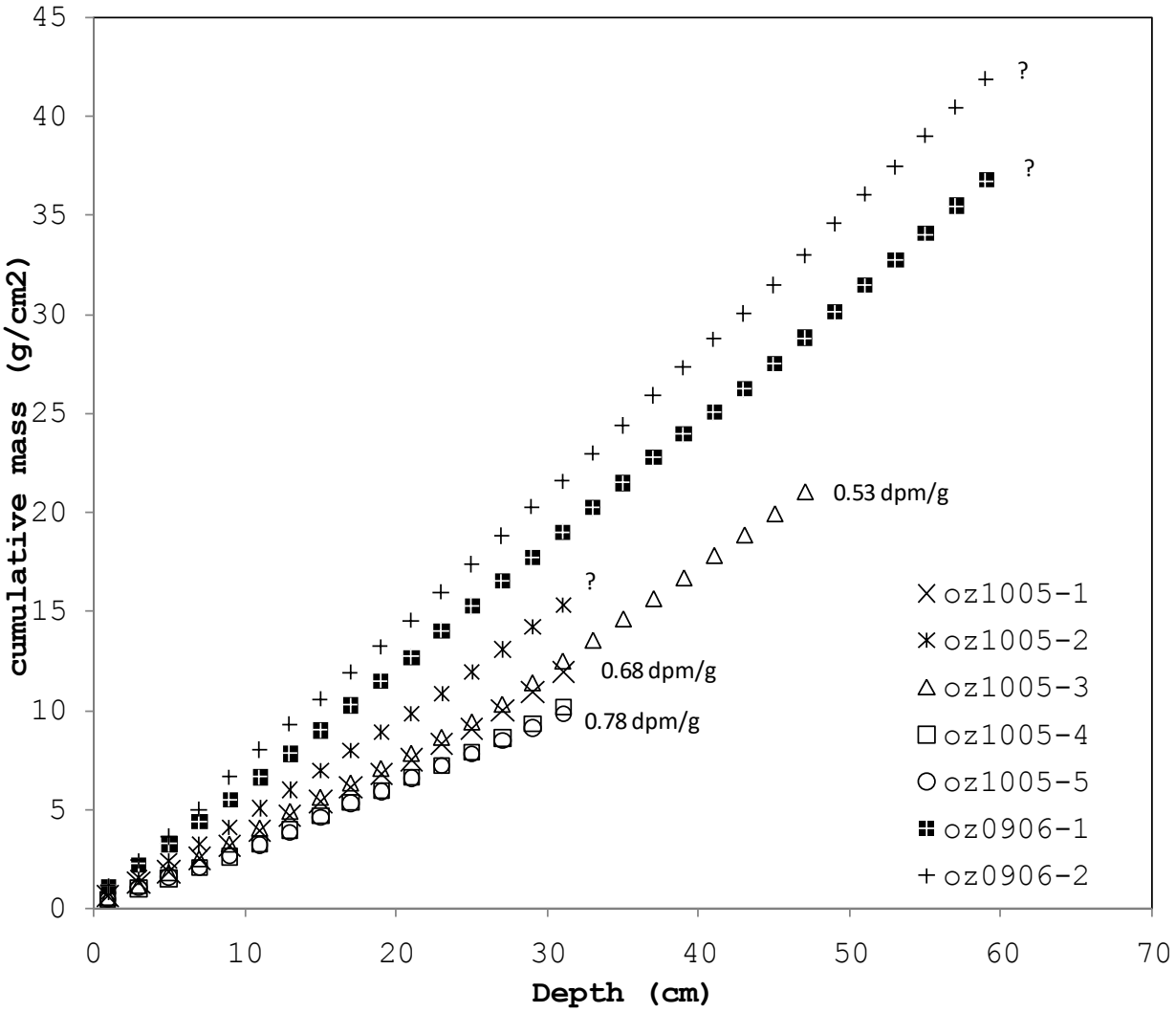

Figure 31. Cumulative mass by depth for 7 cores used for ^{210}Pb datingof sediment accumulation rates in Lake Ozette. Supported (background) ^{210}Pb activity values are shown where measured. Supported activity was not determined for cores marked with '?'.

Five of the seven cores processed showed an inflection in mass accumulation rate. In all five of these cores, the inflection indicates a shift to higher accumulation rates. In four of the cores this occurred between 1956 and 1962, and a fifth (in the middle of the North End) showed a shift in 1981. The other two cores (OZ1005-3 and OZ0906-2) exhibited significant noise in their activity profiles (Figure 35). In these cores, no change in accumulation rate was detected. This is likely due the noise, which may be a result of variations in grain size. Supported (background) ^{210}Pb activity was clearly identified on four of the seven cores processed for ^{210}Pb (Figure 33). Background activity was not reached on the remaining three (Figure 34).

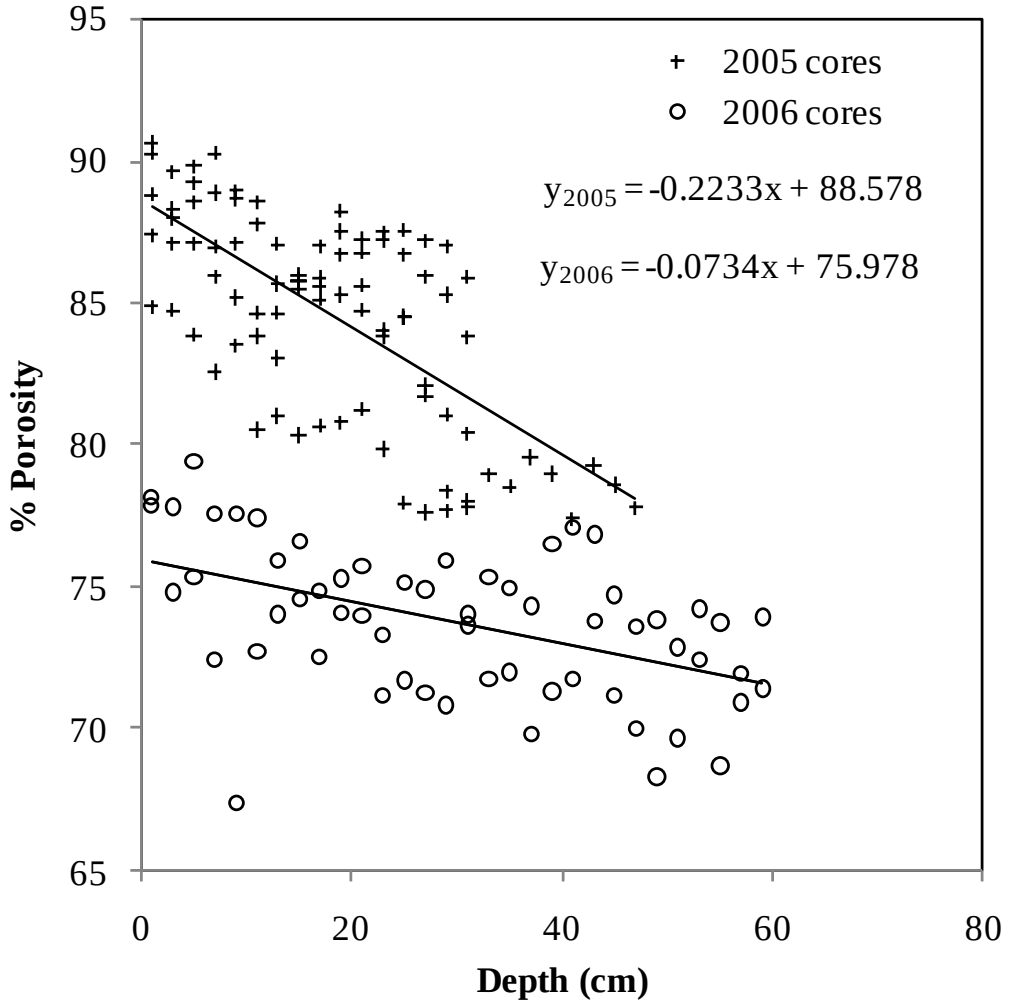

Figure 32. Porosity data and regressions from cores collected in 2005 and 2006.

Lower porosity values in 2006 cores relative to cores collected in 2005 (Figure 32) are consistent with shallower sampling depths in 2006 which were located closer to tributary mouths. As a consequence of targeting areas of more rapid accumulation, these cores necessarily sampled coarser sediment, reflected in higher cumulative mass-depth slopes (Figure 31) and lower compressibility and porosity values (Figure 32).

Plots of cumulative mass vs. excess activity are shown in Figure 36 - Figure 40 for all cores where inflection points were identified. The strongest inflections in mass accumulation rate were seen in core OZ1005-1 (Figure 36) from the center of the North End (Figure 5), and in cores OZ1005-2 (Figure 37) and OZ0906-1 (Figure 40) from Swan Bay (Figure 5).

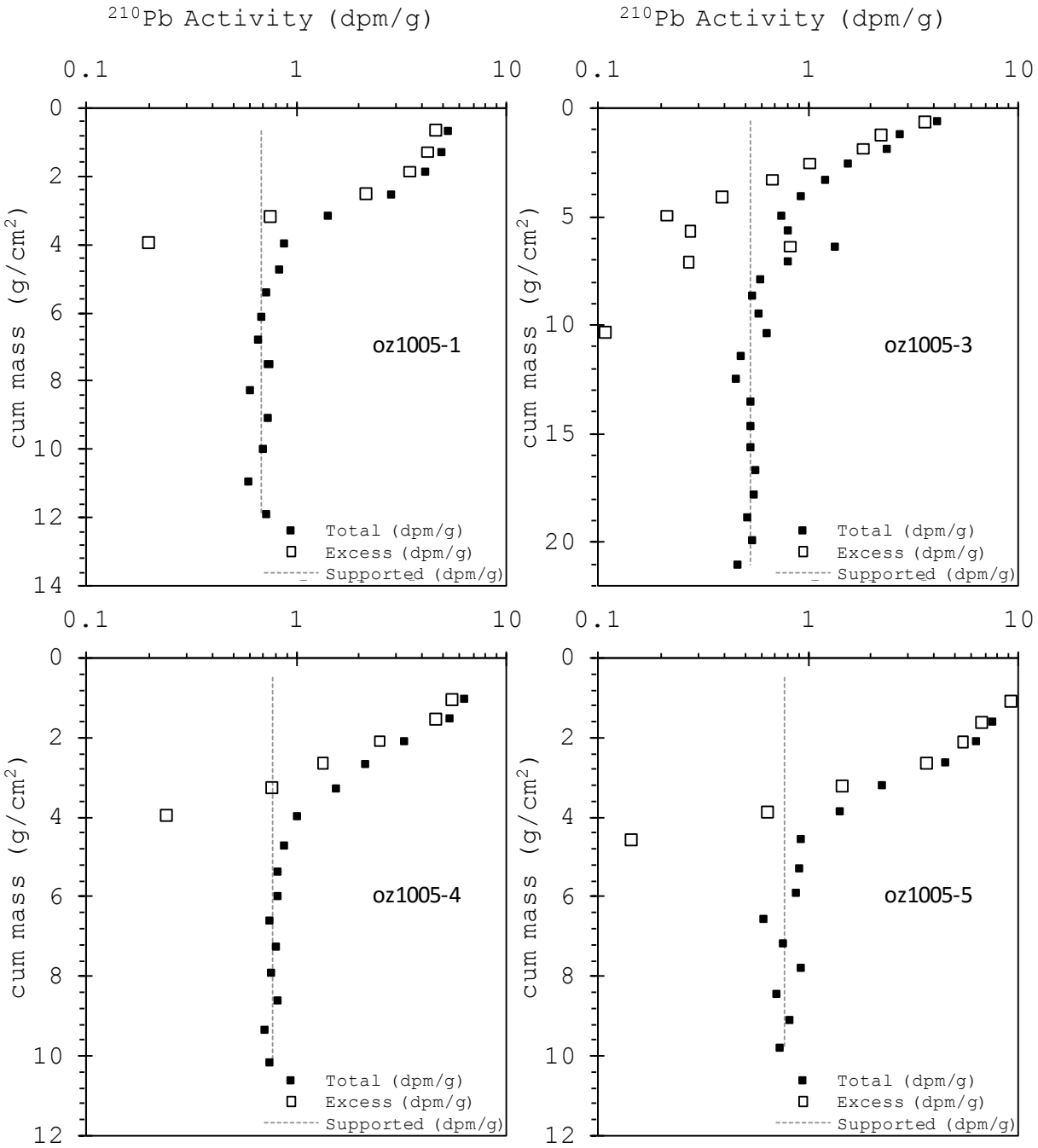

Figure 33. Total and excess ^{210}Pb activity plotted by cumulative mass for four cores where supported activity (background) was clearly identified.

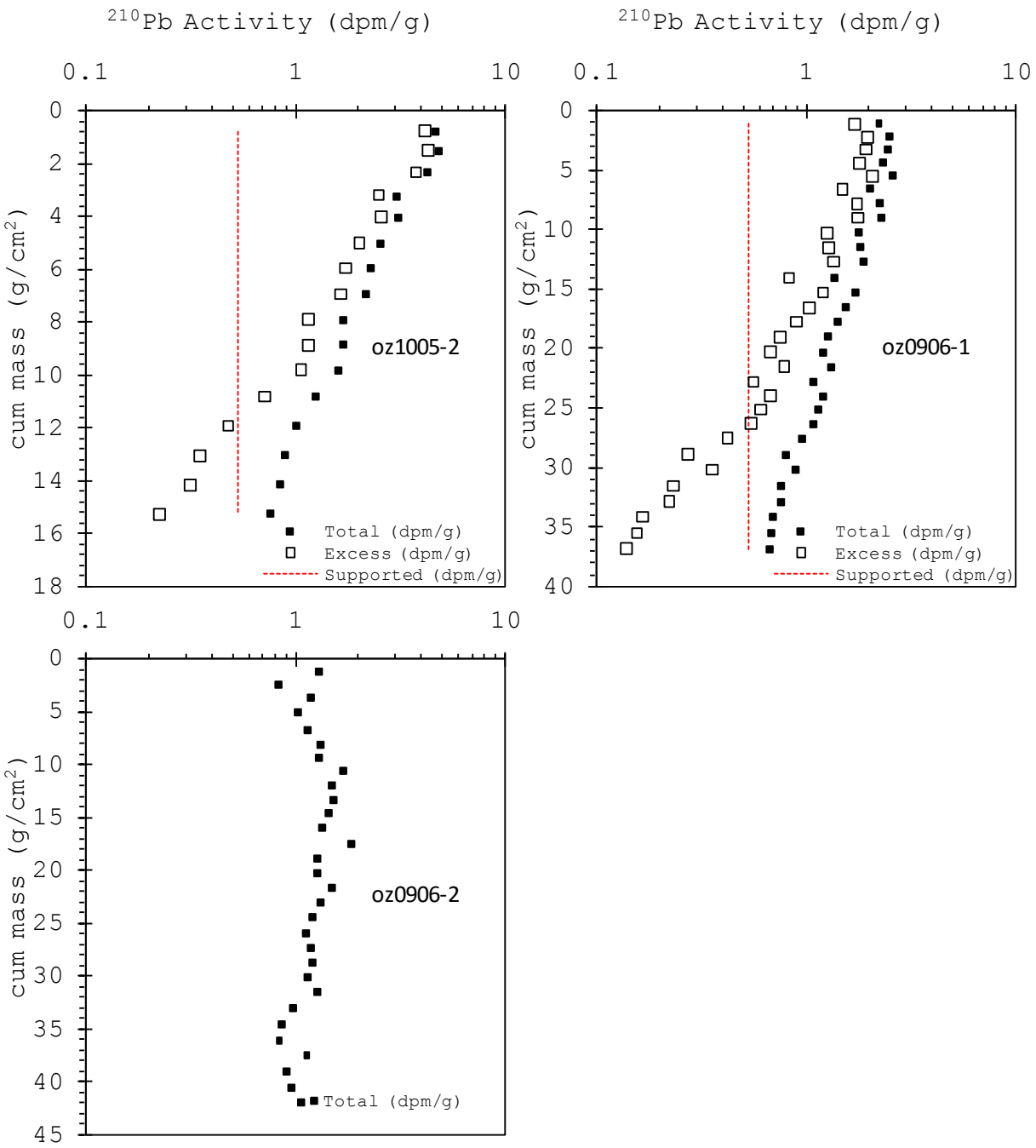

Figure 34. ^{210}Pb activity profiles for three cores where supported (background) ^{210}Pb activity was not determined. Preferred estimate of supported activity is indicated where inferred from nearby cores. No attempt was made to estimate supported activity for core OZ0906-2.

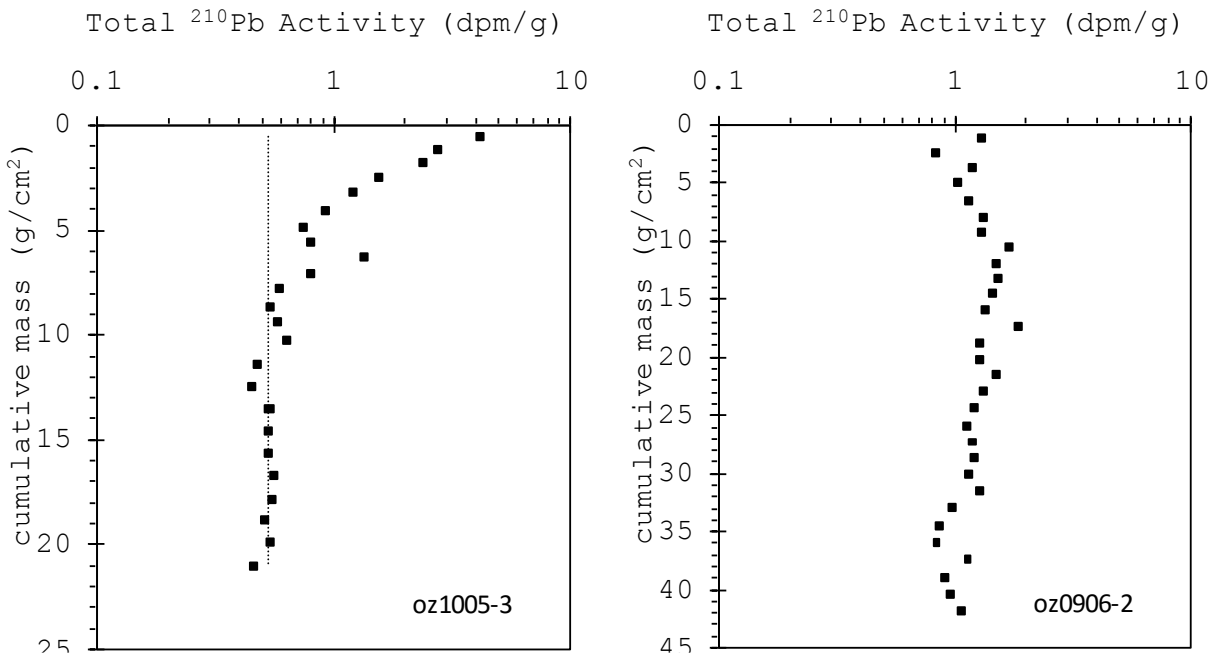

Figure 35. ^{210}Pb activity profiles for core OZ1005-3 and OZ0906-2. Both cores were too noisy to determine whether a change in mass accumulation rate had occurred.

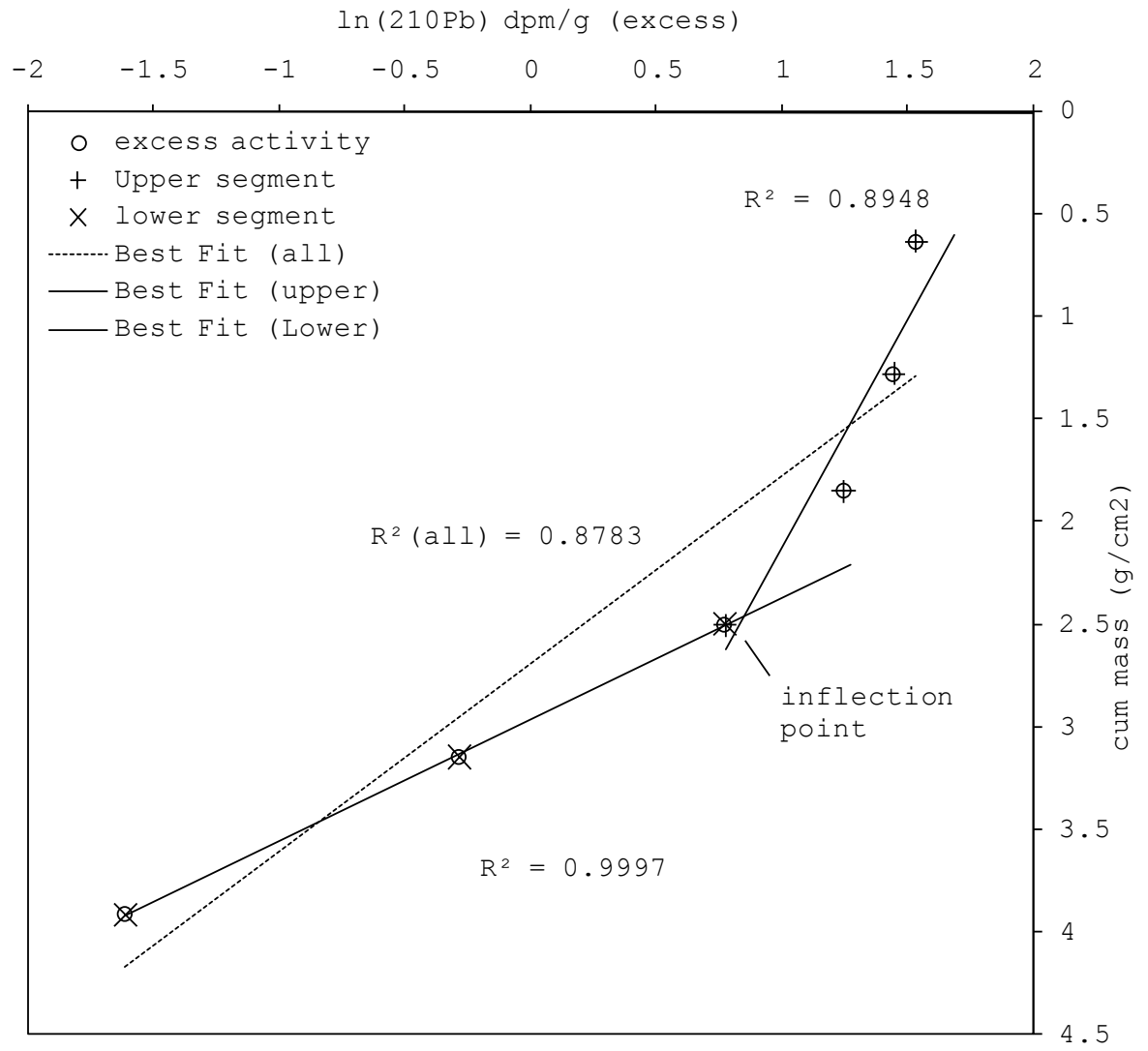

Figure 36. Linear regression of excess ^{210}Pb values by depth for core OZ1005-1 showing relative fit of single-stage and two-stage regression.

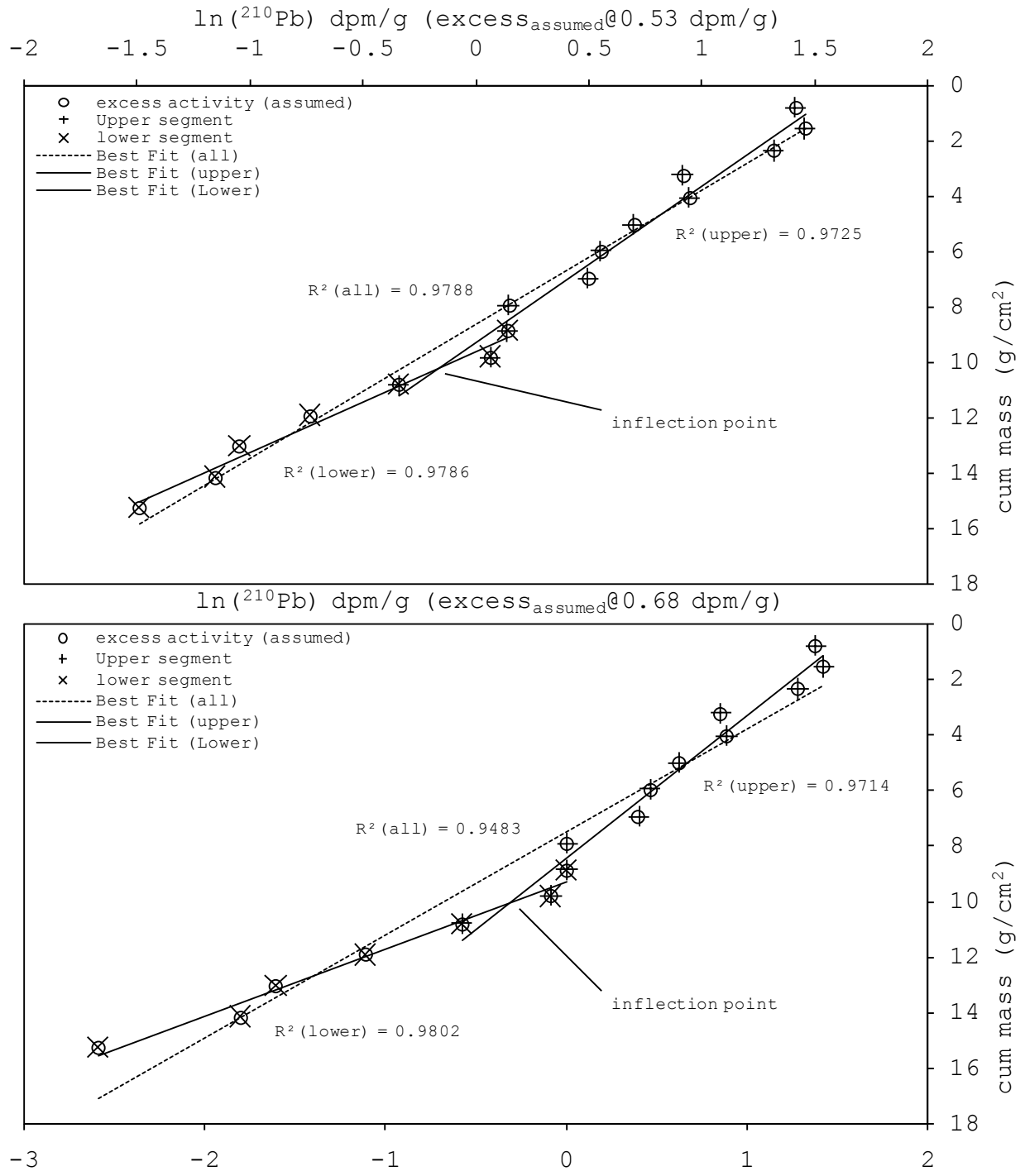

Figure 37. Linear regression of excess ^{210}Pb values by depth for core OZ1005-2 showing relative fit of single-stage and two-stage regression for supported values of 0.53 dpm/g (preferred) and 0.68 dpm/g.

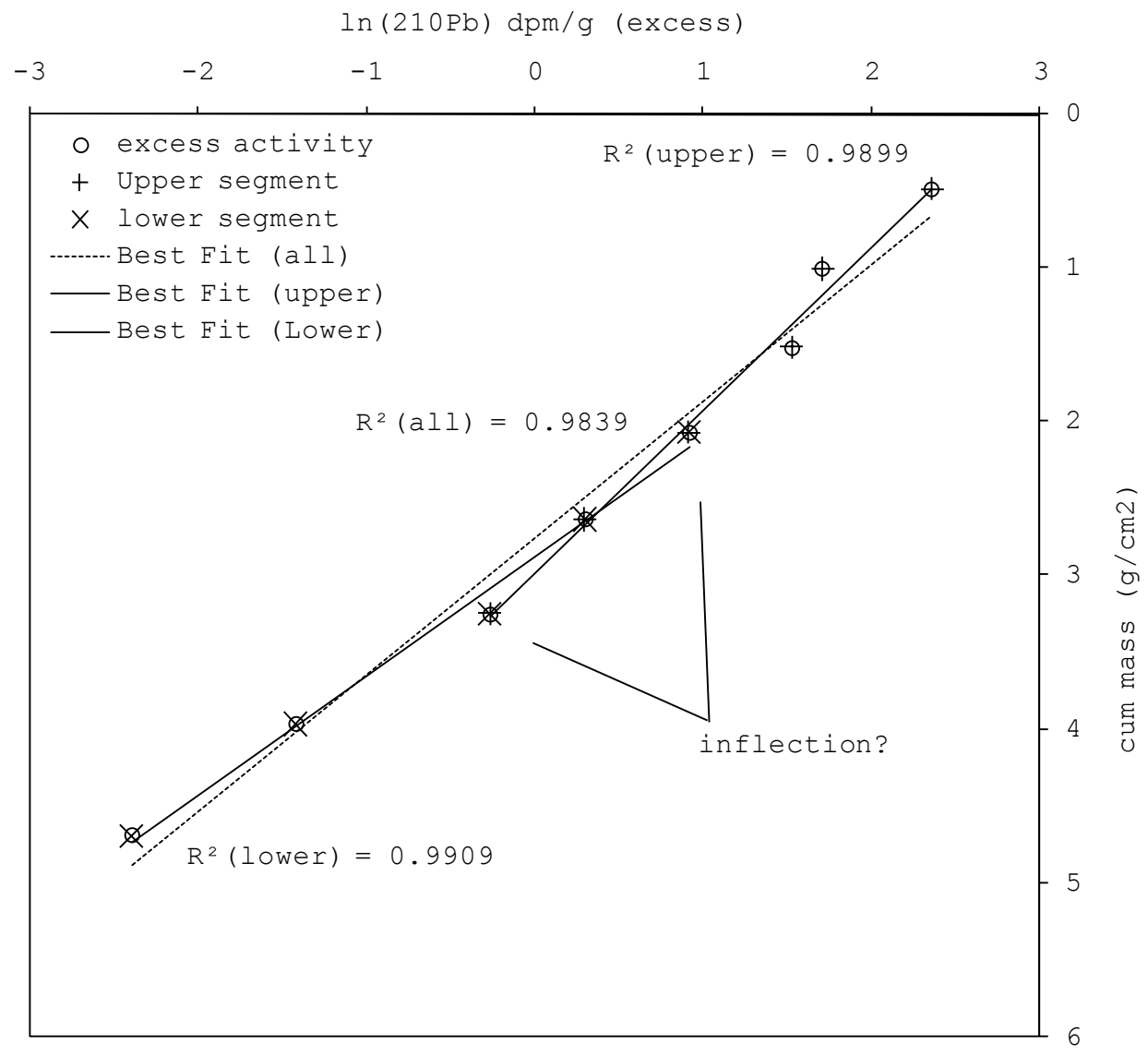

Figure 38. Linear regression of excess 210Pb values by depth for core OZ1005-4 showing relative fit of single-stage and two-stage regression.

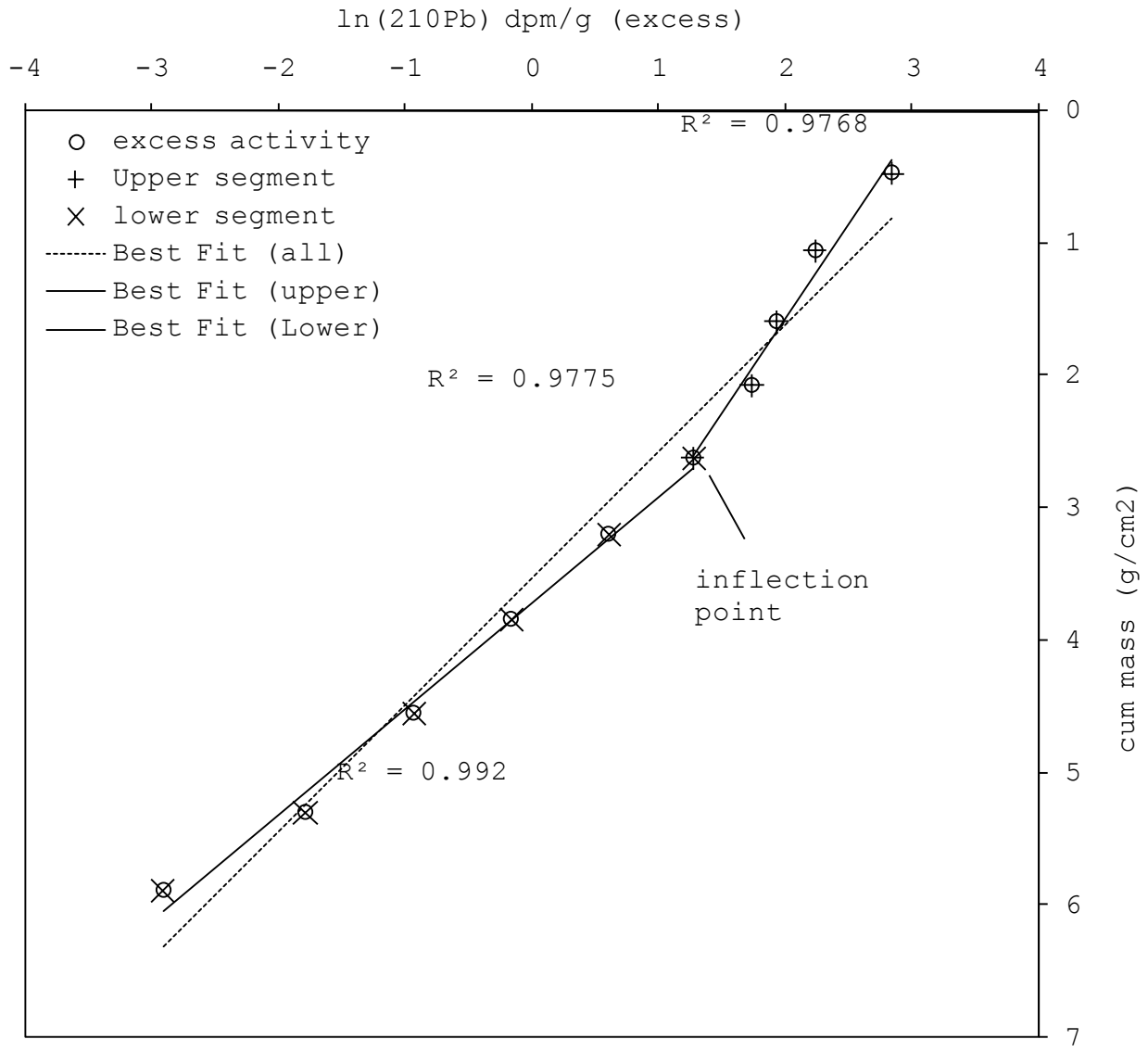

Figure 39. Linear regression of excess 210Pb values by depth for core OZ1005-5 showing relative fit of single-stage and two-stage regression.

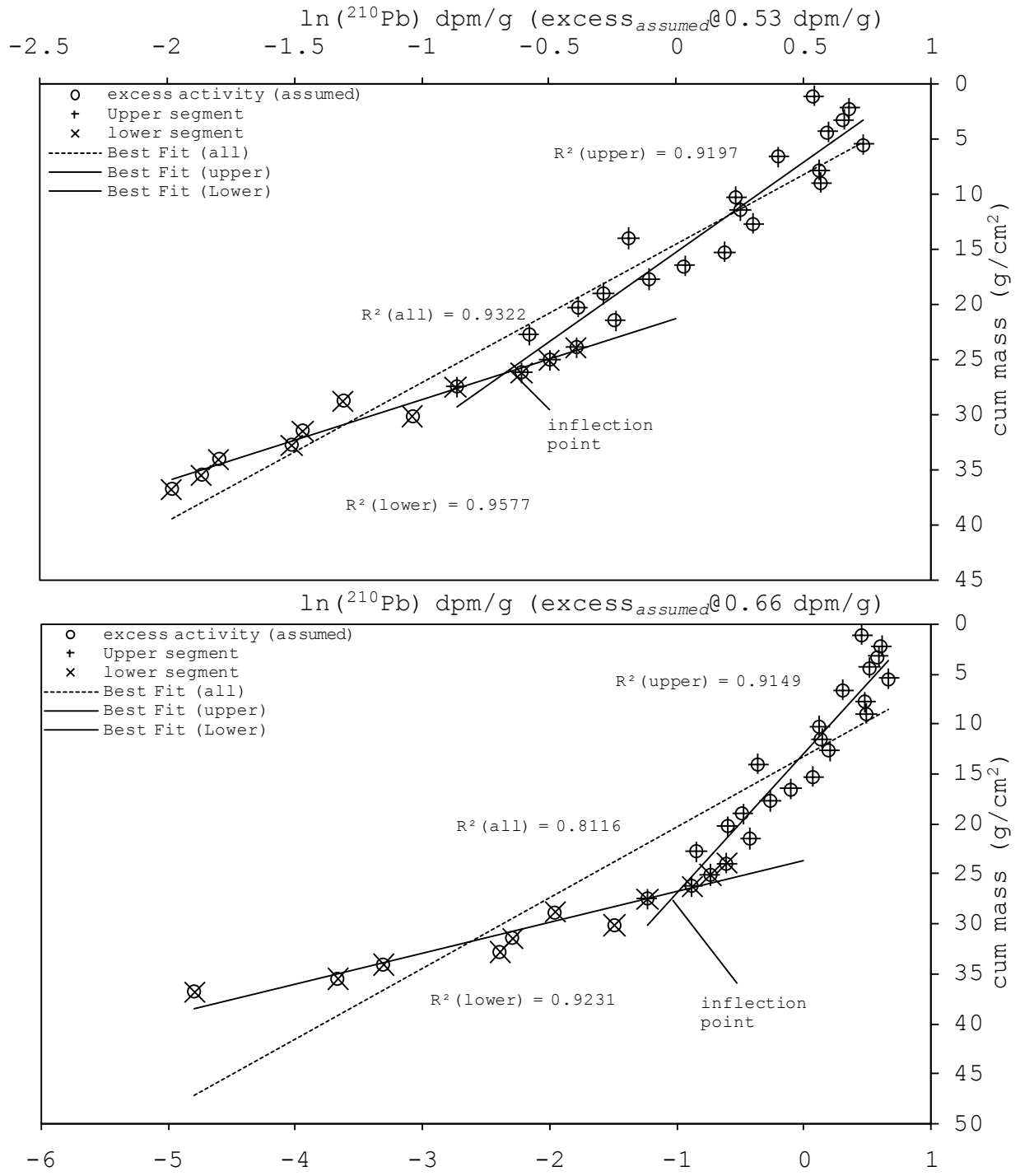

Figure 40. Linear regression of excess ^{210}Pb values by depth for core OZ0906-1 showing relative fit of single-stage and two-stage regression for supported values of 0.53 dpm/g (preferred) and 0.66 dpm/g.

Table 8 summarizes the inferred magnitude and date of the change in mass accumulation rate for each core where an inflection (^{210}Pb date) was detected. Upper and lower dates provide a maximum and minimum age for the sampled interval containing the inflection point. These

bounding ages are based on the ^{210}Pb date at the inflection, with the higher accumulation rate applied to the 1 cm above the sample midpoint, and the lower rate applied to the 1 cm below. Cores OZ1005-2 and OZ0906-1 are shown with various scenarios for supported ^{210}Pb activity. Preferred values are indicated in the table. Note that for non-preferred estimates,

Table 8. Summary of ^{210}Pb profiles in 5 cores from Lake Ozette showing shifts in mass accumulation rate. Preferred value for supported ^{210}Pb activity when estimated is indicated with *.

Core	^{210}Pb *supported*	inflection depth	MAR (g/cm^2) (S) (upper)	MAR (g/cm^2) (S) (lower)	ΔS	^{210}Pb age	^{210}Pb date	upper date	lower date	^{210}Pb age @ depth
oz1005-1	0.68$_m$	7	0.29	0.05	5.5	24.4	1981	1982	1974	101
*oz0906-1**	*0.53$_e$*	*43*	*1.00*	*0.13*	7.9	*36.8*	*1968*	1969	1964	*81**
oz0906-1	*0.66$_e$*	*43*	*1.17*	*0.36*	3.2	*43.0*	*1962*	1962	1960	*169*
*oz1005-2**	*0.53$_e$*	*21*	*0.48*	*0.20*	2.4	*43.5*	*1962*	1962	1959	*94**
oz1005-2	*0.6$_e$*	*21*	*0.47*	*0.17*	2.8	*45.1*	*1960*	1961	1957	*105*
oz1005-2	*0.68$_e$*	*21*	*0.45*	*0.12*	3.6	*47.2*	*1958*	1959	1954	*128*
oz1005-2	*0.75$_e$*	*21*	*0.43*	*0.11*	3.8	*49.1*	*1956*	1957	1952	*216*
oz1005-4	0.78$_m$	7	0.15	0.08	2.0	46.6	1958	1960	1955	122
oz1005-5	0.78$_m$	9	0.19	0.08	2.3	46.6	1958	1960	1955	165

$_m$ - measured 210Pb activity

$_e$ - estimated supported 210Pb activity

* - Preferred estimate of supported activity

Because supported ^{210}Pb activity was not reached on core OZ0906-1 and OZ1005-2, the date for the timing of this shift in accumulation rate is less certain. However, upper and lower bounds for supported activity can be reasonably well constrained. The upper bound for supported activity was the lowest total activity measured in the core (rounded down 0.01 dpm/g). The lower bound was the lowest supported activity measured in any core. This value, 0.53 dpm/g, was measured in core OZ1005-3, which was also the closest site where supported activity was measured. It is the preferred estimate of supported ^{210}Pb activity for both cores.

Upper and lower ages (upper date and lower date in Table 8) were calculated for each 2 cm subsample where inflection points were identified by applying the mass accumulation rate from the slope of the upper line to the upper half, and the slope of the lower line to the lower half of the subsample. This assumes equal mass above and below the ^{210}Pb date (essentially a well-mixed subsample). The resulting date range represented for each 2 cm subsample in cores where inflection points were identified is shown in Figure 41.

Lower accumulation rates are indicated by longer lines, and more lopsided lines indicate a greater shift in accumulation rates. The highlighted portion of the timeline shows the minimum time interval which intersects all preferred ^{210}Pb dates (light gray) and sample intervals, excluding Umbrella Creek (dark gray). The light gray bar spans the period from 1960 – 1982, and the dark gray bar spans the period from 1963 – 1964. Grayed-out sample names show results using other (non-preferred) estimates of background activity.

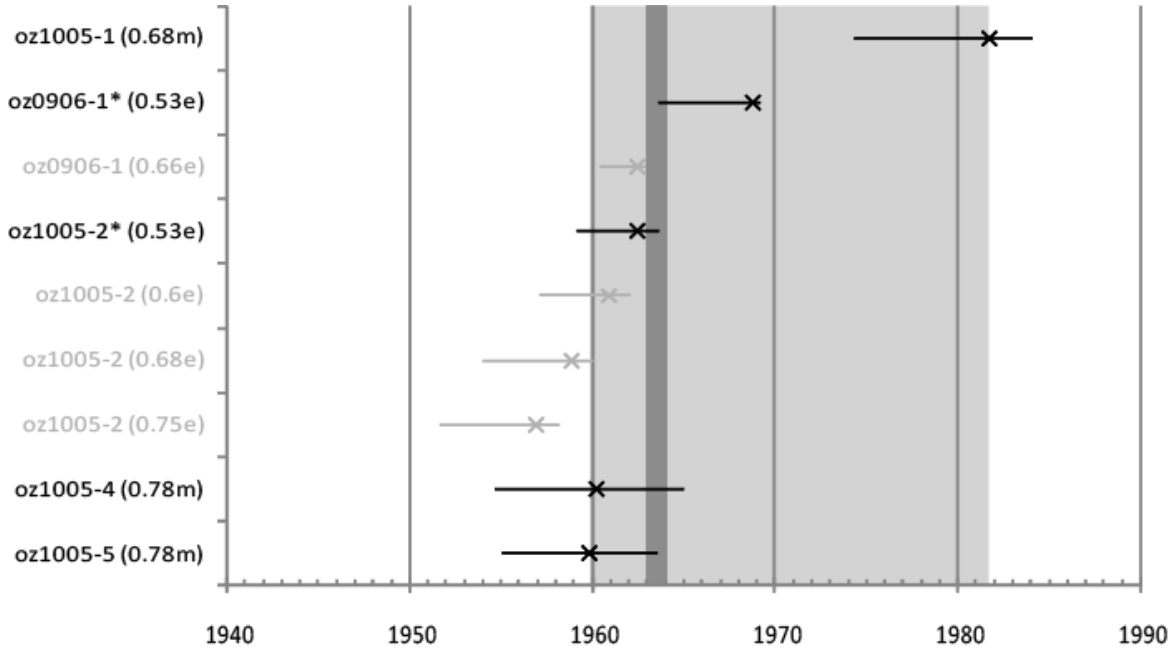

Figure 41. ^{210}Pb dates of inflection points in ^{210}Pb activity profiles, from north to south. Supported activity is in parentheses. Measured supported values are indicated by an "m", and estimated values by an "e") following the activity. Preferred values when supported activity is estimated are indicated with a "*". Lines represent upper and lower age of sample interval assuming 2 cm subsamples are well mixed. Outer and inner gray vertical bars show best fit to all preferred ^{210}Pb dates, and 2 cm intervals, excluding the North End, respectively.

Core locations (Figure 5) do not appear to differentiate timing of the inflection point within the resolution of the analysis, with the possible exception of core OZ1005-1, This core showed a later inflection than other cores, as well as a six-fold increase in accumulation rate. The core was located in the middle of the North End, and one possible explanation for this is a lag between an increase in deposition near tributary mouths and transport northward toward the lake outlet.

Interestingly, this lag is not apparent in core OZ1005-4 and OZ1005-5, located in depocenters in the deeper main east and west basins. It is also possible that this is an artifact of sampling intervals being coarse relative to the pre-inflection accumulation rates in cores such as OZ1005-1, that have low long-term (and pre-inflection) accumulation rates.

3.2.2 Long-term accumulation rates (^{14}C isotope analysis)

All ^{14}C samples processed yielded valid ^{14}C age determinations. Probability distributions are shown for all samples in Figure 42, and Table 9 shows raw and calibrated dates for each sample. The age of sediment at the base of each core ranged from a minimum of ~300 years in Swan Bay to a maximum of ~2900 years in the western main basin of the lake.

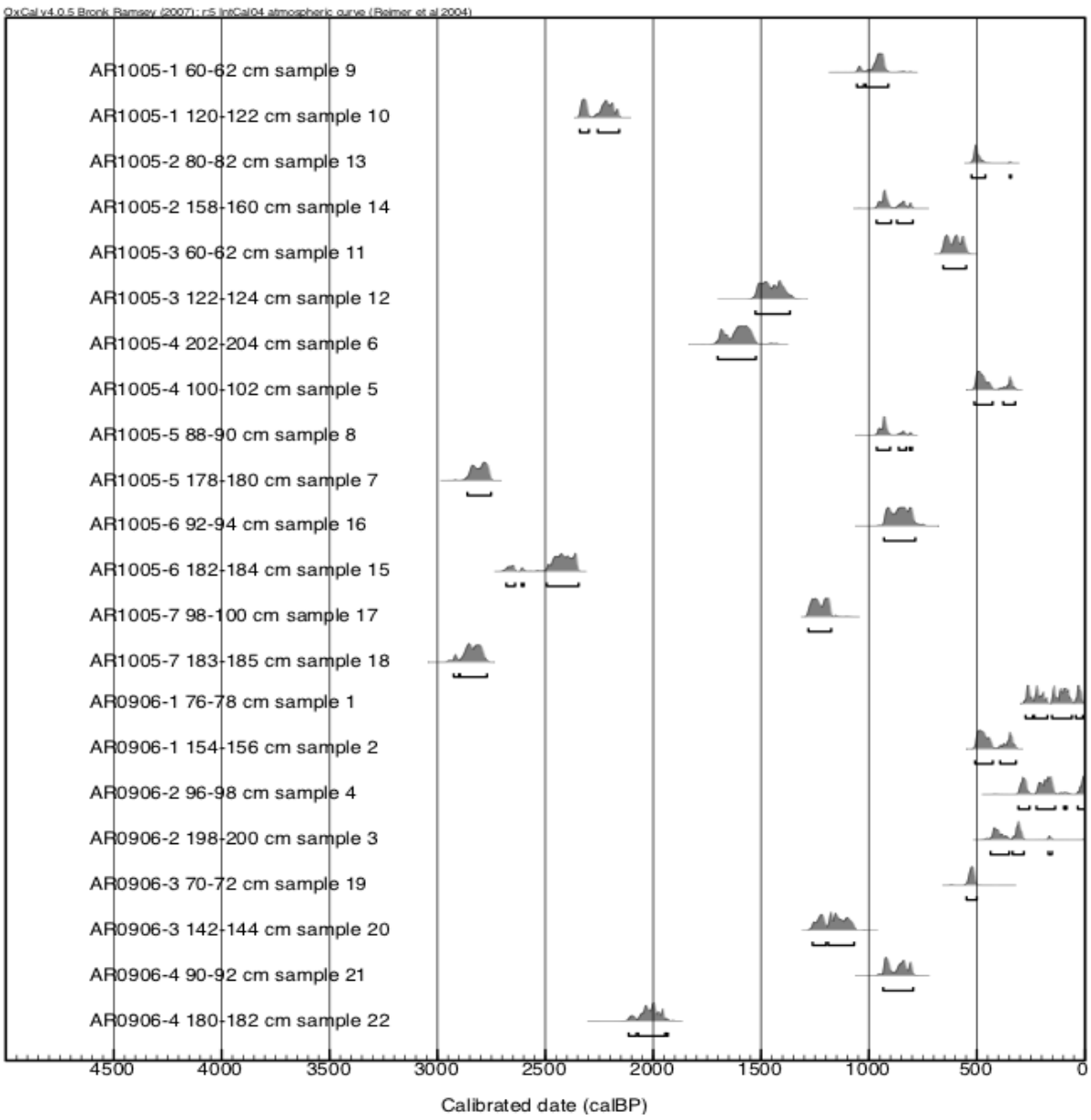

Figure 42. Probability distribution of calibrated ^{14}C dates (calendar years BP) for all cores. Bracketed ranges are for the 95.4% probability distribution for a given date.

Three dates from the cores OZ0906-1 and OZ0906-2 have insufficient age control to allow extraction of meaningful information. This is demonstrated by the large RSD of the calibrated age shown in Table 9. These ages and accumulation rates derived from them are gray in Table 9 and Table 10.

Table 9. Uncalibrated and calibrated ages (years BP) for ^{14}C samples from Ozette sediment cores. Gray values have RSD > 30%.

Core	*Sample depth (cm)*	*NOSAMS 14-C BP*		*OxCal cal BP (2σ)*		*RSD*
		R_Date	*error +/-*	*oldest*	*youngest*	*(σ/μ)*
OZ1005-1	60-62	1040	35	1056	911	10%
	120-122	2250	25	2340	2158	6%
OZ1005-2	*80-82*	*430*	*25*	*525*	*342*	*30%*
	158-160	995	30	965	797	13%
OZ1005-3	60-62	615	30	656	550	12%
	122-124	1550	35	1526	1366	8%
OZ1005-4	*100-102*	*395*	*30*	*512*	*322*	*32%*
	202-204	1690	40	1701	1524	8%
OZ1005-5	88-90	1000	25	964	801	13%
	178-180	2700	35	2861	2752	3%
OZ1005-6	92-94	945	35	930	785	12%
	182-184	2400	30	2681	2346	9%
OZ1005-7	98-100	1280	25	1281	1175	6%
	183-185	2750	30	2925	2770	4%
OZ0906-1	*76-78*	*135*	*20*	*274*	*9*	*132%*
	154-156	*385*	*30*	*508*	*319*	*32%*
OZ0906-2	*96-98*	*200*	*35*	*307*	*-4*	*145%*
	198-200	*275*	*30*	*437*	*153*	*68%*
OZ0906-3	70-72	490	30	548	500	6%
	142-144	1230	30	1261	1069	12%
OZ0906-4	90-92	970	30	934	795	11%
	180-182	2050	25	2114	1932	6%

Table 10. Long-term sediment accumulation rates (cm/yr) for all cores derived from calibrated ^{14}C dates and decompacted sample depths. Gray values have high RSD and were not used to evaluate accumulate rate changes (ΔAR).

	upper core (U)		*whole core (W)*		*lower core (L)*		*mean accumulation rate*			*Δ AR*
Core ID	*min*	*max*	*min*	*max*	*min*	*max*	*U*	*W*	*L*	*(U/L)*
OZ1005-1	0.06	0.07	0.06	0.07	0.05	0.07	0.07	0.06	0.06	1.1
OZ1005-2	*0.17*	*0.26*	0.21	0.25	*0.18*	*0.41*	*0.22*	0.23	*0.30*	
OZ1005-3	0.10	0.12	0.10	0.11	0.08	0.11	0.11	0.10	0.10	1.1
OZ1005-4	*0.23*	*0.36*	0.17	0.19	*0.12*	*0.17*	*0.29*	0.18	*0.14*	
OZ1005-5	0.10	0.13	0.08	0.09	0.07	0.08	0.12	0.08	0.07	1.6
OZ1005-6	0.11	0.13	0.09	0.10	0.07	0.10	0.12	0.10	0.09	1.4
OZ1005-7	0.09	0.10	0.08	0.09	0.08	0.09	0.09	0.09	0.08	1.1
OZ0906-1	*0.29*	*8.91*	*0.33*	*0.53*	*0.18*	*1.97*	4.60	*0.43*	1.07	
OZ0906-2	*0.33*	*-25.53*	*0.51*	*1.45*	*0.27*	*-0.78*	-12.60	0.98	-0.25	
OZ0906-3	0.13	0.15	0.12	0.14	0.11	0.16	0.14	0.13	0.13	1.1
OZ0906-4	0.10	0.12	0.09	0.10	0.08	0.10	0.11	0.10	0.09	1.2

Three additional ^{14}C dates from the midpoints of core OZ1005-2 and OZ1005-4, and the base of core OZ0906-1 have RSDs of about 30%. These dates and accumulation rates derived from them are shaded. Basal dates are better constrained for OZ1005-2 and OZ1005-4 (Table 9), and long-term accumulation rates still provide useful information for these cores (Table 10).

Sediments younger than about 400 ^{14}C years are often difficult to constrain with ^{14}C dates because fluctuations in the ^{14}C calibration curve, combined with error in the uncalibrated ^{14}C date, allow for age solutions over a wide range of values relative to the total age. This is the primary reason for the "bad" dates shown in gray in Table 9 and Table 10. Even at a depth of 1.5 – 2 m (the base of cores OZ0906-1 and OZ0906-2), sediments were young enough that the difference between minimum and maximum age was a large fraction of the total age (Figure 43).

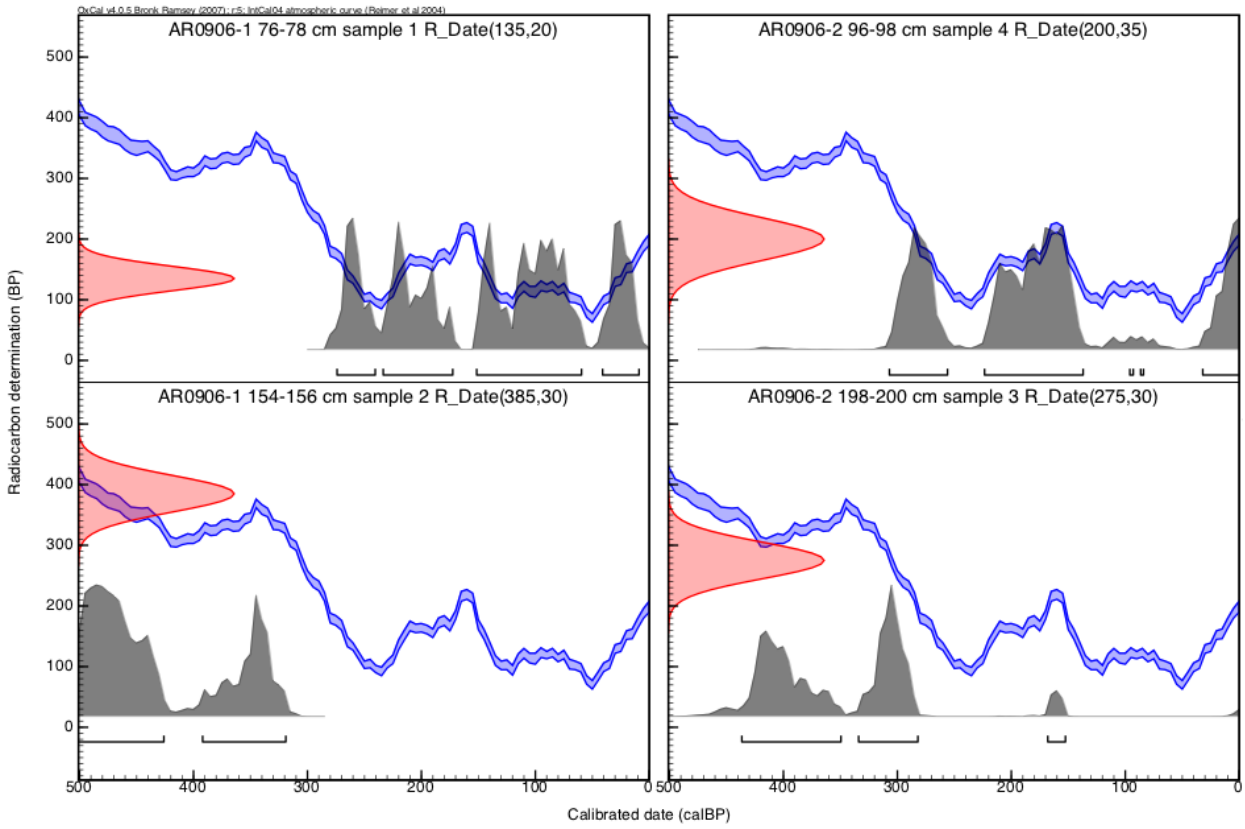

Figure 43. ^{14}C age (red) and calibrated date probability distribution (gray). Brackets are 2σ (95.4%) probability distribution. The blue line is the IntCal04 atmospheric radiocarbon calibration curve for the Northern Hemisphere derived from tree-ring data (Reimer et al 2004).

When all cores with dates having a RSD > 30% are excluded (bold and gray entries in Table 10), the seven remaining cores all show higher accumulation rates in the upper half of the core than in either the whole core or the lower half of the core. For these seven cores, mean upper core accumulation rates are 14% higher than whole-core accumulation rates, and 24% higher than lower core accumulation rates.

Because ^{14}C samples were processed from just the midpoint and bottom of each core, only a coarse scale comparison of recent and more ancient accumulation rates could be calculated using these data. Table 10 shows these calculations - the maximum, minimum, and mean decompacted accumulation rates for the upper (U), whole, (W), and lower (L) section of each core.

Results of sediment accumulation calculations from ^{14}C dates point convincingly to an increase in sediment accumulation rates in the recent past. A single core (OZ1005-2), with relatively poor age control on the upper core date, seen by a RSD of 30% - (Table 9) indicates a higher accumulation rate in the basal half of the core. Eight other cores show higher accumulation rates in the upper half of core than in either the whole core or the lower core. Two cores (gray records in Table 9 and Table 10) were excluded from this analysis.

3.3 $\delta^{13}C$ and $\delta^{15}N$ isotope values in Lake Ozette

The range in both $\delta^{13}C$ and $\delta^{15}N$ values was relatively small in sampled sediments. The range of $\delta^{13}C$ values in this study was -27.7‰ to -26.7‰. Isotope values for $\delta^{15}N$ showed a wider range, from 0.6‰ to 3.1 ‰. C:N mass ratio varied from 11.5 to 20, %C from 1% to 6.1%, and %N from 0.1% to 0.4%. The strongest signals in these profiles are a down core increase in C:N ratio (6 of 7 profiles), down-core decrease in $\delta^{15}N$ values (5 of 7 profiles), and down core variations (increase and decrease) in $\delta^{13}C$ profiles.

Stable isotope profiles by depth are shown in Figure 44 - Figure 50 for the seven sampled cores. The three cores from 2005 were sampled to a depth of 60 cm. Two cores from 2006 were sampled throughout their depth, and two were sampled to a depth of 60 cm.

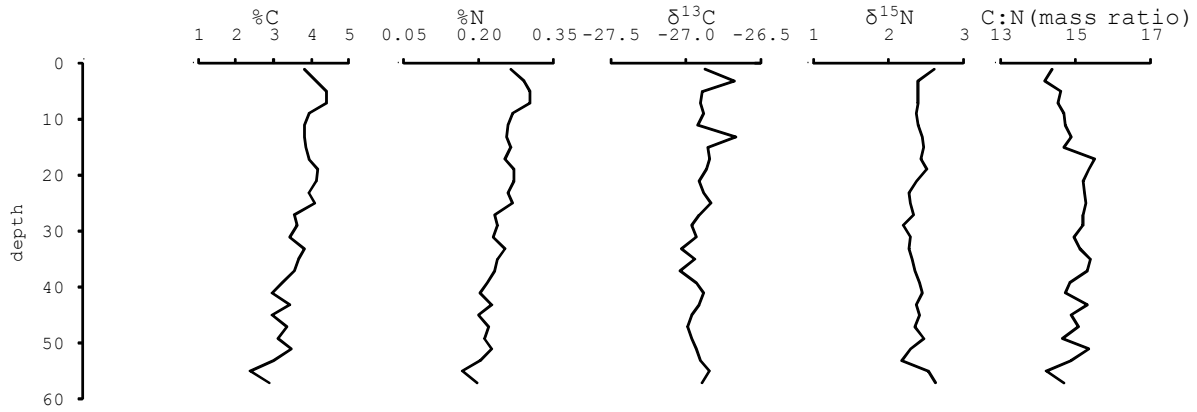

Figure 44. Carbon and nitrogen elemental and isotope values for core OZ1005-1

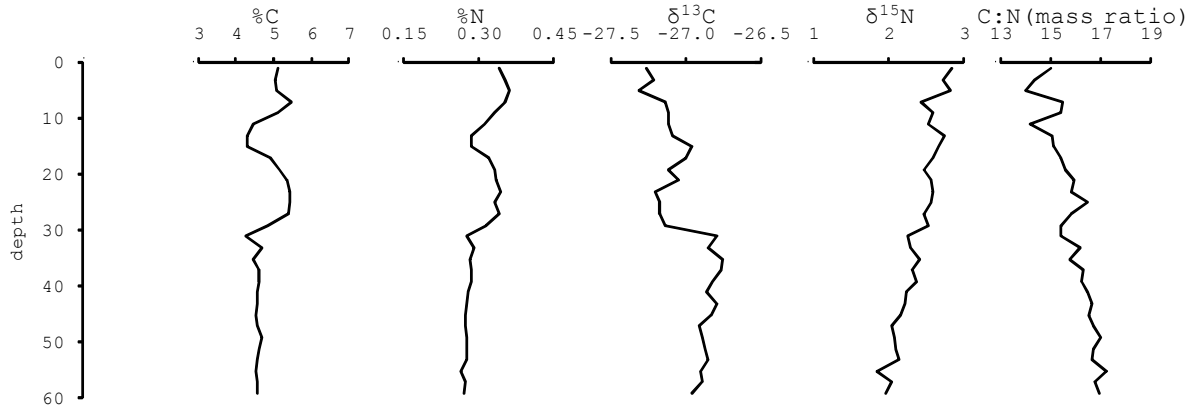

Figure 45. Carbon and nitrogen elemental and isotope values for core OZ1005-4

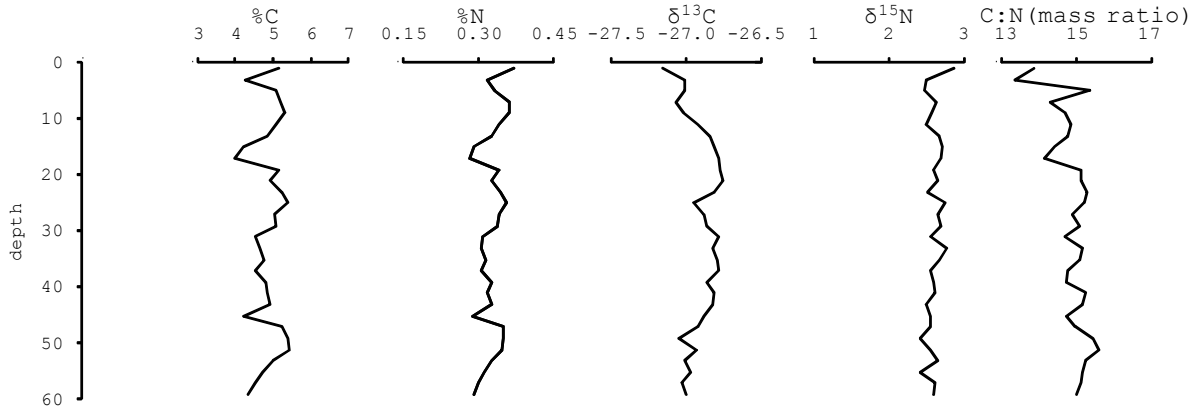

Figure 46. Carbon and nitrogen elemental and isotope values for core OZ1005-5.

Cores from 2005 are not well constrained below about 15 cm. ^{210}Pb data indicate that a depth of about 15 cm is approximately 100 years old in all three samples. However, ^{14}C dates are only available at the base, or below the sampled intervals. These dates indicate that OZ1005-1 is about 1000 years at 60 cm, OZ1005-4 is about 400 years at 100 cm, and OZ1005-5 is about 1000 years at 90 cm. Accordingly, isotope values from core OZ1005-1 represent about the last 1000 years, core OZ1005-4 is less than 400 years, and OZ1005-5 is less than 1000 years. This complicates comparison between cores to analyze stable isotope trends.

Samples from 2006 are somewhat better constrained than those from 2005, and in particular, core OZ0906-1 has good agreement between ^{210}Pb age profiles and ^{14}C age profiles. Since this core is also proximal to the largest tributary, it represents probably the best record of trends in stable isotope values of inputs to Lake Ozette over the last several hundred years.

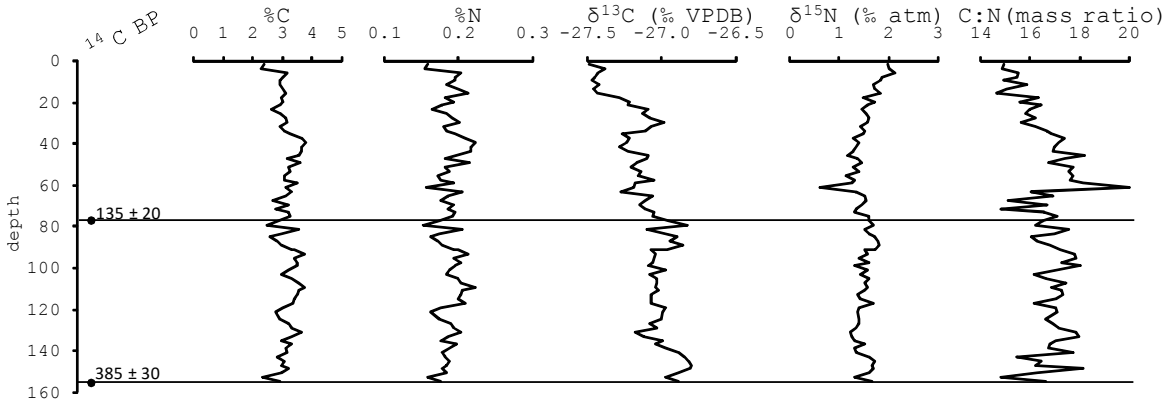

Figure 47. Carbon and nitrogen elemental and isotope values for core OZ0906-1.

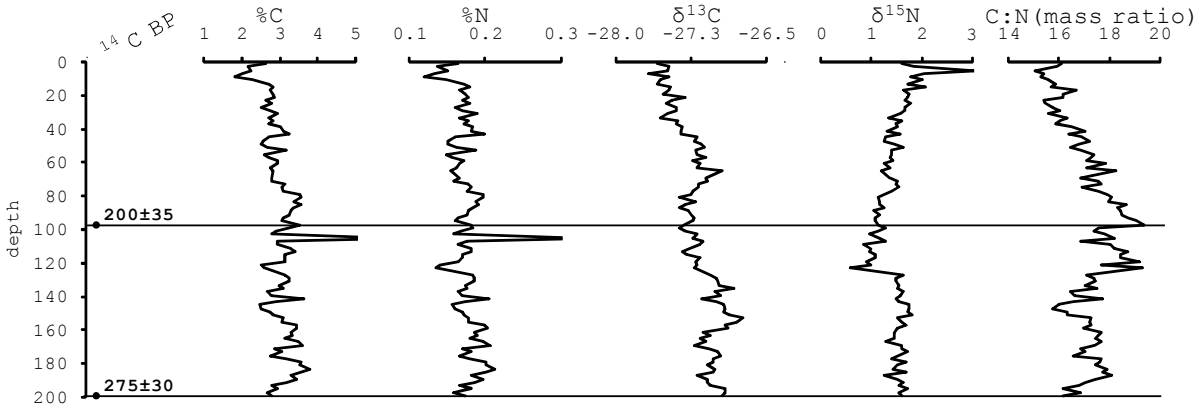

Figure 48. Carbon and nitrogen elemental and isotope values for core OZ0906-2.

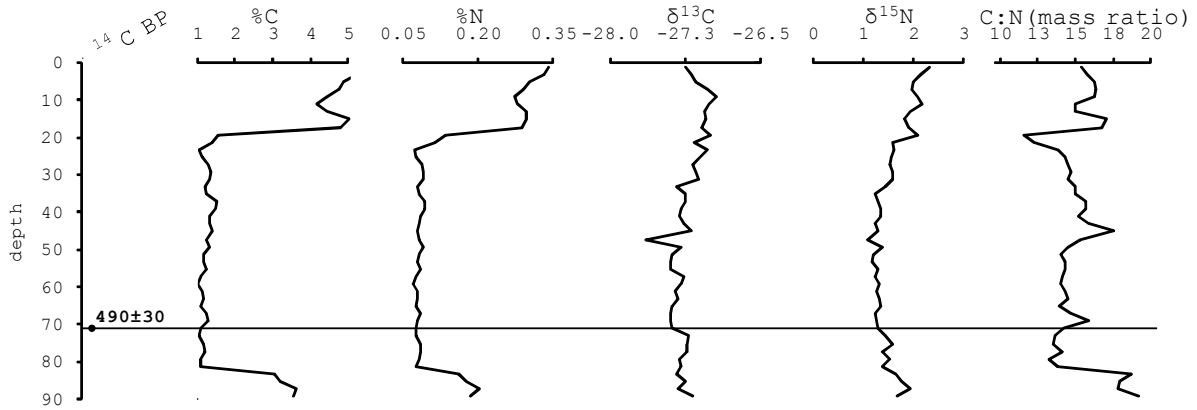

Figure 49. Carbon and nitrogen elemental and isotope values for core OZ0906-3.

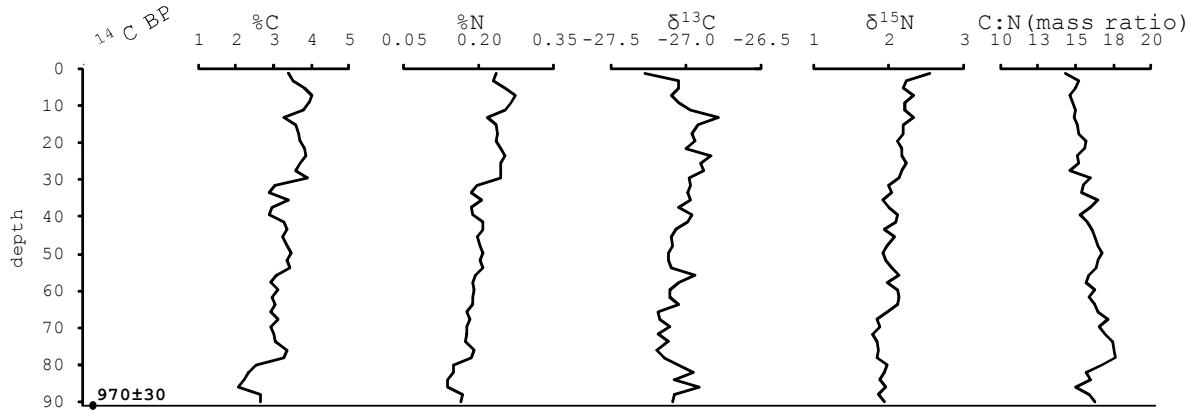

Figure 50. Carbon and nitrogen elemental and isotope values for core OZ0906-4.

Similarities in profiles of $\delta^{13}C$, $\delta^{15}N$, and C/N ratio in cores OZ0906-1 and OZ0906-2 (Figure 47 and Figure 48) suggest that the accumulation rate in OZ0906-2 is roughly twice that of OZ0906-1. However, care should be used in this interpretation. Core OZ0906-4 shows similar trends in $\delta^{15}N$ and C/N ratio, with a much older basal date (Figure 50). Perhaps equally significant is that cores from the eastern side of the lake show a down-core decrease in $\delta^{15}N$, while cores OZ1005-1 and OZ1005-5, taken from the west basin (Figure 5), show relatively stable values.

Anomalously low values in core OZ0906-3 (Figure 49) between about 22 and 80 cm may indicate an event deposit here. Several distinct sand lenses are visible in x-rays of the core at depths of about 30 and 80 cm (Appendix A).

A comparison of $\delta^{13}C$ vs. $\delta^{15}N$ values (Figure 51) does not show a correlation between $\delta^{13}C$ and $\delta^{15}N$ values. Other researchers have reported positive correlations (Hodell and Schelske 1998) as well as negative correlations (Herczeg et al 2001), although isotope values in these studies have spanned a much wider range than those reported here. There is overlap between 2005 and 2006

cores, but interestingly the 2005 cores show both $\delta^{13}C$ values and $\delta^{15}N$ values which are more positive than the 2006 cores, with little overlap in the $\delta^{15}N$ ranges. Core OZ1005-4, from the deepest portion of the lake, is intermediate between the 2006 cores (in the eastern half of the lake) and the two other 2005 cores, which are in the deepest portions of the west basin.

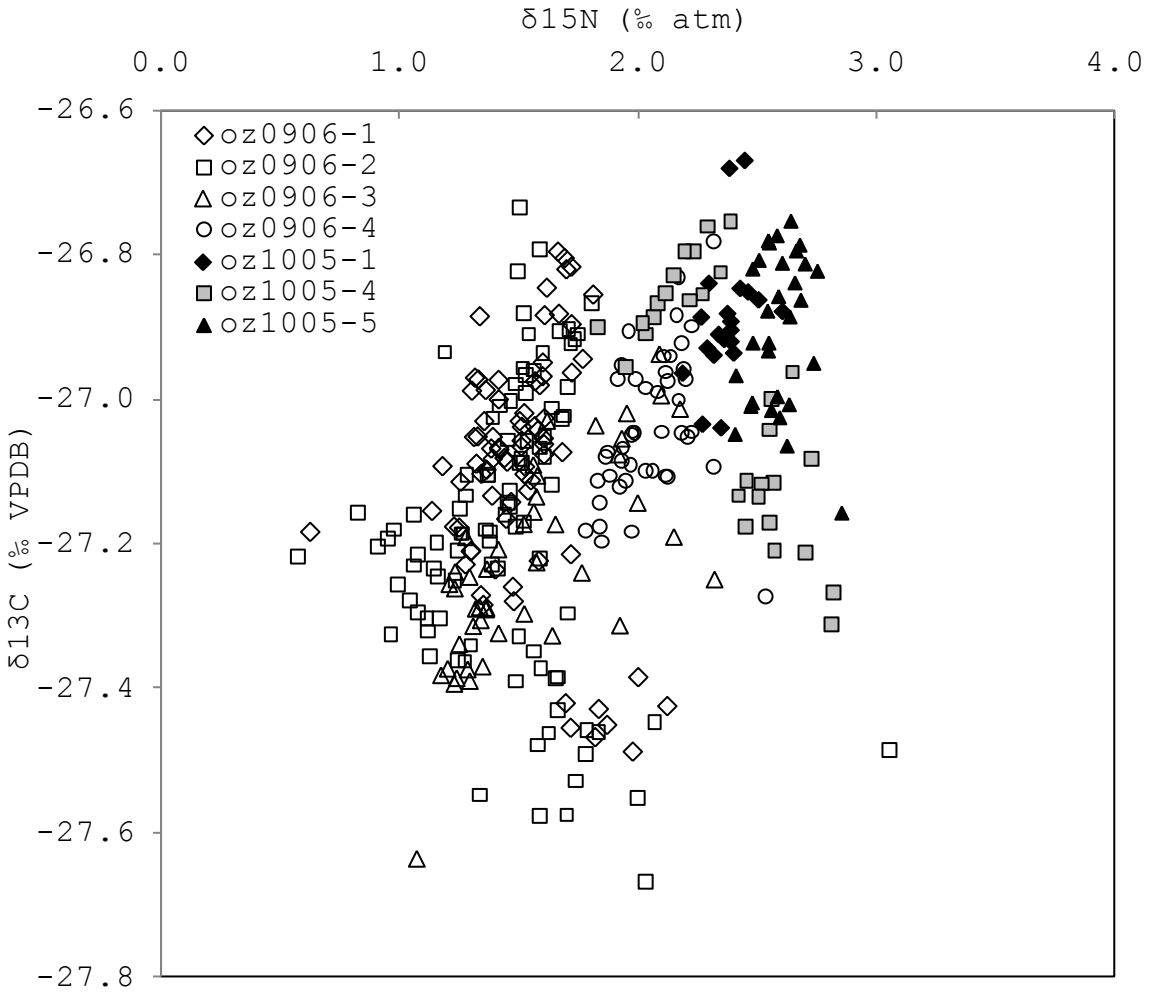

Figure 51. Relationship between $\delta^{13}C$ and $\delta^{15}N$ in sampled cores from 2005 (solid markers) and 2006 (hollow markers).

The offset seen in $\delta^{13}C$ vs. $\delta^{15}N$ is also apparent when comparing the C:N ratio (Figure 52), particularly if the two cores from the west basin are grouped together. Again, core oz1005-4 is intermediate between the 2006 cores and the two west basin cores from 2005. This offset between entire cores suggests that variations in isotope values and C:N ratios are a function of differences in the core locations, such as depth or distance from terrestrial inputs.

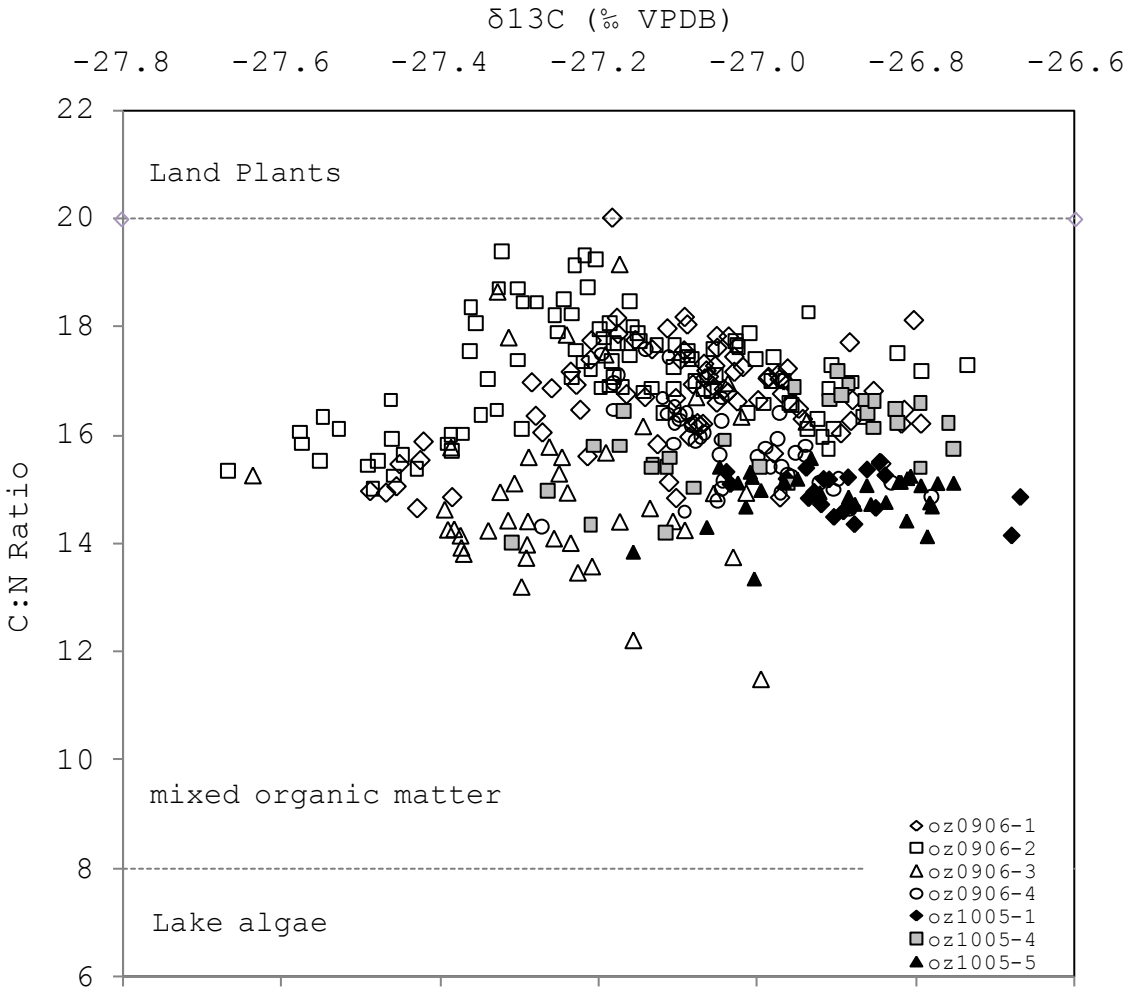

Figure 52. Comparison of C:N ratio and $\delta^{13}C$ values for all samples sampled for stable isotope values.Representative ranges of terrestrial and aquatic values from Meyers (1994).

4 DISCUSSION

4.1.1 Shoreline and watershed changes

The U.S. Forest Service (USDA 1993) uses both road density and hydrologic maturity to develop a watershed risk rating. Their metrics are percent of watershed in stands less than 30 years, and road density. Based on current road densities in the Ozette watershed (Figure 25) and annualized sub-basin harvest rates (Table 6), the entire watershed, and all of the major sub-basins fall into the highest watershed risk rating for cumulative risk of adverse effects (Figure 53).

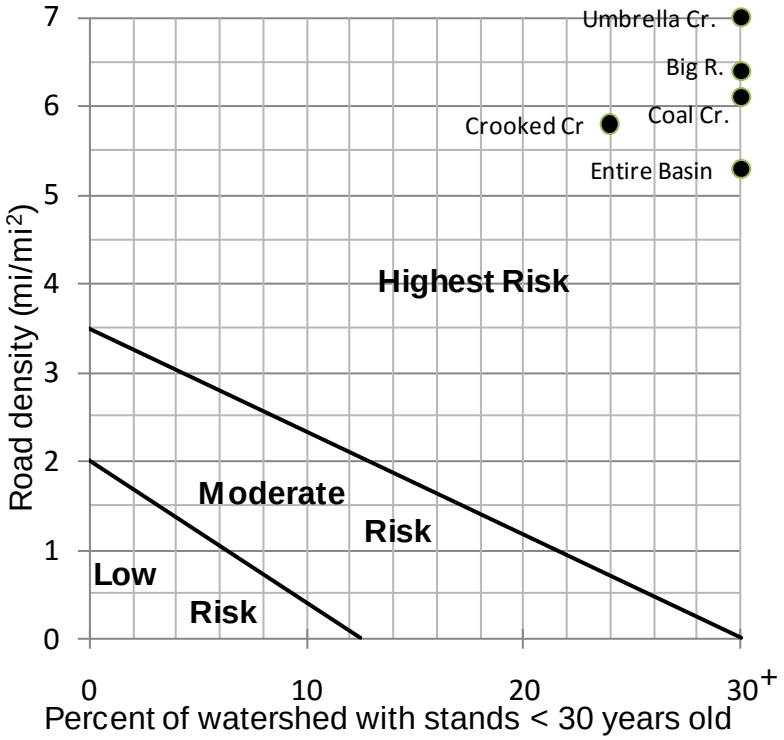

Figure 53. Watershed risk rating with representative values from the Ozette basin plotted for reference (after USDA 1993).

Beechie et al (2003) identified road densities of greater than 2.0 km/km^2 as likely impaired. Ratings for watershed hydrologic condition developed as part of NOAA Fisheries Matrix of Pathways and Indicators (NMFS 1996) considers watersheds with road densities greater than 1.9 km/km^2 (3 mi/mi^2) as not properly functioning due to significant (e.g., 20-25%) increase in the drainage network density due to roads. Current road densities in the Ozette basin are more than double this density, averaging 4.0 km/km^2 (6.4 mi/mi^2) on private lands, and ranging from 3.6 to 4.6 km/km^2 (5.8 – 7.4 mi/mi^2) for the four largest tributaries, with the highest densities found in the Umbrella Creek sub-basin.

Virtually the entire privately held portion of the Ozette basin has been heavily roaded and converted from primary forest to commercial forest in <50 year rotations between 1953 and 2003. Between 1953 and 1994, 70% of the Ozette watershed, and about 80% of privately held

land, was harvested. Umbrella Creek, the third-largest sub-basin in Ozette, experienced the most rapid road-building and most complete removal of original forest.

As a result of increased sediment flux from timber harvest and road building in the Umbrella Creek watershed, the Umbrella Creek delta has grown substantially. During the 15 years of peak timber harvest and road building between 1964 and 1979, the delta grew by about 2.4 ha, and sockeye salmon stopped using the delta for spawning. In the same 15-year period, 72% of the watershed was harvested (Figure 21), and road densities increased four-fold, from about 1 km/km^2 (1.6 mi/mi^2) to about 4km/km^2 (6.4 mi/mi^2) (Figure 29). By 1981, sediment accumulation rates offshore from the delta increased more than five-fold over pre-disturbance rates (Figure 36; Table 5). In contrast to virtually everywhere else along the lakeshore, open beach area on the Umbrella Creek delta increased between 1953 and 2003.

In the shoreline analysis only one other area (tributary 20.0078, a small, steep stream east of Baby Island) showed an increase in open beach area in the shoreline analysis. The increase in unvegetated area in these two locations, and nowhere else, and the dramatic growth of Umbrella Creek delta and its associated spits (Figure 18 and Figure 19) indicates that sediment flux into the lake at these locations probably overwhelms colonizing vegetation. Herrera (2006) found that Umbrella Creek delta was the coarsest delta sampled. During research at the mouth of tributary 20.0078 in the winter of 2008-2009, instruments were buried by a ~50 cm wedge of sediment deposited in a single event. This sediment was subsequently scoured out and transported into deeper water south of the delta (Aaron Brooks, pers. comm. 26 Feb. 2009).

Both the loss of sockeye spawning grounds and the increase in open beach area at the Umbrella Creek delta can be explained by rapid deposition on the delta. Delta growth requires high sediment flux, which in combination with peak storm discharges and fluctuating lake levels, has created an unstable environment where vegetation cannot become established. The increase in unvegetated area is a consequence of increased sediment flux, which also makes the delta unsuitable for spawning sockeye salmon. In this environment, eggs are easily buried or scoured, and survival to emergence is unlikely.

These observations, and data presented here, indicate that sediment delivery into the lake is potentially significantly higher than current estimates, such as those by Herrera (2006). The Umbrella Creek delta progrades into deep water (20 to 60 m), and a substantial amount of sediment is necessary to grow the delta surface by ~2 ha. For example, if the delta prograded onto a flat surface at 20 m depth and maintained its current clinoform, 2 ha of progradation would represent about 400,000 m^3 of sediment delivery to the lake. This is about 4x more sediment than would be delivered by current sediment production rates estimated by Herrera (2006) over the last 50 years.

Without accurate bathymetry and sub-bottom imagery of Lake Ozette, it is difficult to constrain the depth or aerial extent of delta progradation, and estimates of sediment volume represented by the delta should be treated with caution. Delta clinoforms are complex, and while generally the clinoform is maintained as the delta progrades (Pratson et al 2007), more data are needed to constrain the volume of sediment represented by delta growth. The amount of progradation, combined with lake depths off the delta, implies higher sediment inputs than have been estimated

by other researchers. This warrants further investigation, and more data are needed to accurately calculate the volume of sediment represented by delta growth. Regardless, until sediment flux at the delta is reduced, it is difficult to imagine that it can provide suitable spawning substrate for sockeye salmon.

Between 1953 and 2003, more than half of the open beach area along the shore of Lake Ozette was covered by vegetation. This marked change is possibly related to increased fine sediment input, to changes in lake hydroperiod (the timing of water-level fluctuations), or both (Haggerty et al 2009). Increased fine sediment around the lakeshore would provide more suitable substrate for vegetation to grow, and a change in the hydroperiod could both reduce wave energy acting on a given shoreline elevation, and reduce the time that the lakeshore is inundated, leading to a longer growing season at lower elevations on lake beaches, and thus more favorable growing conditions for vegetation. The loss of open beach is detrimental to spawning sockeye. In the last 50 years, more than 2/3 of the open beach area has disappeared on the two existing sockeye spawning beaches in Lake Ozette, Olsen's Beach and Allen's Beach. This contrasts to Umbrella Creek delta, where increasing open beach area is a symptom of high sediment flux which also creates an unsuitable environment for spawning sockeye.

In the Ozette watershed, a persistent shift to higher sediment flux and altered hydrologic function occurred between 1964 and 1980. Rather than transient changes during peak old-growth harvest, data reported herein on land cover, road density and sediment accumulation rates indicate that these shifts continue to impair proper watershed function. Therefore it can be concluded that if either hydrologic alterations or fine sediment inputs are to blame, vegetation and high sediment flux will continue to impair existing, historic, and potential sockeye spawning habitat around the lakeshore. If the trend toward less open beach and consequently less lakeshore spawning habitat is to be reversed, investigation of the causal mechanisms for vegetation colonization on lake beaches should be a research priority. Furthermore, it appears that in order to ensure continued availability of open beach area for sockeye spawning, some vegetation removal may be required to mitigate the environmental response to changes outside the watershed. However, understanding why vegetation is growing on formerly open beaches should have at least equal priority to removing the vegetation to mitigate loss of spawning habitat. Furthermore, if sockeye spawning is to be restored to the Umbrella Creek delta, upstream sediment reduction should be a priority.

4.1.2 The sedimentary record in Lake Ozette

Sediments from Lake Ozette contain a well-preserved record of sediment accumulation throughout the Holocene. Acoustic profile data show parallel reflectors indicating flat-lying sediment to depths of about 20 m below the lakebed in the North End, and to about 30 m below the lakebed in the western basin. X-radiographs from cores in these locations revealed mm-scale laminae, which may be varves (annual layers), although the annual nature of the layering has not been confirmed. Both ^{210}Pb and ^{14}C-derived accumulation rates are below 1mm/yr prior to the last 50 years, and terrestrial macrofossils are plentiful and well preserved. The potential is good for sediments in these locations to contain a high-resolution paleoenvironmental record extending for 20 – 30 ka, well into the last glacial period.

Multiple proxies indicate that sediment inputs to Lake Ozette have increased in the latter half of the 20th century (Figure 54, Table 8).

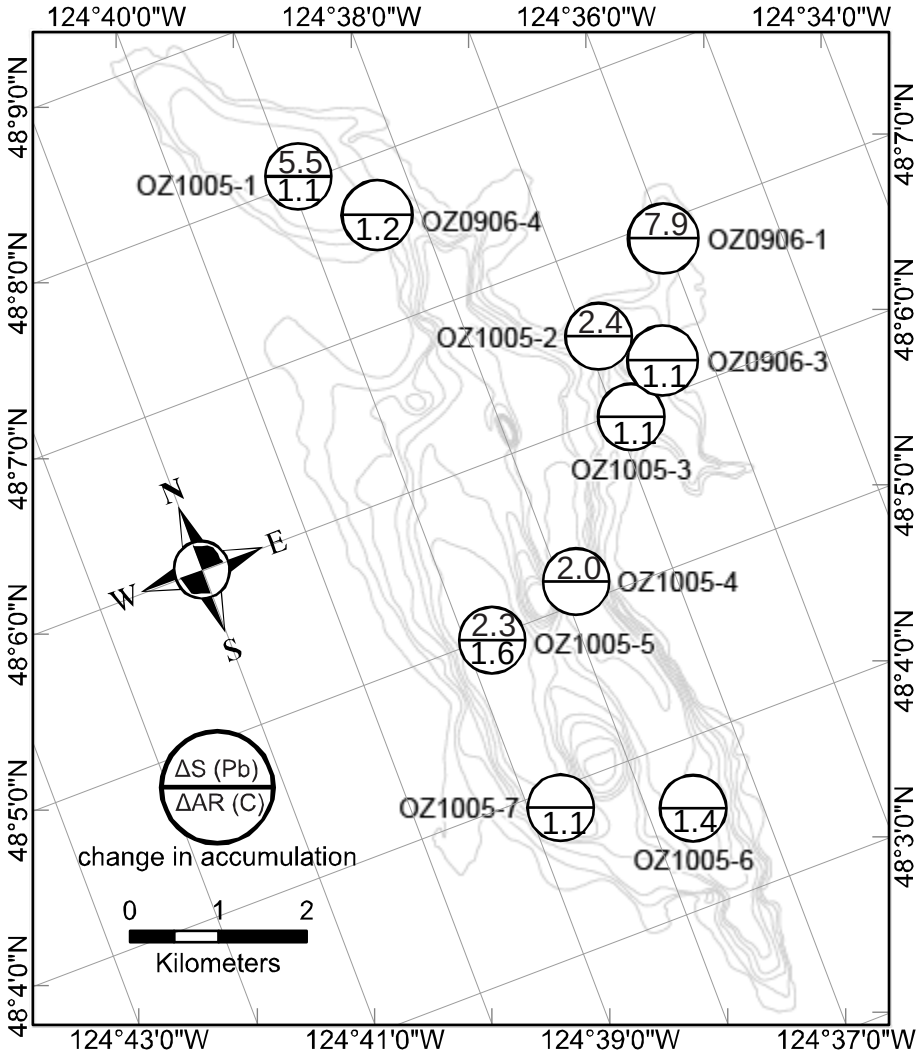

Figure 54. Calculated change in accumulation rates for ten cores in Lake Ozette based on ^{210}Pb and ^{14}C. Upper number is mass accumulation from ^{210}Pb (ΔS), and lower number is vertical accumulation from ^{14}C, adjusted for compaction (ΔAR).

Both ^{210}Pb-derived mass accumulation rates and ^{14}C-derived long-term accumulation rates show an increase in sediment accumulation at the top of cores taken from locations throughout the lake, including areas far from coarse sediment sources (OZ1005-1 and OZ1005-5). ^{14}C dates from the base of cores in areas of low accumulation rates indicate that for about the last 3 ka, long-term accumulation rates have been from one-half to one-eighth of what they are now. ^{210}Pb profiles constrain the timing of the increase to between 1960 and 1982, depending on location. Accumulation rates in most areas of the lake increased between 1960 and 1970, and remained high thereafter.

Every core that had sufficiently clear ^{210}Pb data to calculate mass accumulation rates showed an increase in the accumulation rate (Figure 54; $\Delta S > 1$). The magnitude of change ranged from nearly eightfold near Big River (core OZ0906-1), to about double in the eastern and western basins of the main body of the lake (core OZ1005-4 and OZ1005-5). While the greatest increases in mass accumulation rates were measured near Umbrella Creek (core OZ1005-1; $\Delta S = 5.5$) and Big River (core OZ0906-1; $\Delta S = 7.9$), even areas isolated from direct sediment delivery showed that accumulation rates have more than doubled since 1960 (core OZ1005-5; $\Delta S = 2.3$).

Carbon dates from the middle and bottom of the cores also indicate an increase in recent accumulation rates over long-term rates (Figure 54; $\Delta AR > 1$). Data from ^{14}C dating are more useful for long term accumulation rates than for calculating short-term changes, especially in the modern era, and especially when changed accumulation rates occupy only a small portion of the total core. However, when I compared the accumulation rates based on ^{14}C from the upper half and the lower half of the cores, without exception the upper half of the cores (containing the modern era), showed an increase in accumulation rates. By themselves, these data are meaningless, since any sediment-generating event of low frequency and high magnitude during deposition of the upper half of the core (e.g. earthquake-triggered landslides, submarine landslides, or fires) could cause this difference. But when viewed in combination with ^{210}Pb data, the ^{14}C data support the finding that modern accumulation rates are significantly higher than long-term rates.

The core showing the most recent time of the shift in accumulation rates, OZ1005-1 (Figure 55), also had the lowest measured pre-disturbance accumulation rate, and one of the highest recent increases (from 0.05 g/cm^2 to 0.29 g/cm^2; Table 8). There are several possible explanations for this. First, it is possible that the temporal lag in increased accumulation rates is real. Timber harvest in the Umbrella watershed lagged behind that in Big River by about a decade (Figure 55), and the North End of the lake is more isolated from direct sediment inputs from Big River and Crooked Creek than the other core sites because a sill separates the North End from the main body of the lake (Figure 54). Any inputs from Big River or Crooked Creek would have to remain suspended at depths shallower than this sill and to drift about 4 km through the lake before contributing to sedimentation in the North End.

Sampling limitations (2-cm intervals) may have contributed to this apparent later timing of the change in accumulation rates in the North End (core OZ1005-1). Applying the lower and upper accumulation rate from Table 8 to each half of the 2 cm interval below and above the inflection point respectively results in an age range of 6.3 years for the 1 cm below the inflection point, and 1.1 years for the 1 cm above. With low accumulation rates and a large shift in rates, slight errors in sample-interval collection could include a higher fraction of younger, more active sediment, which would bias the results toward a later shift in accumulation rates. Also in this core, ^{210}Pb levels decayed to background within 14 cm of the surface, so only six samples in the core were above background. While there clearly is a change in accumulation rates, and the best fit of a two-stage regression has a higher R^2 value than a single-stage regression, exactly where to draw the inflection (which sample interval to ascribe it to) can be problematic. Finer-scale sampling (e.g. freeze coring) could help to better resolve the precise timing of the change in accumulation. However it is clear that significant changes in mass accumulation rates have occurred at this site.

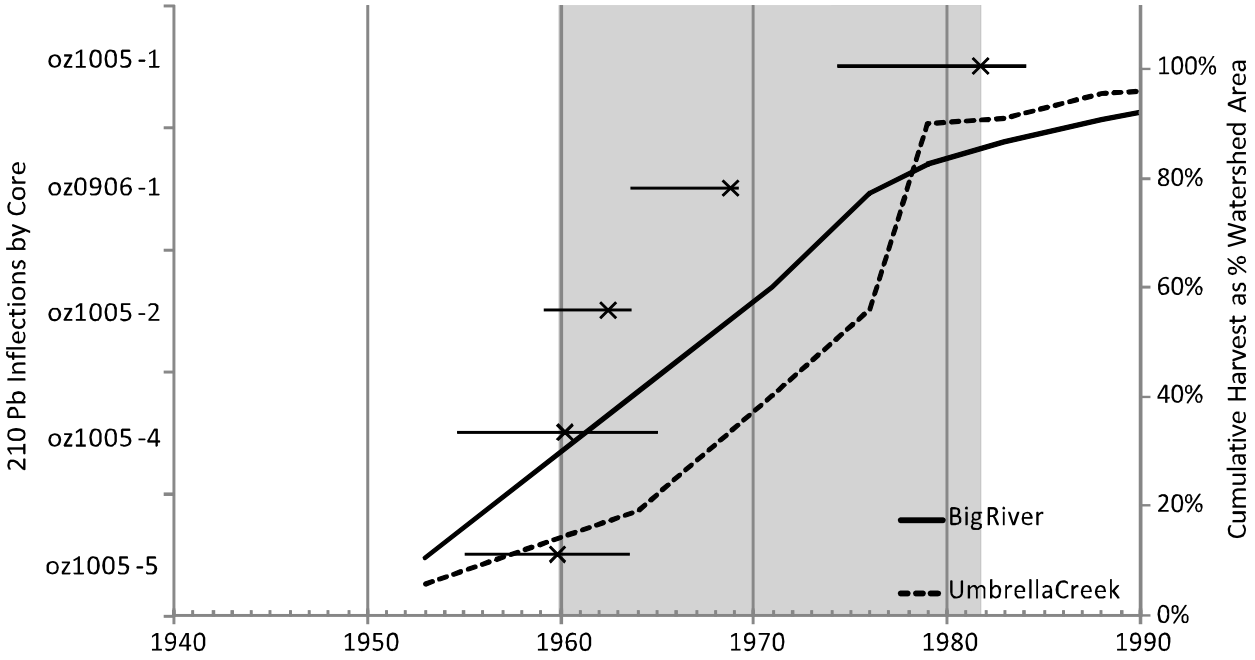

Figure 55. ^{210}Pb inflection points and cumulative harvest for Big River and Umbrella Creek. Shaded area encompasses the time period where accumulation rates increased in cores.

The best-constrained shift in accumulation rates, near the largest tributary, comes from core 0906-1, in the center of Swan Bay (Figure 54). While supported ^{210}Pb activity was not reached in the ^{210}Pb profile of this core, the timing of the shift is constrained to the period between 1960 and 1970 by the high and low estimates of supported activity (Figure 41). Measured supported (or background) activities for each core allow for a more accurate determination of dates down-core because ^{210}Pb dates are calculated based on the amount of unsupported (or atmospherically derived) activity remaining in the core. In the absence of a measured supported activity, supported activity from nearby cores with similar mass-depth ratios was used.

Long-term estimates of accumulation rates from ^{14}C dates do not provide sufficient temporal resolution to quantify changes in sediment inputs in the last century. However, ^{210}Pb profiles do give us this resolution. Close to the mouth of Big River, mass accumulation rates increased between 3- and 6-fold, while in more distal locations, mass accumulation rates increased 2- to 5-fold (Figure 54). Sediment accumulation rates are thus at least 200% of background in all cases, even in cores far from tributary inputs. It is interesting that the core from the North End (OZ1005-1) shows both the most recent shift and one of the greatest increases in accumulation rates. If accurate, this could be a function of lag time from circulation patterns in the lake. Given the well preserved nature of sediments at this location, and the relative ease of access for sampling, this location seems ideal for additional higher-resolution work.

4.1.3 Spatial distribution and timing of changes in sediment accumulation in relation to watershed disturbance.

Shifts in accumulation rates identified in ^{210}Pb profiles indicate that a transition to higher accumulation rates occurred between about 1960 and 1980, coinciding with rapid road-building and deforestation in the watershed (Figure 25; Figure 55), as well as significant delta growth in Umbrella Creek (Figure 20). Longer-term estimates of accumulation rates from ^{14}C dates indicate that these recent elevated accumulation rates are not duplicated in the sedimentary record over the last several thousand years. Similarly, it appears that the increase in the accumulation rate has been sustained into the present. None of the accumulation rate profiles indicates a peak during the early period of land disturbance, or a decrease as road networks were completed and forest practices became more regulated. Subsamples at 2-cm intervals from core OZ0906-1, in the center of Swan Bay, provide roughly biennial resolution from about 1960, when accumulation rates increased to about 1 cm/yr. Figure 40 from core OZ0906-1 shows clearly that after the inflection, accumulation rates remain elevated in Swan Bay, despite slowed rates of road construction and timber harvest in the last few decades.

The similar magnitude of shifts in accumulation rates measured in cores in the western basin and the North End to those seen in Swan Bay implies that land-use impacts are not confined to an area near the tributary mouths. Since sands and silts settle out relatively quickly, and are isolated from both the North End and the western basin, it is likely that increases in accumulation rates measured in both the western basin and the North End are due to transport of the clay fraction far from the input sources.

If the clay fraction is remaining in suspension and being distributed throughout the lake, it could help to explain lake-wide changes in vegetation distribution along the shoreline, although other mechanisms, such as changes in the hydroperiod of the lake, cannot be discounted (see Haggerty et al, 2008). It is likely that watershed changes at the temporal and spatial scale seen in Ozette in the last 50 years have significantly impacted watershed hydrology. With a ~3 m annual fluctuation in lake levels from wet to dry season, it seems equally likely that a change in timing and/or magnitude of lake-level fluctuations is responsible – or at least partially responsible, for the lake-wide changes in vegetation cover.

4.1.4 Stable isotope signatures in Lake Ozette.

Stable-isotope data do not indicate that trophic-level changes have occurred in Lake Ozette surrounding the collapse of Ozette sockeye in the 1950s. This is not particularly surprising because while research in Alaskan lakes has found strong correlations between δ^{15}N values and salmon population variability, research in temperate locales similar to Ozette has failed to identify such correlations. Relative to studies which have used δ^{15}N to track salmon abundance (Finney et al 2000; Finney et al 2002; Gregory-Eaves et al 2004; Schindler et al 2005), isotope values and ranges in the Ozette cores are low, with little variation within or between cores. However, values reported in Ozette are comparable to those found in salmon lakes in southwestern Vancouver Island and Kodiak Island (Holtham et al 2004) and coastal British Columbia (Brahney et al 2006; Hobbs and Wolfe 2008). Measured δ^{13}C varied in Ozette varied by only 1‰ (from -27.7‰ to -26.7‰), and δ^{15}N varied by 2.5‰ (between 0.6‰ and 3.1‰). In

contrast, isotope values in lakes where $\delta^{15}N$ has been correlated with sockeye abundance are typically in the range of 5‰ to 10‰ (e.g. Finney et al 2000). Both stable isotope and C:N ratio data should be interpreted cautiously, but warrant further investigation.

Although Lake Ozette sediments appear to be rich in organics, down-core variation in C and N isotope ratios and values is not necessarily a function of changes in inputs, such as watershed productivity or lake processes. Diagenetic processes can also alter isotope ratios, and even elemental ratios, after deposition.

Lehmann et al (2002) measured changes in all of these parameters in the laboratory under oxic and anoxic conditions, and in a multi-year comparison of sediment cores with data collected from sediment traps during the same years. They found that $\delta^{13}C$ decreased by about 1.8‰ in the laboratory during oxic bacterial decomposition of algae, and by 1.65‰ during anoxic decomposition. In situ measurements showed that $\delta^{13}C$ in varves was about 1.5‰ lower than in sediment collected in sediment traps in the same year as the varve was deposited. In the same study, $\delta^{15}N$ was found to decrease by about 1.2‰ in cores, and by about 2.8‰ during laboratory microbial decomposition experiments. C:N changed less, with an increase of about 1.1.

In Lake Ozette cores, down-core variations in stable isotope values do not appear to correlate with changes in accumulation rate, and variability is well within the range reported by Lehmann et al (2002) for sediments undergoing diagenesis. C:N ratios in cores with stable depositional facies show a decrease in the C:N ratio in more recent sediments (Figure 44 - Figure 46). However, care should be exercised in interpreting these trends, because sampling intervals encompass multiple years, and because diagenesis has not been studied in these sediments.

Some correlation between cores is apparent. However further research into the nutrient web in the Ozette Basin is necessary to determine whether isotope values change as a function of pre- or post-depositional processes. For example, Kaushal and Binford (1999) found a rise in the C:N ratio in lake sediments in Lake Pleasant, Massachusetts, which corresponded to deforestation. They attributed this rise to an increase in terrestrially sourced carbon. On the other hand, Brahney et al (2006) found that the C:N ratio decreased as sockeye escapement increased in sockeye nursery lakes in coastal British Columbia, Canada, which they attributed to a reduction of nitrogen limitation to primary productivity.

Both of the above studies are inconsistent with data from Lake Ozette, which shows a decline in the C:N ratio in the recent (upper) portion of the majority of the cores (Figure 44 - Figure 49). Because we know that salmon populations declined markedly in Ozette in the 1950s (Jacobs et al 1996; Haggerty et al 2008), and that timber harvest occurred largely in the latter half of the 20th century (this paper), another mechanism must explain the down-core decrease in the C:N ratio in data from this study. The most logical explanation is that, rather than reflecting trophic changes in Lake Ozette, these data demonstrate diagenetic changes in sediment characteristics. A study of varved sediments in a Swedish lake found a similar patterns to those observed in C:N ratios in Ozette. In that study, over a period of 27 years, the C concentration in sediment decreased by 23% and the N concentration by 35%, resulting in a change in C:N ratios from ~10 to ~12 over the same period (Gälman and Rydberg 2008). For comparison, the C:N ratio in Ozette sediments generally increases from about 14 to 17 down-core. However, substantial

variability exists, and likely there is a great deal of information to be gleaned from additional research. Such research should take care to collect and sample cores in a way that preserves the maximum amount of structure and information.

A possible explanation for higher isotopic values for both C and N in the deeper cores (which are also farther from sources of terrestrial inputs) is a relatively higher contribution of algal sources. The most common form of dissolved inorganic nitrogen (DIN) used by algae is NO_3^-, which typically has a $\delta^{15}N$ value that is 7 - 10‰ higher than atmospheric N_2 fixed by soil bacteria for terrestrial plants (Meyer 2003). However, as stated before, care must be taken in interpreting these results without a more complete understanding of biogeochemical processes at work throughout the watershed, however. For example, Peterson and Fry (1987) point out that very different isotopic fractionation could occur in nitrogen-limited vs. phosphorus limited systems.

It is hypothesized that Ozette is phosphorus-limited (Meyer and Brenkman 2001), but there are insufficient data to support this assumption. Results from this study do shed light on the fate of phosphorus in the lake though. The presence of vivianite ($Fe_3(PO_4)_2 \cdot 8H_2O$) in cores from Lake Ozette is indicative of a reducing environment, and implies that sediments in Lake Ozette contain a significant reservoir of phosphorus, a limiting nutrient to algal production. Vivianite was identified in five of nine X-rayed cores, and was absent only from cores where rapid accumulation was common (OZ0906-1,2, & 3), or where there was evidence of episodic sedimentation (OZ1005-4). Vivianite is commonly formed authigenically as an early byproduct of diagenesis in organic rich lake sediments and occurs when organic-rich sediments are depleted of sulfate and enriched in Fe^{2+} (Burnett and Riggs 1990). Precipitation and dissolution is believed to be an important regulator of phosphorus in lake waters (Nriagu and Dell 1974; Olsson et al 1997), An increase in nutrients, and particularly an increase in sulfur, can result in dissolution of vivianite, and consequent release of phosphorus into the water column (Olsson et al 1997). Modern forest fertilization practices in the Pacific Northwest have used nitrogen and $MgSO^4$ fertilization to increase productivity (Harrison et al 1993; Chappell et al 1990). In light of this, and the presence of vivianite in sediments in Lake Ozette, sulfur loading should be monitored to minimize the risks of anthropogenic release of phosphorus from lake sediments (e.g. Olsson et al 1997).

5 REFERENCES

Aalto, K.R., Sharp, W.D. & Renne, P.R. 1998. 40Ar/39Ar dating of detrital micas from Oligocene-Pleistocene sandstones of the Olympic Peninsula, Klamath Mountains, and northern California Coast Ranges: Provenance and palaeodrainage patterns, Canadian Journal of Earth Science, 35, 735-745.

Aalto, R., and Dietrich, W., 2005, Sediment accumulation determined with Pb-210 geochronology for Strickland River flood plains, Papua New Guinea, in Walling, D.E., and Horowitz, A.J., eds., Sediment Budgets I: Wallingford, UK, IAHS Press, v. 291, p. 303-309.

Alaback, P. B. 1996. Biodiversity patterns in relation to climate: The coastal temperate rainforests of North America. Pgs. 105-133 in: Lawford, R. G., Alaback, P. B. and Fuentes, E. (eds.) High-Latitude Rainforests and Associated Ecosystems of the West Coast of the Americas: Climate, Hydrology, Ecology and Conservation. New York, Springer-Verlag.

Appleby, P.G., P. Nolan, D.W. Gifford, M.J. Godfrey, F. Oldfield, N.J. Anderson, and R.W. Battabee. 1986. Pb-210 dating by low background counting. Hydrobiologia 142:21-27.Alaback, P.B. 1996. Biodiversity patterns in relation to climate: The coastal temperate rainforests of North America. In High-latitude rainforests and associated ecosystems of the west coast of the Americas: climate, hydrology, ecology and conservation. Edited by R.G. Lawford, P.B. Alaback, and E. Fuentes. Springer-Verlag, New York pp. 105-133.

Atwater, B.F. and Hemphill-Haley, E. 1997. Recurrence intervals for great earthquakes of the past 3,500 years at northeastern Willapa Bay, Washington. U.S. Geological Survey, Professional Paper 1576.

Azevedo, J. and D.L. Morgan. 1974. Fog precipitation in coastal California. Ecology 55:1135-1141.

Babcock, R.S., Burmester, R.F., Engebretson, D.C., Warnock, A., Clark, K.P., 1992, A rifted margin origin for the Crescent basalts and related rocks in northern Coast Range volcanic province, Washington and British Columbia: Journal of Geophysical Research, v. 97, p. 6799-6821.

Beechie, T.J., E.A. Steel, P. Roni, and E. Quimby (editors). 2003. Ecosystem recovery planning for listed salmon: an integrated assessment approach for salmon habitat. NOAA Tech. Memo. NMFS-NWFSC-58, 183 p.

Bolsinger, C.L. 1969. Resource Bulletin PNW-RB-031. U.S. Department of Agriculture, Forest Service, Pacific Northwest Research Station. 60 p.

Bortleson, G., Dion, N. 1979. Preferred and observed conditions for sockeye salmon in Ozette Lake and its tributaries, Clallam County, Washington. Tacoma, WA., United States

Department of the Interior, U.S. Geological Survey Water Resources Investigations 78-64, 61pp.

Boudreau, B.P, and Bennett, R.H. 1999. New rheological and porosity equations for steady-state compaction. American Journal of Science, vol 299, p. 517-528.

Brahney J., Bos D.G., Pellatt M.G., Edwards T.W.D., Routledge R. 2006. The influence of nitrogen limitation on $\delta^{15}N$ and carbon:nitrogen ratios in sediments from sockeye salmon nursery lakes in British Columbia, Canada. Limnology and Oceanography 51, p. 2333-2340.

Brandon, M. T.; Calderwood, A. R., 1990, High-pressure metamorphism and uplift of the Olympic subduction complex. Geology, v. 18, no. 12, p. 1252-1255.

Brandon, M.T., Vance, J.A., 1992, Tectonic evolution of the Cenozoic Olympic subduction complex, Washington State, as deduced from fission track ages for detrital zircons. American Journal of Science 292: 565-636.
Bronk Ramsey, C., 2001, Development of the radiocarbon calibration program OxCal, Radiocarbon, 43 (2A): 355-363.

Burnett, W.C., Riggs, S.R. (editors). 1990. Phosphate Deposits of the World, Volume 3: Neogene to modern phosphorites. Cambridge University Press, Cambridge, UK.

Caplanne, S., Laurion, I., 2007. Effect of chromophoric dissolved organic matter on epilimnetic stratification in lakes. Aquatic Sciences - Research Across Boundaries.

Chappell, H.N., Cole, D.W., Gessel, S.P., Walker, R.B. 1991. Forest fertilization research and practice in the Pacific Northwest. Nutrient Cycling in Agroecosystems 27(1): 129-140.

Court, A., Gerston, R.D., Fog Frequency in the United States. Geographical Review 56(4): 543-550.

Daly, C., Neilson, R.P., Phillips, D.L., 1994, A statistical-topographic model for mapping climatological precipitation over mountainous terrain, Journal of Applied Meteorology 33:140–158. Data retrieved from ftp://prism.oregonstate.edu//pub/prism/us/grids/ppt/Normals/us_ppt_1971_2000.14.gz dated 4 Feb 2004.

Dawson, T.E. 1998. Fog in the California redwood forest: ecosystem inputs and use by plants. Oecologia 117: 476-485.

Finney, B.P., Gregory-Eaves I., Sweetman J., Douglas M.S.V. and Smol J.P. 2000. Impacts of climatic change and fishing on Pacific salmon abundance over the past 300 years. Science 290: 795-799.

Finney, B.P., Gregory-Eaves, I., Douglas, M.S.V., Smol, J.P. 2002. Fisheries productivity in the northeastern Pacific Ocean over the past 2,200 years. Nature 416: 729–733

Franklin, Jerry F.; Dyrness, C.T. 1973. Natural vegetation of Oregon and Washington. Gen. Tech. Rep. PNW-GTR-008. Portland, OR: U.S. Department of Agriculture, Forest Service, Pacific Northwest Research Station. 427 p.
Gälman, V., Rydberg, J., 2008. Carbon and nitrogen loss rates during aging of lake sediment: Changes over 27 years studied in varved lake sediment. Limnology and Oceanography 53(3): 1076-1082

Gannett, H. 1897. The Administration of the Forests of the Public Domain. Journal of the American Geographical Society of New York 29(2): 181-192.

Gee, NG. 1934. Some New Records of Occurrence of North American Fresh-Water Sponges. Science, New Series 80(2072): 248.

Goldfinger, C., Nelson, C.H., Johnson, J.E., and the Shipboard Scientific Party. 2003. Deep-water turbidites as Holocene earthquake proxies: the Cascadia subduction zone and Northern San Andreas Fault Systems. Annals of Geophysics 46(5): 1169-1194.

Gregory-Eaves, I., Finneym B.P., Douglas, M.S.V., Smol, J.P. 2004. Inferring sockeye salmon (Oncorhynchus nerka) population dynamics and water-quality changes in a stained nursery lake over the past ~500 years. Can J Fish Aquat Sci 61:1235–1246.

Gucinski, H., Furniss, M.J., Ziemer, R.R., Brookes, M.H. 2001. Forest roads: a synthesis of scientific information. Martha H.Gen. Tech. Rep. PNW-GTR-509. Portland, OR: U.S. Department of Agriculture, Forest Service, Pacific Northwest Research Station. 103 p

Guilderson, T.P., Reimer, P.J., Brown, T.A. 2005. The Boon and Bane of Radiocarbon Dating. Science 307: 362-364.

Gustafson, R. G. and Iwamoto, E. M. 2005. A DNA-based Identification Key to Pacific Northwest Freshwater Mussel Glochidia: Importance to Salmonid and Mussel Conservation. Northwest Science 79(4): 233-245.

Haeussler, P. J., Bradley, D. C., Wells, R. E., Miller, M. L., 2003, Life and death of the Resurrection Plate; evidence for its existence and subduction in the northeastern Pacific in Paleocene-Eocene time: Geological Society of America Bulletin 115(7): 867-880.

Haggerty, M.J., Ritchie, A.C., Shellberg, J.G., Crewson, M.J., and Jalonen, J. 2009. Lake Ozette Sockeye Limiting Factors Analysis. Prepared for the Makah Indian Tribe and NOAA Fisheries in Cooperation with the Lake Ozette Sockeye Steering Committee, Port Angeles, WA. Available at: http://www.nwr.noaa.gov/Salmon-Recovery-Planning/Recovery-Domains/Puget-Sound/Ozette-LFA.cfm

Halloin, L.J. 1987. Soil Survey of Clallam County, Washington, USDA Soil Conservation Service in cooperation with Washington State Department of Natural Resources;

Washington State University Agriculture Research Center; and Clallam County Commissioners.

Harr, R.D. 1982. Fog drip in the Bull Run municipal watershed, Oregon, Water Resources Bulletin 18(5): 785-788.

Harrison, R.B., Henry, C.L., Xue, D., 1994. Magnesium deficiency in Douglas-fir and Grand fir growing on a sandy outwash soil amended with sewage sludge. Water, Air, & Soil Pollution, 75(1): 37-50.

Henderson, J.A., Peter, D.A., Lesher, R., Shaw, D.C. 1989. Forested plant associations of the Olympic National Forest. USDA Forest Service PNW Region. R6-ECOL-TP 001-88. 502 pp.

Herrera Environmental Consultants, I. 2006. Reconnaissance study of geomorphic conditions: Lake Ozette watershed. Unpublished report prepared for Olympic National Park, 154 pages plus appendices, Port Angeles, WA.

Heusser, C. J., 1973, Environmental sequence following the Fraser advance of the Juan de Fuca lobe, Washington. Quaternary Research 3(2): 284-306.

Hobbs, W.O., Wolfe, A.P. 2008. Recent Paleolimnology of three lakes in the Fraser River Basin (BC, Canada): no response to the collapse of sockeye salmon stocks following the Hells Gate landslides. Journal of Paleolimnology 40: 295-308.

Hodell, D.A., Schelske, C.L., 1998. Production, sedimentation and isotopic composition of organic matter in Lake Ontario. Limnology and. Oceanography 43: 200-214.

Holtham, A. J., I. Gregory-Eaves, M. G. Pellatt, D. T. Selbie, L. Stewart, B. P. Finney, and Smol, J.P. 2004. The influence of flushing rates, terrestrial input and low salmon escapement densities on paleolimnological reconstructions of sockeye salmon (Oncorhynchus nerka) nutrient dynamics in Alaska and British Columbia. Journal of Paleolimnology 32: 255-271.

Hutchinson, I., McMillan, A.D., 1997, Archaeological Evidence for Village Abandonment Associated with Late Holocene Earthquakes at the Northern Cascadia Subduction Zone, Quaternary Research 48(1): 79

Jacobs, R., Larson, G., Meyer, J., Currence, N., Hinton, J., Adkison, M., and Burgner, R. 1996. The sockeye salmon Oncorhynchus nerka populations in Lake Ozette, Washington, USA. U.S. Department of the Interior, National Park Service, Tech. Report NPS /CCSOSU/NRTR-96 /04.

Kaushal, S., Binford, M.W., 1999. Relationship between C:N ratios of lake sediments, organic matter sources, and historical deforestation in Lake Pleasant, Massachusetts, USA. Journal of Paleolimnology 22: 439-442.

Lehmann, M.F., Bernasconi, S.M., Barbieri, A., McKenzie, J.A., 2002. Preservation of organic matter and alteration of its carbon and nitrogen isotope composition during simulated and in situ early sedimentary diagenesis. Geochim. Cosmochim. Acta 66: 3573-3584.

Lieb, A. A. and Perry, T. W. 2005. Watershed Conditions and Seasonal Variability for Select Streams within WRIA 20, Olympic Peninsula, Washington. U.S. Department of the Interior, Bureau of Reclamation, Technical Services Center, Denver, CO.

Madsen, J. K., D. J. Thorkelson, R. M. Friedman, Marshall, D.D., 2006. Cenozoic to Recant configuration in the Pacific Basin: Ridge subduction and slab window magmatism in western North America, Geosphere 2(1): 11-34.

Meyer, J. and Brenkman, S. 2001. Water quality conditions in the Lake Ozette Basin, Washington and potential impacts to salmonids. Olympic National Park, 81pp, Port Angeles, WA.

Meyers, P.A. 1994. Preservation of source identification of sedimentary organic matter during and after deposition. Chemical Geology 144: 289–302.

Meyers, P.A. 2003. Applications of organic geochemistry to paleolimnological reconstructions: a summary of examples from the Laurentian Great Lakes. Organic Geochemistry 34: 261–289.

McMillan, A.D., 1999, Since the Time of the Transformers: The Ancient Heritage of the Nuu-Chah-Nulth, Ditidaht and Makah, UBC Press.

NCDC (NOAA-National Climate Data Center) 2007. Quillayute Airport weather station data query. Accessed 10 June 2007 http://www4.ncdc.noaa.gov/cgi-win/wwcgi.dll?wwDI~StnSrch~StnID~20027854

Nittrouer, C.A., Sternberg, R.W., Carpenter, R., Bennett, J.T., 1979. The use of ^{210}Pb geochronology as a sedimentological tool: application to the Washington continental shelf. Marine Geology 31:297.

Nriagu, J.O., Dell, C.I. 1974. Diagenetic Formation of Iron Phosphates in Recent Lake Sediments. American Mineralogist 59: 934-946.

Oberlander, G.T. 1956. Summer fog precipitation on the San Francisco Peninsula. Ecology 37:851-852.

Olsson, S., Regn´ell, J., Persson, A., Sandgren, P. 1997. Sediment-chemistry response to land-use change and pollutant loading in a hypertrophic lake, southern Sweden. Journal of Paleolimnology 17: 275-294.

Pater, D. E., S. A. Bryce, T. D. Thorson, J. Kagan, C. Chappell, J. M. Omernik, S. H. Azevedo, and A. J. Woods. 1997. Ecoregions of western Washington and Oregon (color poster with map). U.S. Geological Survey.

Peterson, B.J., Fry, B., 1987. Stable isotopes in ecosystem studies. Annual Reviews of Ecological Systems 18: 293–320.

Phillips, E.L., 1960, Climate of Washington, in Climatography of the United States: U.S. Department of Commerce, no. 60-45.

Pratson, L.F., Nittrouer, C.A., Wiberg, P.L., Steckler, M.S., Cacchione,D.A., Karson, J.A., Mullenbach, B.L., Swenson, J.B., Murray, A.B., Spinelli, G.A., Fulthorpe, C.S. O'Grady, D.B. Parker, G. Driscoll, N.W., Burger, R.L., Paola, C., Orange, D.L., Wolinsky, M., Field, M.E., Friedrichs, C.T., Fidelez, J.J., 2007. Seascape evolution on clastic continental shelves and slopes, in C.A. Nittrouer et al. (eds.) Continental-Margin Sedimentation: From Sediment Transport to Sequence Stratigraphy, Blackwell.

Reimer, P. J., Baillie, M. G. L., Bard, E., Bayliss, A., Beck, J. W., & Bertrand, C. J. H., et al. (2004). IntCal04 terrestrial radiocarbon age calibration, 0-26 cal kyr BP. Radiocarbon, 46(3): 1029-1058.

Renker, Ann. 1994 "The Makah". In Native America in the Twentieth Century: An Encyclopedia. New York: Garland.

Revil, A., Pezard, P.A., and de Larouzière, F.D., 1999. Fluid overpressures in western Mediterranean sediments, Sites 974-979. In Zahn, R., Comas, M.C., and Klaus, A. (Eds.), Proc. ODP, Sci. Results, 161: College Station, TX (Ocean Drilling Program), 117-128. doi:10.2973/odp.proc.sr.161.274.1999

Riley, CL., 1968. The Makah Indians: A Study of Political and Economic Organization. Ethnohistory 15(1): 57-95

Schasse, H. W. 2003. Geologic map of the Washington portion of the Cape Flattery 1:100,000 quadrangle. Washington Division of Geology and Earth Resources Open File Report 2003-5, 1 sheet, scale 1:100,000.

Schindler, D.E., Leavitt, P.R., Brock, C.S., Johnson, S.P., Quay, P.D. 2005. Marine-derived nutrients, commercial fisheries, and production of salmon and lake algae in Alaska. Ecology, Vol. 86 No. 12, pp. 3225-3231.

Sells, C., 1915. Report of the Commissioner of Indian Affairs, In Reports of the Department of the Interior for the fiscal year ended June 30 1915, Vol II p. 69. Washington, Government Printing Office.

Stone, R.G., 1936. Fog in the United States and Adjacent Regions, Geographical Review, Vol. 26, No. 1. pp. 111-134.

Sumioka, S. S.; Kresch, D. L.; Kasnick, K. D. 1998, Magnitude and Frequency of Floods in Washington. Water Resources Investigation Report no 97-4277. United States Geological Survey, Denver, CO.

Stewart, R. J., Brandon, M. T., 2004, Detrital-zircon fission-track ages for the "Hoh Formation": implications for late Cenozoic evolution of the Cascadia subduction wedge: Geological Society of America bulletin, v. 116, n. 1/2, p. 60-75.

Stuiver, M. and Polach, H.A., 1977, Discussion: Reporting of 14C data. Radiocarbon, 19:355-363.

Stuiver, M., 1980, Workshop on 14C data reporting. Radiocarbon, 22:964-966.

Swindell, E.G. 1941. Transcript of minutes a meeting between Mr. E. G. Swindell, Jr. (U.S. Attorney Office, representing Taholah Indian Agency) and Makah Indians, discussing traditional fishing locations. Makah Museum, Makah Language Program, adapted version (contains Makah spelling and pronunciation of place names), Neah Bay, WA.

Tabor, R.W. and Cady, W.M., 1978, The structure of the Olympic Mountains, Washington--analysis of a subduction zone: U.S. Geological Survey Professional Paper 1033, 133 p.

Törnqvist, T.E., Wallace, D.J., Storms, J.E.A., Walling, J. van Dam, R.L., Blaauw, M. Derksen, M.S., Klerks, C.J.W., Meijneken, C., Snijders, E.M.A. 2008. Mississippi Delta subsidence primarily caused by compaction of Holocene strata. Nature Geoscience, vol 1, p. 173-176.

U.S. Department of Agriculture (USDA) 1993. Determining the risk of cumulative watershed effects resulting from multiple activities. U.S. Department of Agriculture, U.S. Forest Service.

U.S. Geological Survey. Ozette Lake quadrangle, Washington [map]. 1:62,500. 1935. War Department. Corps Of Engineers, U.S. Army. Washington D.C.

U.S. Geological Survey. Ozette Lake quadrangle, Washington [map]. 1:62,500. 1956. Publication MR 7056. Washington D.C.

U.S. Geological Survey. Ozette quadrangle, Washington [map]. 1:24,000 7.5 Minute Series. 1984. Washington D.C.

U.S. Geological Survey. Allens Bay. Dickey Lake, Ozette, and Umbrella Creek quadrangles, Washington [map]. 1:24,000 7.5 Minute Series. 1984. Washington D.C.

U.S. Geological Survey. 1994 1:24,000. Digital Raster Graphics (DRG) maps on cd-rom 7.5 Minute Series. Washington D.C.: USGS, 1994. Available as of January 2008. < http://gis.ess.washington.edu/data/raster/drg/>

Vander Schaaf, D., G. Wilhere, Z. Ferdaña, K. Popper, M. Schindel, P. Skidmore, D. Rolph, P. Iachetti, G. Kittel, R. Crawford, D. Pickering, and J. Christy. 2006. Pacific Northwest Coast Ecoregion Assessment. Prepared by The Nature Conservancy, the Nature Conservancy of Canada, and the Washington Department of Fish and Wildlife. The Nature Conservancy, Portland, Oregon.

Walcott, E.E., 1973, Lakes of Washington. Water Supply Bulletin #14, WA Department of Ecology.

Washington Native Plant Society (WNPS). Unpublished. Native Plant List for Lake Ozette. Available at: http://www.wnps.org/plant_lists/counties/clallum/lake_ozette.doc (retrieved 12 Dec 2007).

Wemple, B.C., Jones, J.A., Grant, G.E. 1996. Channel network extension by logging roads in two basins, western Cascades, Oregon. Water Resources Bulletin 32:1-13 .

Western Regional Climate Center (WRCC). 2003. Average Number of Days with Heavy Fog. Available at http://www.wrcc.dri.edu/htmlfiles/westcomp.fog.html (accessed on 2 May 2007).

Wray, J., Anderson, M.K., 2003, Restoring Indian-Set Fires to Prairie Ecosystems on the Olympic Peninsula. Ecological Rest. 2003 21: 296-301.

APPENDIX A: Acoustic profiles

APPENDIX B: Core X-radiograph negatives